
Chiral dynamics for open-charm systems at PANDA

Chirale Dynamik von Open-Charm-Systemen für PANDA

Zur Erlangung des Grades eines Doktors der Naturwissenschaften (Dr. rer. nat.)

genehmigte Dissertation von Xiaoyu Guo, M.Sc. [REDACTED]

Tag der Einreichung: 24.01.2017, Tag der Prüfung: 15.02.2017

Darmstadt 2018 – D 17

1. Gutachten: Prof. Dr. Matthias F.M. Lutz
2. Gutachten: Prof. Dr. Achim Schwenk



TECHNISCHE
UNIVERSITÄT
DARMSTADT

Fachbereich Physik
GSI Theorie

Chiral dynamics for open- charm systems at PANDA
Chirale Dynamik von Open-Charm-Systemen für PANDA

Genehmigte Dissertation von Xiaoyu Guo, M.Sc. [REDACTED]

1. Gutachten: Prof. Dr. Matthias F.M. Lutz
2. Gutachten: Prof. Dr. Achim Schwenk

Tag der Einreichung: 24.01.2017

Tag der Prüfung: 15.02.2017

Darmstadt 2018 – D 17

Bitte zitieren Sie dieses Dokument als:

URN: urn:nbn:de:tuda-tuprints-72058

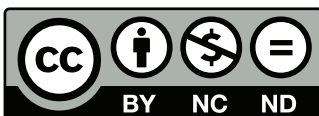
URL: <http://tuprints.ulb.tu-darmstadt.de/7205>

Dieses Dokument wird bereitgestellt von tuprints,

E-Publishing-Service der TU Darmstadt

<http://tuprints.ulb.tu-darmstadt.de>

tuprints@ulb.tu-darmstadt.de



Die Veröffentlichung steht unter folgender Creative Commons Lizenz:

Namensnennung – Keine kommerzielle Nutzung – Keine Bearbeitung 4.0 International

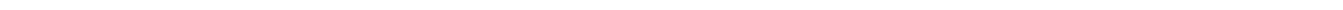
<http://creativecommons.org/licenses/by-nc-nd/4.0/>

Erklärung zur Dissertation

Hiermit versichere ich, die vorliegende Dissertation ohne Hilfe Dritter nur mit den angegebenen Quellen und Hilfsmitteln angefertigt zu haben. Alle Stellen, die aus Quellen entnommen wurden, sind als solche kenntlich gemacht. Diese Arbeit hat in gleicher oder ähnlicher Form noch keiner Prüfungsbehörde vorgelegen.

Darmstadt, den January 17, 2018

(Xiaoyu Guo)



Abstract

This thesis aims to study low-energy strong interaction effects of open-charm mesons. Our studies are based on the chiral Lagrangian supplemented by constraints from the heavy-quark spin symmetry. The pseudoscalar and vector open-charm-meson masses are calculated up to next-to-next-to-next leading order ($N^3\text{LO}$) corrections. Different assumptions on the counting rules are investigated. It is illustrated that a chiral expansion uniformly converges rapidly up to Goldstone boson masses as heavy as the kaon masses if formulated in terms of physical meson masses. First estimates of the relevant low-energy parameters are extracted from lattice QCD data on the quark mass dependence of the D meson masses. Such low-energy parameters are of crucial importance for the low-energy interaction of the Goldstone bosons with the D mesons.

Zusammenfassung

In dieser Arbeit untersuchen wir stark wechselwirkende Mesonsysteme mit nicht verschwindenden Charminhalt ($C \neq 0$). Es kommt zur Anwendung der chiralen Lagrangian, wobei die Konsequenzen der Quarkspinsymmetrie der schweren Quarks eingearbeitet werden. Die Massen der pseudoskalaren und vektoriellen D Mesonen mit $C = 1$ werden zu N³LO berechnet. Verschiedene Annahmen für das chirale Zählchema werden untersucht. Es wird gezeigt, dass ein Zählchema, welches mit Hilfe der physikalischen Mesonmassen formuliert ist, uniform konvergiert bis zu Massen der Pionen und Kaonen von ca 600 MeV. Erste Abschätzungen für die Niederenergieparameter des chiralen Lagrangian werden aus Gitter QCD Daten für die D Mesonmassen bei verschiedenen unphysikalischen Quarkmassen abgeleitet. Diese Parameter bestimmen die Niederenergiewechselwirkung der Goldstonebosonen mit den D Mesonen.

Contents

1. Introduction	7
2. Low Energy QCD and Effective Theories	9
2.1. Chiral Perturbation Theory	9
2.1.1. Chiral symmetry	10
2.1.2. Chiral Lagrangian in the pure Goldstone boson sector	12
2.1.3. Inclusion of Heavy Meson Fields	14
2.2. Heavy-Quark Reduction	16
2.2.1. Symmetries in heavy-light mesons	16
2.2.2. Heavy Meson Reduction	22
2.3. Heavy-quark constraints on the chiral Lagrangian involving open-charm mesons	23
2.3.1. Leading order chiral Lagrangian	24
2.3.2. Higher order Lagrangian	25
3. Chiral extrapolation for open-charm meson masses	29
3.1. Chiral corrections for the masses of open-charm mesons up to $N^3\text{LO}$	30
3.1.1. Self-energies for the 0^- and 1^- open-charm mesons	30
3.1.2. The χ - $\overline{\text{MS}}$ subtraction scheme	36
3.1.3. Renormalization of the low energy constants	38
3.1.4. Numerical estimate on the importance of the bubble-loop corrections	39
3.2. The convergence of chiral expansions on the loop corrections	40
3.2.1. The convergence behavior in the heavy-quark mass limit	41
3.2.2. The convergence behavior in the light-quark mass limit	42
3.2.3. The convergence behavior in a small-scale expansion	45
3.2.4. A novel chiral-expansion pattern	47
3.3. Chiral Extrapolation	53
3.3.1. Lattice simulations for open-charm meson masses	53
3.3.2. Fitting the D -meson chiral mass formula to lattice data	57
3.3.3. Comparison of the values of LECs from different works	59
4. Summary	64
A. Conventions	65
B. Vector versus tensor representations for vector particles	66
C. Large N_C approximation	67
D. Passarino-Veltman Integrals	70
D.1. Passarino-Veltman integrals in an infinite volume	70
D.2. Finite-volume corrections	71
E. Chiral expansions	73
E.1. Basic definitions	73
E.2. $O(Q^5)$ results according to the small-scale expansion scheme	75



E.3. $O(Q^5)$ results according to the novel chiral expansion scheme	76
F. A complement of the lattice data for the D-meson masses	78
Bibliography	80
Acknowledgements	89

1 Introduction

In the standard model, elementary particles are divided into quarks, leptons and gauge bosons. There are 6 different flavors of quarks, the lighter ones up, down and strange, and heavier ones charm, bottom and top. The quarks experience strong interactions with each other via gluons described by quantum chromodynamics (QCD). QCD features asymptotic freedom: the magnitude of the QCD coupling constant increases when the energy transfer decreases. As a consequence, low-energy QCD is characterized by a plethora of non-perturbative phenomena.

In understanding the low-energy behavior of QCD, studies of open-charm mesons, mesons consisting with a single charm quark, are believed to be of crucial importance (for reviews, see Refs. [1, 2]). They may be described by QCD-motivated quark models [3, 4]. However, open-charm states with exotic properties have been discovered (see e.g. [5–7], and [8] for a recent review), that cannot be reasonably accommodated by conventional quark models [9–13]. More systematic approaches based on QCD are required for studies of open-charm systems.

Low-energy QCD systems have been extensively studied using chiral effective field theory approaches [14–16]. For open-charm systems, the heavy-quark symmetry [17, 18] poses additional constraints in the construction of the relevant effective Lagrangians [19–21]. Chiral effective field theories are based on a power counting scheme which permits the systematic and perturbative expansion of physical observables in a small parameter, like the masses of the Goldstone bosons. Non-perturbative extensions implement the coupled-channel unitarity constraint [22–26]. Such approaches are successful in describing exotic open-charm states as molecular resonances generated by final state interactions [27–31]. Higher order improvements rely on a set of low-energy constants (LECs) from counter terms in the effective Lagrangian. As shown in Ref. [28], the knowledge of such LECs are crucial in predicting properties of scalar and axial-vector open-charm resonances. Such studies are of great importance for the open-charm physics program at PANDA [32].

As a non-perturbative approach, lattice QCD has gained great progress in describing low-energy QCD properties during the last decades [33]. Accurate results are available mainly for ground-state masses of hadrons at different quark masses with Goldstone-boson masses off their physical values. Low-energy constants of effective Lagrangians may be extracted from such QCD lattice data. For a long time, lattice simulations for charm quark systems were suffering from large discretization errors such that no faithful results on open-charm meson or baryon masses were available. But recently, significant progress has been made by improved actions that reduce the discretization errors and the use of larger lattices with a smaller size of the lattice spacing [34–40].

This work aims to determine the low-energy constants of the chiral Lagrangian formulated with the pseudo-scalar and vector D mesons. The masses of the D mesons are computed as a function of such LECs at next-to-next-to-next leading order ($N^3\text{LO}$). The resulting mass formulae are applied to two lattice data sets [41, 42].

In Chapter 2, we first briefly introduce the chiral Lagrangian properly constrained by the heavy-quark symmetry. A full relativistic flavor $SU(3)$ Lagrangian with pseudo-scalar and vector D mesons is considered. In particular all counter terms needed for the computation of the D -meson masses at $N^3\text{LO}$ are constructed for the first time.

In Chapter 3, chiral loop corrections for the D -meson masses are computed in a finite spatial box following the method suggested recently in [43]. The results are analyzed in the infinite volume limit first. There is a controversy to what extent a flavour $SU(3)$ chiral Lagrangian leads to convergent results at physical values of the Goldstone boson masses [44–51]. Are the physical kaon and η meson masses small enough so that the chiral expansion converges rapidly enough to obtain significant results? We study this issue by considering four different counting rules and working out their respective convergence domains. In particular a novel chiral expansion approach formulated in terms of physical meson masses

is investigated Ref [52]. The Chapter closes with some first results obtained from a fit to the lattice data sets. Here the finite-box computations for the D -meson masses are used. First estimates of the LECs are discussed and compared with previous studies. A brief summary will be drawn in the last chapter.

2 Low Energy QCD and Effective Theories

QCD has been established as an SU(3) gauge theory to describe the strong interaction. The Lagrangian is

$$\mathcal{L}_{\text{QCD}} = \bar{\psi}(i\gamma_\mu \mathcal{D}^\mu - M_q^0)\psi - \frac{1}{4} F_{a,\mu\nu} F_a^{\mu\nu}, \quad (2.1)$$

in which ψ is a N_f -component quark field with N_f flavors and M_q^0 is the current quark mass matrix. The index a runs through the gauge degrees of freedom that are called gluons in QCD. The quark fields come in the basic gauge representation with three different colours. It is convenient to consider the gauge covariant derivative and the gluon field tensor

$$\mathcal{D}^\mu = \partial^\mu - ig A_a^\mu \frac{\lambda_a}{2} \quad (2.2)$$

$$F_a^{\mu\nu} = \partial^\mu A_a^\nu - \partial^\nu A_a^\mu + g f_{abc} A_b^\mu A_c^\nu \quad (2.3)$$

where A_a^μ is the vector representation of the gluon field and λ_a are the eight Gell-Mann matrices. A perturbative calculation of the coupling constant shows the asymptotic freedom of the strong interaction. At the one-loop level, the running coupling constant tends to be divergent when the renormalization scale goes down to $\Lambda_{\text{QCD}} \approx 200\text{MeV}$. This divergence is just an artifact: it implies that perturbation theory turns invalid at small momentum transfer. A non-perturbative calculation in the low energy region can give a distinct running behavior of the coupling constant. The divergence of the coupling constant will no longer appear. Nevertheless the one-loop result suggests a characteristic scale for QCD, $\Lambda_{\text{QCD}} \approx 200\text{ MeV}$.

The strong interaction at low energies has got various unique features that can not be obtained from perturbation theory. The most notable phenomena of non-perturbative QCD are the color confinement and the spontaneous breaking of chiral symmetry. The colored degrees of freedom like quarks and gluons are always grouped into colorless degrees like mesons and baryons. This is color confinement: the normal physical world is color neutral. The breaking of chiral symmetry brings about a large dynamical quark mass for light quarks and is responsible for the relatively low masses of the pseudoscalar meson ground states.

Effective field theories provide powerful tools when dealing with complicated physical systems. The effective degrees of freedom need not to be the same as the ones in the underlying theory. Effective field theories implement simplified and systematic approaches to study non-perturbative QCD. Various effective field theories for QCD were developed. For instance, at low energies chiral perturbation theory (ChPT) can be applied (for reviewing see, for example, Refs. [53, 54]). Here an expansion according to the small momenta of the Goldstone bosons is performed. On the other hand, in some systems involving a heavy quark, the inverse of the heavy quark mass $1/M_Q$ is a small quantity that one can perturbatively deal with. The heavy quark effective theory (HQET) is based on this assumption (for reviewing see Refs. [55, 56]).

In this thesis, we will apply the effective theory method for the study of open-charm processes. Our first step is to determine the effective chiral Lagrangian. Concepts from heavy quark effective theory are used as well in order to take open-charm mesons into account. We will concentrate on the construction of the effective Lagrangian in this chapter.

2.1 Chiral Perturbation Theory

As an effective theory, Chiral perturbation theory (ChPT) suitably describes the low-energy behavior of the strong interaction, by asserting the theory possessing the same global symmetry as QCD, which is

the chiral symmetry. In this work we focus on chiral SU(3) symmetry. This means that the strange quark is treated as light as the u - and d -quark. In the low-energy regime of the strong interaction, the chiral symmetry is spontaneously broken, i.e. the vacuum state of the low-energy strong interaction doesn't respect the symmetry of the Lagrangian. This leads to a large mass gap between the lowest lying pseudo-scalar mesons, π and K , and other hadrons, due to Goldstone mechanism. We will have a more detailed discussion of the spontaneous broken of SU(3) chiral symmetry in the following subsection.

2.1.1 Chiral symmetry

Chiral symmetry is an approximate global symmetry of the QCD Lagrangian with light quarks. The three lightest quarks, u , d , s , have current masses of about $2 \sim 5$ MeV for the u , d quarks and about 100 MeV for the s quark [57]. These masses are much smaller than the typical hadronic scale of ~ 1 GeV. Therefore it is useful to consider the Lagrangian with up, down and strange quarks only

$$\mathcal{L}_{\text{QCD}}^0 = \bar{q} i \gamma_\mu \mathcal{D}^\mu q - \frac{1}{4} F_{a,\mu\nu} F_a^{\mu\nu}, \quad (2.4)$$

where we have neglected the quark mass matrix. The quark fields $q = u, d, s$ can be decomposed into left- and right-handed fields

$$q = q_L + q_R, \quad q_L = \frac{1 - \gamma_5}{2} q, \quad q_R = \frac{1 + \gamma_5}{2} q. \quad (2.5)$$

In terms of those fields the Lagrangian $\mathcal{L}_{\text{QCD}}^0$ can be written as

$$\mathcal{L}_{\text{QCD}}^0 = \bar{q}_L i \gamma_\mu \mathcal{D}^\mu q_L + \bar{q}_R i \gamma_\mu \mathcal{D}^\mu q_R - \frac{1}{4} F_{a,\mu\nu} F_a^{\mu\nu}. \quad (2.6)$$

One can verify that this Lagrangian is invariant under two independent SU(3) \times U(1) global transformations

$$q_L \rightarrow \exp\left(-i\theta^L - i \sum_a \theta_a^L \frac{\lambda_a}{2}\right) q_L, \quad q_R \rightarrow \exp\left(-i\theta^R - i \sum_a \theta_a^R \frac{\lambda_a}{2}\right) q_R, \quad (2.7)$$

where λ_a represent the 8 Gell-Mann matrices. The Lagrangian preserves a global SU_L(3) \times SU_R(3) \times U_L(1) \times U_R(1) symmetry called chiral symmetry. In contrast, the mass term

$$\bar{q} \hat{m} q = \bar{q}_L \hat{m} q_R + \bar{q}_R \hat{m} q_L, \quad (2.8)$$

is not invariant under independent right and left handed SU(3) \times U(1) transformations. Here $\hat{m} = \text{dia}(m_u, m_d, m_s)$ is the quark mass matrix. If the masses of the light quarks are sufficiently small the Lagrangian (2.4) serves as a good starting point to approximate strong interaction.

In the chiral limit, the chiral transformations on the Lagrangian (2.6) result in the Noether currents

$$V_a^\mu(x) = \bar{q}(x) \gamma^\mu \frac{\lambda_a}{2} q(x), \quad A_a^\mu(x) = \bar{q}(x) \gamma^\mu \gamma^5 \frac{\lambda_a}{2} q(x), \quad a = 1, \dots, 8, \quad (2.9)$$

$$V^\mu(x) = \bar{q}(x) \gamma^\mu q(x), \quad A^\mu(x) = \bar{q}(x) \gamma^\mu \gamma^5 q(x), \quad (2.10)$$

which are only conserved at the classical level. The U_A(1) symmetry is explicitly broken due to a quantum effect and will be mentioned later. If the remaining symmetry SU_L(3) \times SU_R(3) \times U_V(1) were respected in hadronic states, hadrons with same quantum numbers but opposite parities would be degenerate. This conclusion contradicts the observed hadronic spectrum. Moreover, the lightest pseudoscalar octet

mesons are much lighter than all other hadrons. To be consistent with these facts, a spontaneous breaking of the chiral symmetry is expected. When a symmetry is spontaneously broken, the ground state no longer respects the symmetry of the Lagrangian. The approximate $SU_L(3) \times SU_R(3)$ symmetry is spontaneously broken down to $SU_V(3)$ symmetry in hadronic states. The lightest pseudoscalar mesons are identified with the Goldstone bosons of the spontaneously broken chiral symmetry.

The eight Noether charges of the $SU_A(3)$ symmetry are defined by the zeroth components of the corresponding Noether currents,

$$Q_A^a(t) = \int d^3x A_0^a(x). \quad (2.11)$$

If the $SU_A(3)$ symmetry is spontaneously broken, the Noether charges give non-zero results when acting on the vacuum state, $Q_A^a(t)|0\rangle \neq 0$. The resulting state vector has a non-vanishing overlap with the Goldstone boson state $|\phi^a\rangle$:

$$\langle 0|Q_A^a(t)|\phi^a\rangle \neq 0. \quad (2.12)$$

Because of the Lorentz covariance, the matrix element of the corresponding current A_μ^a between $|0\rangle$ and $|\phi^b\rangle$ has the form (see e.g. [58])

$$\langle 0|A_\mu^a(0)|\phi^b(p)\rangle = if_0\delta^{ab}p^\mu, \quad (2.13)$$

where p^μ is the four-momentum of the Goldstone boson. The factor f_0 is recognized as the decay constant of the Goldstone bosons in the chiral limit, with the value $f_0 \simeq 93\text{MeV}$ [59]. Furthermore, the matrix element of the pseudoscalar quark density $\langle 0|\bar{q}(x)i\gamma_5\lambda_a q(x)|\phi_a\rangle$ is supposed to be non-zero. This assumption is sufficient to give a time-independent vacuum expectation (see e.g. [58, 54])

$$\langle 0|i[Q_A^a(t), \bar{q}(0)i\gamma_5\lambda_b q(0)]|0\rangle = \frac{2}{3}\delta_{ab}\langle \bar{q}(0)q(0)\rangle, \quad (2.14)$$

which can be identified with an order parameter of the spontaneous chiral symmetry breaking. Because the translational invariance of the vacuum requires $\langle \bar{q}(0)q(0)\rangle \equiv \langle \bar{q}(x)q(x)\rangle$, the quark condensate is space-time-independent, and can be abbreviated to $\langle \bar{q}q\rangle$. If the quark condensate $\langle \bar{q}q\rangle \neq 0$, the chiral symmetry will be spontaneously broken. In a strict chiral symmetric system, the spontaneous breaking of chiral symmetry gives rise to the massless pseudoscalar meson octet, while the existence of small quark masses shifts the meson masses to a small finite value. This phenomenon is illustrated by the Gell-Mann-Oakes-Renner (GOR) relations [60]

$$\begin{aligned} m_\pi^2 &= -\frac{\langle \bar{q}q\rangle}{3f_0^2}2m, \\ m_K^2 &= -\frac{\langle \bar{q}q\rangle}{3f_0^2}(m + m_s), \\ m_\eta^2 &= -\frac{\langle \bar{q}q\rangle}{3f_0^2}\left(\frac{2m + 4m_s}{3}\right), \end{aligned} \quad (2.15)$$

where the M 's and m 's are meson masses and current quark masses respectively. Throughout the thesis, we assume an exact $SU(2)$ isospin symmetry ($m_u = m_d \equiv m$). These relations relate the current quark mass and the quark condensate to the Goldstone boson mass.

As mentioned before, the $U_A(1)$ symmetry is not conserved at the quantum level [61]. This effect is attributed to $U_A(1)$ anomaly which originates from an ambiguity in defining the measure of the path integrals for fermions [62]. The result is a non-vanishing term of the derivative of the corresponding singlet axial-vector current in the chiral limit [63]

$$\partial_\mu A^\mu = \frac{3g_s^2}{32\pi^2}\epsilon^{\mu\nu\rho\sigma}F_{\mu\nu}^a F_{\rho\sigma}^a. \quad (2.16)$$

Thus, no Goldstone modes are provided by the breaking of the $U_A(1)$ symmetry.

2.1.2 Chiral Lagrangian in the pure Goldstone boson sector

As an effective low-energy theory, chiral perturbation theory is constructed with hadronic degrees of freedom. Because there's a mass gap between the Goldstone bosons and heavier hadrons only Goldstone fields need to be included in an effective Lagrangian describing the strong interaction between Goldstone bosons at low energies. The Goldstone fields can be treated as group parameters of a transformation belonging to the quotient G/H [64]. Here G is the spontaneously broken symmetry group $SU_L(3) \times SU_R(3)$ and the subgroup H is the unbroken symmetry group $SU_V(3)$. All transformations of the spontaneous broken symmetry belong to G/H . A group element $U(x)$ belonging to G/H can be chosen to transform according to

$$U(x) \xrightarrow{G} g_R U(x) g_L^\dagger, \quad g_L, g_R \in SU(3), \quad (2.17)$$

under a chiral rotation $(g_L, g_R) \in G$. A convenient choice of $U(x)$ is

$$U(x) = \exp\left[i \frac{\phi(x)}{f_0}\right], \quad (2.18)$$

where

$$\phi(x) = \sum_{a=1}^8 \lambda_a \phi_a = \begin{pmatrix} \pi^0 + \sqrt{1/3}\eta & \sqrt{2}\pi^+ & \sqrt{2}K^+ \\ \sqrt{2}\pi^- & -\pi^0 + \sqrt{1/3}\eta & \sqrt{2}K^0 \\ \sqrt{2}K^- & \sqrt{2}\bar{K}^0 & -2/\sqrt{3}\eta \end{pmatrix}. \quad (2.19)$$

Under the parity transformation (\mathcal{P}) and the charge conjugation (\mathcal{C}), the field $U(x)$ transforms respectively as

$$U(x) \xrightarrow{\mathcal{P}} U^\dagger(x), \quad U(x) \xrightarrow{\mathcal{C}} U^T(x). \quad (2.20)$$

Respecting C, P, T invariance, the effective Lagrangian with two derivatives reads [14–16]

$$\mathcal{L} = \frac{f_0^2}{4} \text{Tr}[\partial_\mu U^\dagger \partial^\mu U], \quad (2.21)$$

where ‘Tr’ specifies a trace over flavor indices. This term is the minimal term that recovers the kinetic term for the Goldstone bosons. The presence of the non-zero quark mass in QCD requires a finite-mass term to the effective Lagrangian,

$$\mathcal{L}_\chi = \frac{f_0^2}{4} \text{Tr}[\chi U^\dagger + U \chi^\dagger], \quad (2.22)$$

where an explicit chiral symmetry breaking term is defined by

$$\chi = 2B_0 \begin{pmatrix} m_u & 0 & 0 \\ 0 & m_d & 0 \\ 0 & 0 & m_s \end{pmatrix}, \quad B_0 = -\frac{\langle \bar{q}q \rangle}{3f_0^2}. \quad (2.23)$$

This term transforms nonlinearly under the chiral transformation group G

$$\chi \xrightarrow{G} g_R \chi g_L^\dagger. \quad (2.24)$$

Besides the terms shown above, one can in principle construct infinitely many terms respecting the chiral symmetry. If one could not tell the relative importance among the infinite many terms, one would not make reliable predictions out of this theory. To this end, a power counting scheme is entailed. One

can arrange the infinitely many interaction terms in respect with the relative importance according to the power counting. And a finite number of interactions can be picked up for a required accuracy.

Fortunately, the power counting scheme of ChPT can be cheerfully established. It is based on the fact that at low energies, the interactions among the Goldstone bosons tend to vanish when the energy of the interaction approaches zero. This is the unique feature of the low energy strong interaction due to the partial conservation of axial current (see [65, 64]). To this end, the power counting scheme has been established according to the power of the momentum of a Goldstone boson p , which has been firstly proposed by Weinberg [66]. The chiral Lagrangian is re-expressed as,

$$\mathcal{L} = \mathcal{L}_2 + \mathcal{L}_4 + \cdots. \quad (2.25)$$

The indices imply the chiral orders of the terms. The power counting rule is [14–16]

$$U \sim O(Q^0); \quad \partial_\mu U \sim O(Q); \quad \chi \sim O(Q^2). \quad (2.26)$$

We assign Q to be the characteristic value of $Q \sim m_{\pi,K,\eta}/\Lambda_\chi$, whereas Λ_χ is some hard scale around 1GeV. According to the rule, the Lagrangians (2.21) and (2.22) are of the leading chiral order $O(Q^2)$. The chiral counting rule for χ comes from the fact that GOR relations (2.15) are valid at leading chiral order, which provides

$$\chi = \frac{1}{3}(m_\pi^2 + 2m_K^2)\mathbb{1} + \frac{2}{\sqrt{3}}(m_\pi^2 - m_K^2)\lambda_8. \quad (2.27)$$

Corrections of the meson masses come from higher chiral order terms. The advantage of adopting the non-linear realization of Goldstone bosons (expressing the Goldstone bosons in terms of U) is that in this manner all the Goldstone interactions involve derivatives acting on the Goldstone fields. This enables one to count the chiral order of each vertex out of the Lagrangian by simply enumerating the number of derivatives acting on U . This is the power of a non-linear realization of the Goldstone bosons, which was illustrated by Coleman, Callan, Weiss and Zumino [67–69].

Up to now, the tree-level power counting rule has been demonstrated. To fully establish the chiral power counting scheme for a quantum effective theory, one needs to estimate the importance of the loop effects of the Goldstone bosons as well. In principle, if we consider loop corrections within an effective theory, some counter terms at an unexpected order may be needed in perturbation theory as to cancel the divergent part from the loops. This process makes the theory unrenormalizable and may cause problems in determining the power counting. But fortunately, the power counting is not harmed by this process when only Goldstone bosons are considered. Since all the energy scales the loop integrals depend on are soft (which is comparable to the Goldstone-boson mass), the loop contributions can be categorized according to the powers of soft scales and a power counting scheme can be well defined. The power counting scheme for pure Goldstone-meson systems has been introduced firstly by Weinberg in 1970s [66], and it has been treated as the foundation of the chiral perturbation theory.

For any given Feynman diagram, the corresponding amplitude depends on some external momenta. In the framework of chiral perturbation theory including only the Goldstone bosons, the size of the external momenta are comparable to the mass of Goldstone bosons. Thus in order to determine the power counting of the amplitude, we need only to count the dimension of the amplitude. We know every propagator of a Goldstone boson has mass dimension -2 , and every $O(Q^n)$ vertex has dimension n . And for every loop, an integration over a 4-momentum is involved, so there is an additional dimension of 4. As a result, the dimension of an amplitude for a given Feynman diagram which involves I_M Goldstone-meson propagator, N_{2n} vertices of order $2n$ as well as N_L loops reads [66]

$$D = -2I_M + \sum_{n=1}^{\infty} 2nN_{2n} + 4N_L = 2 + 2N_L + \sum_{n=1}^{\infty} N_{2n}(2n - 2), \quad (2.28)$$

which is exactly the chiral order (n_q) of the diagram, $n_q \equiv D$. Here we have used the topological relation $I_M = N_L + \sum_n N_n - 1$. And at a certain chiral order n , the number of vertices is finite, $N_n < \infty$, because of symmetry restrictions. If we consider a chiral Lagrangian up to a maximum power counting n_{\max} , it can be inferred from the relation (2.28), the more loops a diagram includes, the higher chiral order it contributes to. So to a certain chiral order, only finite number of loop diagrams we need to consider. On the other hand, considering an additional loop in the calculation will not give any corrections to the lower chiral order. Under the power counting scheme shown by (2.28), a perturbative calculation is feasible according to the chiral order. Another implication of the relation (2.28) is that, up to a given chiral order, only a finite number of loop diagrams contribute, and their divergences can be compensated by introducing finite number of contact counter terms to this order [14–16]. In other words, according to the power counting, the prediction made by chiral perturbation theory (in the pure Goldstone-boson sector) at a given chiral order is renormalization-scale independent.

The perturbative expansion according to the chiral power is convergent in the region close to the threshold. In this region, the energy transferred is up to approximately 1GeV (see e.g. [53]). This region is considered as the applicability domain of ChPT.

2.1.3 Inclusion of Heavy Meson Fields

Up to now we have considered the effective Lagrangian for describing the interaction of Goldstone-bosons. One ends up with the well-established Chiral Perturbation Theory for Goldstone bosons. The task of this thesis is to study the properties of the open-charm mesons in the low-energy regime. Therefore we need to include the open-charm mesons as matter fields in the chiral Lagrangian. The lightest pseudoscalar ($J^P = 0^-$) and vector ($J^P = 1^-$) open-charm mesons are included. We formulate the effective Lagrangian under the flavor $SU(3)$ symmetry. The isospin doublet (D^+, D^0) is combined together with D_s to transform as an anti-triplet under the unbroken $SU_V(3)$ flavor transformation, so do their vector meson partners. We provide the anti-triplets as [27]¹

$$D = (D^0, -D^+, D_s^+), \quad D_{\mu\nu} = (D_{\mu\nu}^0, -D_{\mu\nu}^+, D_{s,\mu\nu}^+). \quad (2.29)$$

Here we have adopted the tensor-field representation for the vector mesons [70, 71]. The relation between the tensor and vector representations are illustrated in Appendix B.

The transformation rule of matter fields under the spontaneously broken chiral symmetry is not uniquely defined, but different transformation forms are related to each other by field redefinitions [56, 72]. We choose the approach to define such a transformation, which was proposed by Coleman et.al. ([67, 68], see also e.g. [69]). According to this method, Goldstone fields can be represented by u ,

$$u^2(x) \equiv U(x), \quad (2.30)$$

where $U(x)$ was already introduced in Eq.(2.18). Under the $SU_L(3) \times SU_R(3)$ chiral transformation, $u(x)$ transforms non-linearly

$$u(x) \xrightarrow{G} g_R u(x) K^\dagger = K u(x) g_L^\dagger. \quad (2.31)$$

K appears as a non-linear realization of $SU_L(3) \times SU_R(3)$ group. And it can be parameterized into

$$K(x) = \exp \left[i \sum_{i=1,\dots,8} \theta_i(x) \frac{\lambda_i}{2} \right]. \quad (2.32)$$

¹ In the identification of the isospin doublet, we adopt the phase-factor convention $|D^+\rangle = |I_3 = 1/2\rangle$ and $|D^0\rangle = |I_3 = -1/2\rangle$. The $|D\rangle$ can be annihilated by the corresponding field operator D . To this end, (D^+, D^0) transforms as an isodoublet under an $SU(2)$ transformation parameterized by $\theta \vec{n}$, $(D^+, D^0) \rightarrow e^{i\vec{\sigma} \cdot \vec{n} \theta / 2} (D^+, D^0)$. We can easily verify that $(D^+, D^0)^T i\sigma_2$ transforms accordingly as an anti-doublet $(D^+, D^0)^T i\sigma_2 \rightarrow (D^+, D^0)^T i\sigma_2 e^{-i\vec{\sigma} \cdot \vec{n} \theta / 2}$. A direct inclusion of D_s provides us the formalism of $SU(3)$ anti-triplet $(D^+, D^0)^T i\sigma_2 \oplus D_s \equiv (D^0, -D^+, D_s)$. By adopting such a convention, we naturally obtain the $-$ phase factor in front of D^+ (and $D_{\mu\nu}^+$) in Eq.(2.29).

It formally resembles an SU(3) transformation, but the group parameters $\theta_i(x)$ vary with x , implicitly depending on Goldstone fields $u(x)$ as well as group elements (g_L, g_R). Under the unbroken $SU_V(3)$ transformation, θ_i reduce to spacetime-independent constants, and $K(x)$ becomes a linear representation of $SU_V(3)$. The works of Coleman et.al. [67, 68] have shown that it is always possible to find a form of $K(x)$ satisfying this property. The explicit expression of $\theta_i(x)$ is irrelevant to the discussion here.

The derivative on the u -field can be collected most economically as

$$U_\mu = \frac{1}{2}[u^\dagger(\partial_\mu u) - u(\partial_\mu u^\dagger)] \quad \text{with,} \quad U_\mu \xrightarrow{G} K U_\mu K^\dagger. \quad (2.33)$$

For instance, the leading order chiral Lagrangian for Goldstone bosons is

$$\mathcal{L} = f_0^2 \text{Tr}[U^\mu U_\mu^\dagger + \frac{1}{2}\chi_+]. \quad (2.34)$$

Explicit chiral breaking effects has been realized by one of the source term

$$\chi_\pm = \frac{1}{2}(u\chi^\dagger u \pm u^\dagger\chi u^\dagger), \quad (2.35)$$

where χ is defined in (2.23). χ_+ and χ_- transform as a Lorentz scalar and a Lorentz pseudoscalar respectively. The Lagrangian (2.34) is equivalent to the Lagrangian (2.21).

We apply this non-linear realization of $SU_L(3) \times SU_R(3)$ transformation to the matter fields D . Here D may refer to either pseudo-scalar or vector open-charm mesons without harming the discussion. The field and its conjugate D and \bar{D} are anti-triplet and triplet respectively under the unbroken subgroup $H = SU_V(3)$ transforming according to

$$D \xrightarrow{H} D g_V^\dagger, \quad \bar{D} \xrightarrow{H} g_V \bar{D}, \quad (2.36)$$

where g_V is a group element of $SU_V(3)$. The conjugate field \bar{D} transforms as a triplet. The transformation of D and \bar{D} under the chiral symmetry $SU_L(3) \times SU_R(3)$ can be assigned to follow

$$D \xrightarrow{G} D K^\dagger, \quad \bar{D} \xrightarrow{G} K \bar{D}. \quad (2.37)$$

According to the previous discussion, under the unbroken $SU_V(3)$ transformation, K reduces to g_V .

Since K depends on x (2.32), it is necessary to introduce a covariant derivative acting on the matter field, $\mathcal{D}_\mu D$, which transforms in the same way as D under the chiral transformation. One can construct the covariant derivative

$$\begin{aligned} \mathcal{D}_\mu D &= \partial_\mu D - D \Gamma_\mu, & \mathcal{D}_\mu \bar{D} &= \partial_\mu \bar{D} + \Gamma_\mu \bar{D}, \\ \text{where} \quad \Gamma_\mu &= \frac{1}{2}[u^\dagger(\partial_\mu u) + u(\partial_\mu u^\dagger)]. \end{aligned} \quad (2.38)$$

Here Γ_μ is recognized as the chiral connection constructed such that $\mathcal{D}_\mu D$ and D have identical transformation properties

$$\mathcal{D}_\mu D \xrightarrow{G} \mathcal{D}_\mu D K^\dagger, \quad \mathcal{D}_\mu \bar{D} \xrightarrow{G} K \mathcal{D}_\mu \bar{D}, \quad (2.39)$$

$$\text{with} \quad \Gamma_\mu \xrightarrow{G} K \Gamma_\mu K^\dagger + K \partial_\mu K^\dagger. \quad (2.40)$$

This formalism is not the only way to implement the symmetry property of a matter field in a chiral Lagrangian. But one merit of this non-linear realization is that it provides a simple form of the parity

transformation for the fields (see e.g. Ref. [56]). Under parity transformation \mathcal{P} , charge conjugation \mathcal{C} , the fields transform according to

$$U_\mu(x) \xrightarrow{\mathcal{P}} -U^\mu(x_p), \quad D(x) \xrightarrow{\mathcal{P}} -D(x_p), \quad D_{\mu\nu}(x) \xrightarrow{\mathcal{P}} D^{\mu\nu}(x_p), \quad \chi_\pm(x) \xrightarrow{\mathcal{P}} \pm\chi_\pm(x_p), \quad (2.41)$$

$$U_\mu(x) \xrightarrow{\mathcal{C}} U_\mu^T(x), \quad D(x) \xrightarrow{\mathcal{C}} \bar{D}(x), \quad D_{\mu\nu}(x) \xrightarrow{\mathcal{C}} -\bar{D}_{\mu\nu}(x), \quad \chi_\pm(x) \xrightarrow{\mathcal{C}} \chi_\pm^T(x), \quad (2.42)$$

where x_p satisfies $x_p^\mu = x_\mu$. It is worth to mention the transformation rule under time reversal \mathcal{T} for light mesons

$$U_\mu(x) \xrightarrow{\mathcal{T}} -U^\mu(-x_p), \quad \chi_\pm(x) \xrightarrow{\mathcal{T}} \chi_\pm(-x_p). \quad (2.43)$$

The time reversal operation will be useful in constructing the heavy-quark reduced formalism of the open-charm Lagrangian, see the next section.

The chiral power counting for a D or D^* is

$$\mathcal{D}_\mu D \sim M_D \sim Q^0, \quad (\mathcal{D}^2 - M_D^2)D \sim Q, \quad (2.44)$$

which is adopted in this thesis. In the effective theory including massive matter fields, the mass of the massive fields serves as an additional scale and may spoil the power counting. In Ref. [73], Gasser et al. calculated the loop corrections for massive matter fields to the next leading order, and found that a naive loop correction will modify the results at lower chiral orders and a power counting scheme cannot be established straight forwardly. A possible approach to solve this problem is to use a heavy-hadron reduction on the massive fields. The massive fields H are treated as infinitely massive, and corrections enter the theory according to powers of $1/M_H$. This approach is adequate to deal with the open-charm mesons. Such kind of mesons possess a remarkable kind of additional symmetries coming from the heavy quark consisted. We will briefly introduce this so-called heavy quark symmetry in the next section. Afterwards we will illustrate how to perform the heavy-meson reduction on a chiral Lagrangian involving an open-charm meson.

2.2 Heavy-Quark Reduction

2.2.1 Symmetries in heavy-light mesons

In QCD, it is a good approximation to take the chiral limit $m_q \rightarrow 0$ when dealing with light quarks u, d, s . In the case of c, b quarks, which have masses of $M_c \approx 1.27 \text{ GeV}$, $M_b \approx 4.18 \text{ GeV}$ [57], the heavy quark limit, when the heavy quark mass $M_Q \rightarrow \infty$, is a good approximation instead [17]. The heavy quark limit is useful to study meson systems including one single heavy quark c or b , which are referred to as open heavy-flavor mesons or heavy-light mesons. In a heavy-light meson, the heavy quark remains static while light degrees of freedom move around it when $M_Q \rightarrow \infty$. This scheme is comparable to an atomic system. In such a system, the nucleus remains static, and neither its mass nor spin orientation is significantly relevant to the dynamics of the system. In a heavy-light meson system, there are similar phenomena from heavy-quark flavour symmetry and heavy-quark spin symmetry. Heavy-quark flavour symmetry states, for a heavy-light meson, that the dynamics of the system remain unchanged when exchanging the heavy quark flavor. Heavy-quark spin symmetry states that the dynamics of a heavy-light meson system are irrelevant to the spin orientation of the heavy quark. Hence the total angular momentum of the light degrees of freedom, which can be expressed as

$$j_l \equiv J - S_Q, \quad (2.45)$$

can be applied to label an open heavy-flavor system in the heavy quark limit. The heavy-quark symmetry breaking effects in QCD caused by the finiteness of heavy quark masses M_Q can be implemented by heavy quark effective theory (HQET). As an effective theory, HQET provides an expansion of QCD in powers of $1/M_Q$ [74–78].

Inside a hadron state, the momentum of the heavy quark is dominated by the on-shell part, while the off-shell part is a soft quantity. The momentum of the heavy quark can be decomposed into

$$p_Q^\mu = M_Q v^\mu + k^\mu, \quad (2.46)$$

where the four-velocity v^μ satisfies $v^2 = 1$. The soft part k^μ is of the Λ_{QCD} scale. The heavy quark field $Q(x)$ can be parameterized into

$$Q(x) = e^{-iM_Q v \cdot x} Q_v^{(+)}(x) + e^{iM_Q v \cdot x} Q_v^{(-)}(x), \quad (2.47)$$

where $Q_v^{(+)}$ and $Q_v^{(-)}$ vary smoothly in space-time. The field operator $Q_v^{(+)}$ annihilates a heavy quark and $Q_v^{(-)}$ creates a heavy antiquark. The QCD Lagrangian in the single heavy-quark sector

$$\mathcal{L}_Q = \bar{Q}(x)(i\not{\partial} - M_Q)Q(x), \quad (2.48)$$

can be written in terms of the smooth fields $Q_v^{(+)}$ and $Q_v^{(-)}$

$$\begin{aligned} \mathcal{L}_v = & \bar{Q}_v^{(+)}[i\not{\partial} - M_Q(1 - \not{v})]Q_v^{(+)} + e^{-2iM_Q v \cdot x} \bar{Q}_v^{(-)}[i\not{\partial} - M_Q(1 - \not{v})]Q_v^{(+)} \\ & + \bar{Q}_v^{(-)}[i\not{\partial} - M_Q(1 + \not{v})]Q_v^{(-)} + e^{2iM_Q v \cdot x} \bar{Q}_v^{(+)}[i\not{\partial} - M_Q(1 + \not{v})]Q_v^{(-)}. \end{aligned} \quad (2.49)$$

The Lagrangian possesses two highly oscillating terms corresponding to heavy quark-antiquark interactions

$$\mathcal{L}_{+-} = e^{-2iM_Q v \cdot x} \bar{Q}_v^{(-)}[i\not{\partial} - M_Q(1 - \not{v})]Q_v^{(+)} + e^{2iM_Q v \cdot x} \bar{Q}_v^{(+)}[i\not{\partial} - M_Q(1 + \not{v})]Q_v^{(-)}. \quad (2.50)$$

It can be proven that these terms vanish up to any given order of $1/M_Q$. Here we use a trick inspired by Ref. [79]. As an example, let us focus on the first term in the Eq.(2.50). Its contribution to the action is

$$\int d^4x e^{-2iM_Q v \cdot x} \bar{Q}_v^{(-)}(x)[i\not{\partial} - M_Q(1 - \not{v})]Q_v^{(+)}(x). \quad (2.51)$$

We notice the identity

$$e^{-2iM_Q v \cdot x} = -\frac{v \cdot \partial}{2iM_Q} e^{-2iM_Q v \cdot x}, \quad (2.52)$$

and find out that the term (2.51) is equivalent to

$$\begin{aligned} & \int d^4x \frac{v^\mu}{-2iM_Q} (\partial_\mu e^{-2iM_Q v \cdot x}) \bar{Q}_v^{(-)}(x)[i\not{\partial} - M_Q(1 - \not{v})]Q_v^{(+)}(x) \\ & = \frac{1}{2iM_Q} \int d^4x e^{-2iM_Q v \cdot x} v \cdot \partial [\bar{Q}_v^{(-)}(x)[i\not{\partial} - M_Q(1 - \not{v})]Q_v^{(+)}(x)] \\ & \quad + \text{surface term.} \end{aligned} \quad (2.53)$$

In the second step, we have applied the integration by parts. The surface term is evaluated at infinity. It has no physical implication since all interactions are turned off at infinity. We can iterate the same process on the right hand side of Eq.(2.53) and obtain an expression with any finite order of $i\partial/M_Q$

exerting on the interaction $\bar{Q}_v^{(-)}[i\cancel{\not{D}} - M_Q(1 - \psi)]Q_v^{(+)}$. As far as k is soft, this term can be removed from the Lagrangian. Here k refers to the momentum involved in the interaction. The same argument can be applied on the second term of (2.50). As a result, heavy quarks and anti-quarks move independently according to

$$\mathcal{L}_v = \bar{Q}_v^{(+)}[i\cancel{\not{D}} - M_Q(1 - \psi)]Q_v^{(+)} + \bar{Q}_v^{(-)}[i\cancel{\not{D}} - M_Q(1 + \psi)]Q_v^{(-)}. \quad (2.54)$$

There are no heavy-quark pair productions or annihilations.

Now we restrict our discussion to the quark sector of the Lagrangian (2.54),

$$\mathcal{L}_+ = \bar{Q}_v^{(+)}[i\cancel{\not{D}} - M_Q(1 - \psi)]Q_v^{(+)}. \quad (2.55)$$

The smoothly varying quark field $Q_v^{(+)}$ can be decomposed into

$$Q_v^{(+)} = Q_{+v}^{(+)}(x) + Q_{-v}^{(+)}(x), \quad (2.56)$$

$$\text{where } Q_{+v}^{(+)} \equiv P_+ Q_v^{(+)}, \quad Q_{-v}^{(+)} \equiv P_- Q_v^{(+)}. \quad (2.57)$$

Projection operators P_{\pm} are defined by

$$P_{\pm} \equiv \frac{1 \pm \psi}{2}, \quad \text{so that } P_{\pm}^2 = P_{\pm}, \quad P_{\pm} P_{\mp} = 0, \quad P_+ + P_- = 1. \quad (2.58)$$

The operators $Q_{+v}^{(+)}$ and $Q_{-v}^{(+)}$ are recognized as the large and small components respectively. In the rest frame, where $v^\mu = (1, 0, 0, 0)$, the large component corresponds to the upper two components of the Dirac spinor while the small component corresponds to the lower ones. The small component can be eliminated by using its equation of motion. This method is equivalent to integrate the small component out in the path integral [80–82]. As a result, one receives a non-local effective Lagrangian for the $Q_{+v}^{(+)}$ field [80]

$$\mathcal{L}_{\text{HQET}}^+ = \bar{Q}_{+v} i v \cdot \cancel{\not{D}} Q_{+v} + \bar{Q}_{+v} i \cancel{\not{D}}_{\perp} (i v \cdot \cancel{\not{D}} + 2M_Q)^{-1} i \cancel{\not{D}}_{\perp} Q_{+v}, \quad (2.59)$$

in which $\cancel{\not{D}}_{\perp}^{\mu} \equiv \cancel{\not{D}}^{\mu} - v^{\mu} v \cdot \cancel{\not{D}}$ is the component orthogonal to the hadron's velocity ($v \cdot \cancel{\not{D}}_{\perp} = 0$). Here we have suppressed the upper index (+). The first term of (2.59) is the Lagrangian in the heavy quark limit. Higher $1/M_Q$ order corrections are provided by the second term of (2.59). The expansion of this term in powers of $i\cancel{\not{D}}/M_Q$ leads to a localized effective Lagrangian. It is easy to see that the leading order Lagrangian respects the heavy-quark flavor and spin symmetry.

A similar discussion can be applied to the anti-quark sector of the Lagrangian (2.54). If we use a decomposition for the anti-quark field $Q_v^{(-)}$

$$Q_v^{(-)} = Q_{+v}^{(-)}(x) + Q_{-v}^{(-)}(x), \quad \text{where, } Q_{+v}^{(-)} \equiv P_+ Q_v^{(-)}; \quad Q_{-v}^{(-)} \equiv P_- Q_v^{(-)}. \quad (2.60)$$

after integrating out the small component $Q_{-v}^{(-)}$, we can get the effective Lagrangian describing the heavy anti-quark field $Q_{+v}^{(-)}$.

We can determine the spin transformation formalism for Q_{+v} . It can be derived from the Lorentz transformation Λ for the full quark field

$$Q(x) \xrightarrow{\Lambda} \exp\left(-\frac{i}{2} \omega_{\mu\nu} \sigma^{\mu\nu}\right) Q(\Lambda^{-1}x), \quad \sigma^{\mu\nu} = \frac{i}{2} [\gamma^{\mu}, \gamma^{\nu}]. \quad (2.61)$$

where Λ is characterized by the antisymmetric tensor $\omega_{\mu\nu}$. A spin rotation R is defined as a Lorentz transformation keeping v^μ intact, $R^\mu{}_{\nu} v^\nu = v^\mu$. Therefore it is a 3-dimensional rotation in the rest frame of the heavy quark moving with the momentum $p = M_Q v$. Without losing generality, we specify a reference frame where $v^\mu = (1, 0, 0, 0)$. Under this condition, the characteristic tensor $\omega_{\mu\nu}$ for a

spin rotation R only has space-like components and can be represented by the rotation angle θ_i , $\omega_{jk} = -\frac{1}{2}\epsilon_{ijk}\theta_i$. So the spinor field is transformed under the spin rotation as

$$Q(x) \xrightarrow{R} \exp(i\boldsymbol{\theta} \cdot \mathbf{S})Q(R^{-1}x), \quad S_i = \frac{1}{4}\epsilon_{ijk}\sigma_{jk}. \quad (2.62)$$

The generator \mathbf{S} can be re-expressed in a 4-dimensional formalism $S_i = \frac{1}{4}\epsilon_{0i\mu\nu}\sigma^{\mu\nu}$, assigning $\epsilon_{0ijk} = \epsilon_{ijk}$. Since $\epsilon_{\mu\nu\rho\sigma}\sigma^{\rho\sigma}$ equals to $-\frac{i}{2}\gamma_5\sigma_{\mu\nu}$, S_i can be expressed as $S_i = -\frac{i}{2}\gamma_5\sigma_{0i}$, which is equivalent to

$$S_i = \frac{1}{2}\gamma_5\gamma_0\gamma_i. \quad (2.63)$$

We can generalize the expression into a covariant formalism in terms of v^μ and three orthonormal basis e_i^μ perpendicular to v^μ , $v \cdot e_i = 0$, $e_i \cdot e_j = -\delta_{ij}$,

$$S_i = \frac{1}{2}\gamma_5\psi\phi_i. \quad (2.64)$$

It satisfies the commutation relations

$$[S_i, S_j]_- = i\epsilon_{ijk}S_j, \quad [\psi, S_i]_- = 0. \quad (2.65)$$

From (2.62), one can observe that the heavy-quark reduced field Q_{+v} under spin rotation transforms as

$$e^{-iM_Q v \cdot x} Q_{+v}(x) \xrightarrow{R} e^{-iM_Q v \cdot x} \exp(i\boldsymbol{\theta} \cdot \mathbf{S}) Q_{+v}(R^{-1}x), \quad (2.66)$$

where $R(\boldsymbol{\theta}) \cdot v = v$. This transformation superficially change the space-time index from x to $R^{-1}x$. But actually the effect of this change is suppressed by $1/M_Q$. Using the plane-wave expansion, the space-time rotation effect of $Q_{+v}(R_h^{-1}x)$ can be implemented by a phase factor

$$Q_{+v}(R^{-1}x) = \exp\left(\frac{R-1}{M_Q}x \cdot i\partial\right)Q_{+v}(x). \quad (2.67)$$

To this end, the rotation $R^{-1}x$ amounts to a redefinition of 4-velocity, $e^{-iM_Q v \cdot x} Q_{+v}(R^{-1}x) = e^{-iM_Q v' \cdot x} Q_{+v}(x)$, where $v'_\mu = v_\mu + \frac{R-1}{M_Q}i\partial_\mu$ satisfying the 4-velocity condition $v'^2 = 1$. Here the condition $v'^2 = 1$ is fulfilled because of the relation $R(\boldsymbol{\theta})v = v$. So the leading order result is irrelevant to the choice of the 4-velocity, and the effect of changing the 4-velocity $v \rightarrow v'$ contributes to $O(1/M_Q)$ (see [83]). Therefore in the heavy quark limit, the heavy quark field Q_{+v} transforms under the heavy-quark rotation as

$$Q_{+v}(x) \xrightarrow{R} \exp(i\boldsymbol{\theta} \cdot \mathbf{S})Q_{+v}(x), \quad (2.68)$$

$$S_i = \frac{1}{2}\gamma_5\psi\phi_i. \quad (2.69)$$

With the help of the heavy quark formalism, we can discuss heavy-light mesons. The pseudoscalar and vector states are denoted by $|P\rangle$ and $|P^*(\epsilon)\rangle$ respectively. They are normalized via the relativistic convention

$$\langle P(p)|P(p')\rangle = 2E_p(2\pi)^3\delta^3(\mathbf{p}-\mathbf{p}'), \quad \langle P^*(p)|P^*(p')\rangle = 2E_p(2\pi)^3\delta^3(\mathbf{p}-\mathbf{p}'). \quad (2.70)$$

The corresponding field annihilation operators $P_+(x)$ and $P_+^\mu(x)$ can be normalized as [84]

$$\langle 0|P_+(0)|P(p)\rangle = \sqrt{M_0}, \quad \langle 0|P_+^\mu(0)|P^*(p, \epsilon)\rangle = \epsilon^\mu \sqrt{M_0}, \quad (2.71)$$

We denote the characteristic heavy meson mass as M_0 , which can be recognized as the spin average of the degenerate heavy mesons respecting the heavy-quark spin symmetry. So operators $P(x)$ and $P^*(x)$ have the dimension $\frac{3}{2}$, and differs by a factor $\sqrt{M_0}$ from the conventional normalization of boson fields. We adopt the convention (2.71) throughout this section since it makes the heavy-meson fields to be of the same dimension as the heavy-quark fields and simplifies our discussion. Under the Lorentz transformation Λ and parity transformation \mathcal{P} , the field operators (2.71) transform like

$$P_+(x) \xrightarrow{\Lambda} P_+(x'), \quad P_+(x) \xrightarrow{\mathcal{P}} -P_+(x_P), \quad (2.72)$$

$$P_+^\mu(x) \xrightarrow{\Lambda} \Lambda^\mu{}_\nu P_+^\nu(x'), \quad P_+^\mu(x) \xrightarrow{\mathcal{P}} P_{+P}^\mu(x_P), \quad (2.73)$$

where $x'^\mu = (\Lambda^{-1})^\mu{}_\nu x^\nu$, $x_P^\mu = x_\mu$. Here P_{+P}^μ satisfies $P_{+P}^\mu = P_{+\mu}$. In the heavy quark limit, the heavy pseudoscalar and vector mesons are degenerate and can be labeled by $j_l^P = \frac{1}{2}^-$ from Eq.(2.45). As mentioned before, such a meson can be considered as the composite of the heavy quark and light degrees of freedom. The heavy quark is annihilated by the field $Q_{+v}(x)$. In the heavy quark limit, it moves in the same velocity of the meson. So Q_v satisfies the projection relation $\psi Q_{+v} = Q_{+v}$. Here v is the 4-velocity of the meson, satisfying $v^2 = 1$. In a $j_l^P = \frac{1}{2}^-$ state, the light degrees of freedom as a whole transform as an anti-fermion spinor [85]. It can be effectively annihilated by an anti-fermion operator $\bar{q}(x)$. So the $j_l^P = \frac{1}{2}^-$ states have non-zero overlaps with the interpolating field $Q_{+v}(x)\bar{q}(x)$,

$$\langle 0|Q_{+v}(0)\bar{q}(0)|P\rangle = M_0^2 \Gamma_\nu^P, \quad \langle 0|Q_{+v}(0)\bar{q}(0)|P^*(\epsilon)\rangle = M_0^2 \Gamma_\nu^{P^*}(\epsilon), \quad (2.74)$$

where Γ_ν^P and $\Gamma_\nu^{P^*}$ are certain Dirac structures. The parameter M_0^2 is attributed to the normalization. Up to the normalization factor, the interpolating field $Q_{+v}(x)\bar{q}(x)$ serves as an operator annihilating either a pseudoscalar or a vector open-charm meson state, which is equivalent to a meson field operator

$$\langle 0|H_\nu(0)|P\rangle = \sqrt{M_0} \Gamma_\nu^P, \quad \langle 0|H_\nu(0)|P^*(\epsilon)\rangle = \sqrt{M_0} \Gamma_\nu^{P^*}(\epsilon). \quad (2.75)$$

The field $H_\nu(x)$ transforms in the same way as $Q_{+v}(x)\bar{q}(x)$, which transforms as a Dirac bispinor. The spinor field ψ transforms under the Lorentz and parity transformation according to

$$\psi \xrightarrow{\Lambda} \exp\left(-\frac{i}{2}\omega_{\mu\nu}\sigma^{\mu\nu}\right)\psi, \quad \psi \xrightarrow{P} \gamma_0\psi. \quad (2.76)$$

To this end, the corresponding transformation laws for the field $H_\nu(x)$ are expressed as

$$H_\nu(x) \xrightarrow{\Lambda} e^{-\frac{i}{2}\omega_{\mu\nu}\sigma^{\mu\nu}} H_{\nu'}(x') e^{\frac{i}{2}\omega_{\mu\nu}\sigma^{\mu\nu}}, \quad H_\nu(x) \xrightarrow{P} \gamma_0 H_{\nu_P}(x_P) \gamma_0, \quad (2.77)$$

where $a'^\mu = (\Lambda^{-1})^\mu{}_\nu a^\nu$, $a_P^\mu = a_\mu$, for $a = \nu$ or x . The projection relation $\psi Q_{+v} = Q_{+v}$ ensures that H_ν satisfies

$$\psi H_\nu = H_\nu. \quad (2.78)$$

Moreover, we can perform a spin rotation R on the heavy-quark component Q_v of the bispinor interpolating field $Q_v(x)\bar{q}(x)$. For a light quark-antiquark interpolating field, this kind of transformation will change the field to be non-local. But as illustrated before, the rotational effect of the space-time index of the heavy quark field is suppressed by $1/M_0$. So in the heavy quark limit, this transformation preserves the locality of the interpolating field up to some higher-order corrections $O(1/M_0)$. With respect to Eq.(2.68), the field $Q_v(x)\bar{q}(x)$ transforms under the heavy-quark spin rotation according to

$$Q_{+v}(x)\bar{q}(x) \xrightarrow{R} \exp(i\boldsymbol{\theta} \cdot \mathbf{S}) Q_{+v}(x)\bar{q}(x). \quad (2.79)$$

Accordingly, the meson H_ν transforms under the heavy-quark rotation R as

$$H_\nu(x) \xrightarrow{R} \exp(i\boldsymbol{\theta} \cdot \mathbf{S})H_\nu(x). \quad (2.80)$$

The open heavy-flavor interactions preserve the heavy-quark spin symmetry in heavy quark limit, so the corresponding Lagrangian is invariant under the transformation (2.80).

Comparing Eq.(2.71) with (2.75), we can identify the field operator H_ν with $P_+(x)$ and $P_+^\mu(x)$ by

$$H_\nu(x) = \Gamma_\nu^P P_\nu(x) + \Gamma_{\nu,\mu}^{P^*} P_\nu^\mu(x), \quad \Gamma_{\nu,\mu}^{P^*} \epsilon^\mu \equiv \Gamma_\nu^{P^*}(\epsilon); \quad (2.81)$$

$$\text{where,} \quad P_\nu \equiv e^{iM_H \nu \cdot x} P_+, \quad P_\nu^\mu \equiv e^{iM_H \nu \cdot x} P_+^\mu, \quad (2.82)$$

The M_H is the mass of the field H . The extraction of the phase factor $\exp[iM_H \nu \cdot x]$ is equivalent to extracting $\exp[iM_Q \nu \cdot x]$ in defining Q_ν . The difference between these two factors, $\exp[i(M_H - M_Q)\nu \cdot x]$, does not affect the result to the heavy quark limit [86]. The transformation laws of P and P^* (2.72) and (2.73) ensure the relation

$$e^{-\frac{i}{2}\omega_{\mu\nu}\sigma^{\mu\nu}} \Gamma_\nu^P e^{\frac{i}{2}\omega_{\mu\nu}\sigma^{\mu\nu}} = \Gamma_\nu^P, \quad \gamma_0 \Gamma_{\nu p}^P \gamma_0 = -\Gamma_\nu^P, \quad (2.83)$$

$$e^{-\frac{i}{2}\omega_{\mu\nu}\sigma^{\mu\nu}} \Gamma_{\nu'}^{P^*,\mu} e^{\frac{i}{2}\omega_{\mu\nu}\sigma^{\mu\nu}} = \Lambda_{\nu'}^\mu \Gamma_\nu^{P^*,\nu}, \quad \gamma_0 \Gamma_{\nu p}^{P^*,\mu} \gamma_0 = \Gamma_{\nu,\mu}^{P^*}. \quad (2.84)$$

Because of the heavy-quark spin symmetry, the heavy-light pseudoscalar meson P and vector meson P^* are degenerate. A spin rotation acting on the heavy quark can lead to an interchange between the two kinds of state. If the states are at rest, the demanded rotation is performed along the direction of the polarization vector of P^* by the rotation angle π [55]

$$|P^*(\epsilon)\rangle \xrightarrow{R(\boldsymbol{\theta}=\pi\boldsymbol{\epsilon})} |P\rangle. \quad (2.85)$$

This relation is fixed up to a phase factor and we set it to be 1. From Eq.(2.75), one can obtain the relation between the wave functions of P and P^* defined in (2.80), $\langle 0|H_\nu(0)|P^*(\epsilon)\rangle = \langle 0|\exp(-i\pi\boldsymbol{\epsilon} \cdot \mathbf{S})H_\nu(0)|P\rangle$. This equation entails a relation between the matrices Γ_ν^P and $\Gamma_\nu^{P^*}$

$$\Gamma_\nu^{P^*}(\epsilon) = -2i\boldsymbol{\epsilon} \cdot \mathbf{S} \Gamma_\nu^P. \quad (2.86)$$

Here we have used the identity $\exp(-i\pi\boldsymbol{\epsilon} \cdot \mathbf{S}) = -2i\boldsymbol{\epsilon} \cdot \mathbf{S}$.

Now we arrive at the point to determine the bispinor matrices Γ_ν^H . They need to satisfy the projection relation (2.78), the transformation property (2.83, 2.84) and the interchange relation (2.86)). It is sufficient to construct Γ_ν^H by

$$\Gamma_\nu^P = i \frac{1 + \boldsymbol{\psi}}{2} \gamma_5, \quad \Gamma_\nu^{P^*}(\epsilon) = \frac{1 + \boldsymbol{\psi}}{2} \boldsymbol{\epsilon}(\epsilon), \quad (2.87)$$

which meet the requirements above. Therefore H_ν is determined by [19],

$$H_\nu = \frac{1 + \boldsymbol{\psi}}{2} (\boldsymbol{\psi}_\nu + iP_\nu \gamma_5), \quad \text{where,} \quad P_\nu \equiv e^{iM_H \nu \cdot x} P_+, \quad P_\nu^\mu \equiv e^{iM_H \nu \cdot x} P_+^\mu, \quad (2.88)$$

which satisfies

$$\boldsymbol{\psi} H_\nu = H_\nu. \quad (2.89)$$

Under Lorentz and parity transformations, H_ν transforms according to Eq.(2.77). And it transforms under the heavy-quark rotation as Eq.(2.80).

In the heavy quark limit, the transverse relation for P_ν^μ reads:

$$\nu \cdot P_\nu = 0. \quad (2.90)$$

Using the equation of motion,

$$\partial^\mu P_{\nu,\mu} - iM_0 \nu^\mu P_{\nu,\mu} = 0, \quad (2.91)$$

it can be proved that corrections to the relation (2.90) contribute to order $1/M_0$. This means that in the heavy quark limit, one can identify an arbitrary ν satisfying $\nu^2 = 1$ with the 4-velocity of the meson. The effect of choosing different 4-velocities arise from the $1/M_0$ order (see [83]). The transverse relation (2.90) entails that in the heavy quark limit H_ν satisfies

$$H_\nu \frac{1 - \not{\nu}}{2} = H_\nu. \quad (2.92)$$

It is worth to emphasize that the field $H_\nu(x)$ only contains the annihilation operator for the heavy-light meson but not the creation operator for the corresponding anti-meson. So one cannot specify a charge conjugation operation for H_ν fields. But the charge-conjugation invariance holds in the non-reduced relativistic field theory. In order to be consistent with the corresponding relativistic theory, the heavy-quark reduced theory should be invariant under time reversal. Therefore the time-reversal invariance is of special importance in constructing the heavy-quark reduced Lagrangian. Under time reversal \mathcal{T} , H_ν transforms according to [87]

$$H_\nu(x) \xrightarrow{\mathcal{T}} T H_{\nu_p}(-x_p) T^{-1}, \quad (2.93)$$

where T is a Dirac matrix satisfying $T = T^{-1} = -T^*$ and can be represented as [88]

$$T = i\gamma_1\gamma_3. \quad (2.94)$$

Later on we will show how to construct the heavy-quark reduced open-charm Lagrangian. The time-reversal operation will give important constraints on the Lagrangian.

2.2.2 Heavy Meson Reduction

In order to study a hadron system involving massive mesons such as the open-charm mesons, we can perform the heavy-meson reduction on the chiral Lagrangian where the heavy meson fields are arranged in powers of the inverse of their masses. For a review, readers may consult Refs. [84, 56]. We will illustrate the reduction of the kinetic terms for the open-charm pseudoscalar and vector meson anti-triplets D and D^* [21, 70]

$$\mathcal{L}_0 = \mathcal{D}_{\mu ab} D_a \mathcal{D}_{bc}^\mu \bar{D}_c - D_a (\hat{M}_D^2)_{ab} \bar{D}_b - \mathcal{D}_{ab}^\mu D_{\mu\rho a} \mathcal{D}_{\nu bc} \bar{D}_c^{\nu\rho} + \frac{1}{2} D_a^{\mu\nu} (\hat{M}_{D^*}^2)_{ab} \bar{D}_{\mu\nu b}, \quad (2.95)$$

where flavor indices are explicitly labeled by a, b, c , and summations over the repeated labels are implicitly implemented. The fields $D, D^{\mu\nu}$ can annihilate an open-charm meson state or create an open-charm anti-meson state. Here the tensor representation has been adopted for D^* . The D - and D^* -meson mass matrices are denoted by \hat{M}_D and \hat{M}_{D^*} respectively. The mass splitting between different elements within one matrix are caused by the SU(3) flavor symmetry breaking effect, which is of the scale $M_{D_s} - M_D \sim 100\text{MeV}$ as well as $M_{D_s^*} - M_{D^*} \sim 100\text{MeV}$. The SU(3) flavor symmetry breaking effect can be implemented by including higher chiral order corrections into the calculation. We will come back to this topic in the next section. Here we restrict our discussion on the leading chiral order by respecting

the strict SU(3) symmetry. And the mass matrices \hat{M}_D and \hat{M}_{D^*} can be substituted by diagonal matrices $\hat{M}_D \text{diag}(1, 1, 1)$ and $\hat{M}_{D^*} \text{diag}(1, 1, 1)$. The mass shift between the \hat{M}_D and \hat{M}_{D^*} is caused by the breaking of heavy-quark spin symmetry, which is characterized by the mass gap $M_{D^*} - M_D \sim 100\text{MeV}$. This quantity is much smaller than the characteristic D and D^* mass $M_0 \sim 2\text{GeV}$. This effect is mainly attributed to the $1/M_0$ corrections. In the heavy quark limit, the mass \hat{M}_D is identical with \hat{M}_{D^*} , and coincide with the characteristic mass M_0 . We can decompose such a meson field into a meson annihilation field P_+ and an anti-meson creation field P_- ,

$$\sqrt{M_0} D = P_+ + P_-, \quad (2.96)$$

where the scale M_0 appears because of the normalization (2.71). Similar to the heavy-quark Lagrangian we have discussed before, the meson and anti-meson fields decouple. We only concentrate on the heavy-meson part. As discussed in the last section, the D meson annihilation field can be factorized by

$$P_+ = \exp[-iM_0 v \cdot x] P_v, \quad (2.97)$$

and the vector representation of D^* is factorized in the same way, $P_+^\mu = \exp[-iM_0 v \cdot x] P_v^\mu$. From Appendix B, the corresponding factorization formalism for the tensor representation of D^* reads [29]

$$P_+^{\mu\nu} = i \exp[-iM_0 v \cdot x] \left[v^\mu P_v^\nu - v^\nu P_v^\mu + \frac{i}{M_0} (\partial^\mu P_v^\nu - \partial^\nu P_v^\mu) \right], \quad (2.98)$$

with a 4-velocity normalized as $v^2 = 1$. Substituting the relations above, we can reduce the Lagrangian (2.95) to the zeroth order

$$\mathcal{L}_{0,kin} = -2P_{va} v \cdot i \mathcal{D}_{ab} \bar{P}_{vb} + 2P_{va}^\mu v \cdot i \mathcal{D}_{ab} \bar{P}_{vb,\mu}. \quad (2.99)$$

We have invoked the transverse condition $v_\mu P^\mu = 0$. The Lagrangian can be further forged in terms of the H_v by definition $H_v = \frac{1+\not{v}}{2} (iP_v \gamma_5 + \not{P}_v)$ as

$$\mathcal{L}_{0,kin} = i \text{tr}_D (H_{va} v_\mu \mathcal{D}_{ab}^\mu \bar{H}_{vb}), \quad (2.100)$$

where tr_D denotes a trace performed on the Dirac indices. This is the heavy-quark reduced form of the kinetic term of the open-charm $j^P = \frac{1}{2}^-$ mesons. This term is invariant under the heavy-quark spin rotation $H_v \xrightarrow{R} e^{i\theta \cdot S} H_v$. So the kinematic term respects the heavy-quark spin symmetry. We notice the normalization condition (2.71) or (2.75) makes $\mathcal{L}_{0,kin}$ to scale with the heavy meson mass $\sim M_0$. This is the typical scaling behavior of the heavy-meson Lagrangian in the limit $M_0 \rightarrow \infty$. This behavior follows from the full covariant kinetic form (2.95), where every derivative acting on a D or $D_{\mu\nu}$ field raises a factor of M_0 :

$$\partial D \sim M_0 [D + O(1/M_0) \text{ terms}]. \quad (2.101)$$

The heavy-quark spin symmetry breaking terms appear as corrections to the next leading $1/M_0$ order. This interaction implicitly involves Goldstone boson fields from the covariant derivative (2.38).

The heavy quark symmetry provides additional correlation between the 0^- and 1^- heavy-light mesons. To this end, the coupling constants of the chiral Lagrangian are correlated. We will illustrate such constraints in the next section.

2.3 Heavy-quark constraints on the chiral Lagrangian involving open-charm mesons

In this section we construct an effective Lagrangian involving open-charm mesons, with an arrangement of the effective interactions according to the chiral power counting scheme. Special attention is paid on how heavy-quark symmetry implies constraints on the involved coupling constants, which are referred to as low-energy constants (LECs).

2.3.1 Leading order chiral Lagrangian

In Sec.2.2.2, we provided the kinetic parts of the D and D^* Lagrangian as (2.95). We have seen that in the heavy-quark limit, $\hat{M}_D = \hat{M}_{D^*}$, the kinetic part of the Lagrangian can be reduced into a compact form (2.99). In this reduced form, the derivative acts on the soft field H_ν , and can be counted as the same scale as the chiral scale Q . The covariant formalism for D and D^* kinetic terms are implicitly involved in Eq.(2.95), which is counted as as order Q . Goldstone fields are implicitly incorporated in the covariant derivative \mathcal{D}^μ via the chiral connection Γ^μ , see Eqs. (2.38,2.40). Noticing the fact that $u^\dagger u = 1$, one can rewrite Γ^μ by $\Gamma^\mu = \frac{1}{2}[u, \partial^\mu u^\dagger]$. The D -meson part in Eq. (2.95) can be expanded with respect to the Goldstone fields as,

$$\mathcal{L}_D = \partial_\mu D \partial^\mu \bar{D} - D \hat{M}_D^2 \bar{D} + \frac{1}{8f^2} \{ \partial^\mu D [\Phi, \partial_\mu \Phi]_- \bar{D} - D [\Phi, \partial_\mu \Phi]_- \partial^\mu \bar{D} \}. \quad (2.102)$$

We assigned the D -meson mass matrix \hat{M}_D as $\hat{M}_D \text{diag}(1, 1, 1)$, which holds in the chiral limit. Here all terms involving higher number of Goldstone fields have been omitted. The last contact interaction term is referred to as the Weinberg-Tomozawa interaction. In the same manner, we can give the Lagrangian involving kinetic and Weinberg-Tomozawa terms for D^* mesons,

$$\mathcal{L}_{D^*} = -\partial_\mu D^{\mu\alpha} \partial^\nu \bar{D}_{\nu\alpha} + \frac{1}{2} D^{\mu\nu} \hat{M}_{D^*}^2 \bar{D}_{\mu\nu} - \frac{1}{8f^2} \{ \partial_\mu D^{\mu\alpha} [\Phi, \partial^\nu \Phi]_- \bar{D}_{\nu\alpha} - D^{\mu\alpha} [\Phi, \partial_\mu \Phi]_- \partial^\nu \bar{D}_{\nu\alpha} \}, \quad (2.103)$$

where the D^* -meson mass matrix \hat{M}_{D^*} is assigned to be the chiral limit $\hat{M}_{D^*} \text{diag}(1, 1, 1)$. The Eqs.(2.102) and (2.103) are part of the order Q chiral Lagrangian for the open-charm mesons. The mass term gives the leading order contribution ($O(Q^0)$) of the charmed-meson masses. The Weinberg-Tomozawa term provides the $O(Q)$ heavy-light meson 4-point interaction.

Besides the Weinberg-Tomosawa terms, there are 3-point interactions shown up at chiral order Q . For 3-point interactions involving Goldstone and heavy mesons, the leading order term is

$$\begin{aligned} \mathcal{L}_3^{(1)} = & 2g_p [D_{\mu\nu} U^\mu \partial^\nu \bar{D} - \partial^\nu D U^\mu \bar{D}_{\mu\nu}] - \frac{i}{2} \tilde{g}_p \epsilon^{\mu\nu\alpha\beta} [D_{\mu\nu} U_\alpha \partial^\tau \bar{D}_{\tau\beta} + \partial^\tau D_{\tau\beta} U_\alpha \bar{D}_{\mu\nu}] \\ & - i \frac{1}{2} g_3 \epsilon^{\mu\nu\alpha\beta} [D_{\mu\nu} U^\tau \partial_\alpha \bar{D}_{\tau\beta} + \partial_\alpha D_{\tau\beta} U^\tau \bar{D}_{\mu\nu}]. \end{aligned} \quad (2.104)$$

Here parameters g_p , \tilde{g}_p , g_3 are both real. The Lagrangian is invariant under parity and charge conjugation (2.41,2.42). The prefactors i before \tilde{g}_p and g_3 are required by hermiticity. There is one more possible interaction, $\epsilon_{\mu\nu\alpha\beta} (D^{\mu\nu} U^\tau \partial_\tau \bar{D}^{\alpha\beta} - \partial_\tau D^{\alpha\beta} U^\tau \bar{D}^{\mu\nu})$. After integrating by parts, it can be proven that the contribution of this term is at least at the next order.

The three parameters g_p , \tilde{g}_p and g_3 are correlated in the heavy quark limit. By means of heavy-quark reduction, we can significantly reduce the number of independent interactions. We follow the way in Sect. 2.2.2 to reduce the full Lagrangian $\mathcal{L}_3^{(1)}$, by using Eqs. (2.97) and (2.98). We have

$$\mathcal{L}_3^{(1)-M_0} = 2g_p (P_\mu U^\mu P^\dagger - P U^\mu P_\mu^\dagger) + 2\tilde{g}_p \epsilon^{\mu\nu\alpha\beta} v_\mu P_\nu U_\alpha P_\beta^\dagger + \dots, \quad (2.105)$$

where terms explicitly including higher orders of $1/M_0$ are omitted. There are no terms corresponding to g_3 in (2.105). This fact implies that the interaction proportional to g_3 contributes at least to the next leading order of $1/M_0$.

The expression (2.105) is comparable with the heavy-quark reduced 3-point Lagrangian to the order Q and $(1/M_0)^0$. We use the multiplet field H_ν (2.88) to construct the requested heavy-quark reduced 3-point Lagrangian. The Lagrangian contains a trace over Dirac indices. To the leading order, the heavy-quark rotation symmetry is respected, which means that the Lagrangian is invariant under the

heavy-quark rotation (2.80). This condition requires \bar{H}_v being always followed by H_v in Dirac space, rejecting any Dirac matrices to exist between \bar{H}_v and H_v . The requested Lagrangian reads [19–21]

$$\mathcal{L}_{3,H}^{(1)} = i G_P \text{tr}_D (H_v U^\mu \gamma_5 \gamma_\mu \bar{H}_v). \quad (2.106)$$

As mentioned before, the constraint of time reversal invariance plays an important role in obtaining the Lagrangian. Actually, the factor i in front of G_P is required by the time reversal invariance. According to the transformation rules for U^μ and H_v (2.43, 2.93), this term transforms under the time reversal as

$$\text{tr}_D (H_v U^\mu \gamma_5 \gamma_\mu \bar{H}_v) \xrightarrow{\mathcal{T}} -\text{tr}_D (H_v U^\mu \gamma_5 \gamma_\mu \bar{H}_v). \quad (2.107)$$

A factor i is necessary since it changes sign under time reversal, such that $i \text{tr}_D (H_v U^\mu \gamma_5 \gamma_\mu \bar{H}_v)$ is invariant under time reversal. Moreover the assignment with the additional factor i is in consistence with the hermiticity². We rewrite $\mathcal{L}_{3,H}^{(1)}$ in terms of open-charm meson fields P and P^μ (2.88), and get

$$\mathcal{L}_{3,H}^{(1)} = -2 G_P (P U^\mu P_\mu^\dagger - P_\mu U^\mu P^\dagger) + 2 G_P \epsilon_{\mu\nu\alpha\beta} v^\nu P^\alpha U^\mu P^{\sigma\dagger}. \quad (2.108)$$

By matching the expressions (2.105) and (2.108), we obtain a relation between g_P , \tilde{g}_P and G_P ,

$$g_P = \tilde{g}_P = G_P. \quad (2.109)$$

Therefore in the heavy quark limit, g_P and \tilde{g}_P are identical while g_3 vanishes. We will see in the next section, the 3-point interaction at $O(Q)$ contributes to chiral order Q^3 self-energy correction of D -mesons. We will suppose the heavy-quark corrections ($\sim 1/M_0$) is of no more importance than the Q^2 chiral correction. It means the self-energy correction from the deviation between g_P and \tilde{g}_P will be numerically compatible with the $O(Q^5)$ chiral correction. Therefore up to $O(Q^4)$, we can suppose the heavy-quark relation [29]

$$g_P = \tilde{g}_P, \quad g_3 = 0. \quad (2.110)$$

At order higher than the leading order, 4-point interaction will appear serving as counter terms. They can be systematically constructed according to the argument of chiral symmetry.

2.3.2 Higher order Lagrangian

As we have seen, the chiral Lagrangian at order Q involves three-point interactions between charmed-mesons and Goldstone bosons. They contribute to $O(Q^3)$ charmed-meson self-energies. In this section we proceed in constructing the counter terms at higher chiral orders that are necessarily involved in the chiral corrections for the self-energies up to $O(Q^4)$. The higher-order counter terms we are considering consist of chiral-symmetry breaking (χ -SB) terms ($\sim \chi_0$) as well as chiral symmetry respecting terms. All of the interactions involve an even number of Goldstone bosons.

At chiral order Q^2 , there are two different kinds of chiral-symmetry breaking (χ -SB) terms for either $[0^-]$ or $[1^-]$ mesons. We collect them as

$$\mathcal{L}_\chi^{(2)} = -(4c_0 - 2c_1) D \bar{D} \text{Tr} \chi_+ - 2c_1 D \chi_+ \bar{D} + (2\tilde{c}_0 - \tilde{c}_1) D^{\mu\nu} \bar{D}_{\mu\nu} \text{Tr} \chi_+ + \tilde{c}_1 D^{\mu\nu} \chi_+ \bar{D}_{\mu\nu}. \quad (2.111)$$

² However this consistence does not always hold for all the possible cases. Some certain kind of interactions may require an additional i to be time-reversal invariant but at the same time violates hermiticity. The consistency requirement makes a selection amongst all possible constructions of the Lagrangian.

Substituting the relation $\chi_+ = \chi_0 - \frac{1}{8f^2} \{\Phi, \{\chi_0, \Phi\}\} + O(\Phi^4)$, we expand these χ -SB NLO terms up to 4-point interactions,

$$\begin{aligned} \mathcal{L}_\chi^{(2)} = & -(4c_0 - 2c_1) D\bar{D}\text{Tr}\chi_0 + \frac{2c_0 - c_1}{f^2} D\bar{D}\text{Tr}(\Phi\chi_0\Phi) - 2c_1 D\chi_0\bar{D} + \frac{c_1}{4f^2} D[\Phi, [\chi_0, \Phi]_+]_+\bar{D} \\ & + (2\tilde{c}_0 - \tilde{c}_1) D^{\mu\nu}\bar{D}_{\mu\nu}\text{Tr}\chi_0 - \frac{2\tilde{c}_0 - \tilde{c}_1}{2f^2} D^{\mu\nu}\bar{D}_{\mu\nu}\text{Tr}(\Phi\chi_0\Phi) + \tilde{c}_1 D^{\mu\nu}\chi_0\bar{D}_{\mu\nu} \\ & - \frac{\tilde{c}_1}{8f^2} D^{\mu\nu}[\Phi, [\chi_0, \Phi]_+]_+\bar{D}_{\mu\nu}. \end{aligned} \quad (2.112)$$

The 2-point terms $D\chi_0\bar{D}$ and $D^{\mu\nu}\chi_0\bar{D}_{\mu\nu}$ give the tree-level χ -SB effect of the D -meson masses, leading to a mass deviation between the strangeness 0 and strangeness 1 D -mesons. One can estimate the value of c_1 and \tilde{c}_1 from the physical mass difference between $D^{(*)}$ and $D_s^{(*)}$. The 2-point terms with once flavor trace ($\sim \text{Tr}\chi_0$) gives an overall chiral correction. This correction is suppressed according to the inverse of N_C (see App.C). The 4-point interactions in (2.112) will generate $O(Q^4)$ loop contributions to the self energy. Detailed calculations will be performed in the next chapter. In the heavy-quark limit, the coefficients c_0 , c_1 and \tilde{c}_0 , \tilde{c}_1 are correlated. We can easily verify the correlation by comparing with the heavy-quark reduced form of the NLO χ -SB term [28]

$$\mathcal{L}_{\chi,H}^{(2)} = \frac{C_0}{\Lambda_\chi} \text{tr}_D(H\bar{H}) \text{Tr}\chi_+ + \frac{C_1}{\Lambda_\chi} \text{tr}_D H \chi_+ \bar{H}. \quad (2.113)$$

In the heavy-quark limit, the hyperfine splitting between \mathring{M}_D and \mathring{M}_{D^*} vanishes. An explicit dependence of the chiral breaking scale Λ_χ is implemented in the denominator. This arrangement entails a dimensionless setup of LECs, C_0 and C_1 ³. The portion of the Goldstone-boson mass m_Q (leading order, from χ_0) and the hard scale Λ_χ implements the suppression according to chiral power counting

$$\frac{m_Q}{\Lambda_\chi} \simeq Q. \quad (2.114)$$

Using the non-relativistic reduction techniques, we observe that if the heavy-quark spin symmetry is respected, the coefficients in Eq.(2.111) satisfy [29]

$$2c_0 - c_1 = 2\tilde{c}_0 - \tilde{c}_1 = \frac{M_0}{\Lambda_\chi} C_0, \quad c_1 = \tilde{c}_1 = \frac{M_0}{\Lambda_\chi} C_1. \quad (2.115)$$

The factor of M_0 is derived from the normalization of H field (2.71). This factor rightly respects with the scale dependence of the heavy-meson Lagrangian. Since numerically M_0 deviates not so much with Λ_χ in the case of open-charm mesons (both of them are $1 \sim 2\text{GeV}$), the combination M_0/Λ_χ may not give a significant modification of the magnitude of the LECs between C_i and c_i, \tilde{c}_i . We can just neglect this scale dependence in the dimensionless LECs c_i and \tilde{c}_i .

Besides the χ -SB terms, there are chiral-symmetry respecting terms reading as

$$\begin{aligned} \mathcal{L}_4^{(2)} = & 4(2c_2 + c_3) D\bar{D}\text{Tr}(U_\mu U^{\mu\dagger}) - 4c_3 D U_\mu U^{\mu\dagger} \bar{D} + \frac{2(2c_4 + c_5)}{\mathring{M}_D^2} \partial_\mu D \partial_\nu \bar{D} \text{Tr}[U^\mu, U^{\nu\dagger}]_+ \\ & - \frac{2c_5}{\mathring{M}_D^2} \partial_\mu D [U^\mu, U^{\nu\dagger}]_+ \partial_\nu \bar{D} + ic_6 \epsilon^{\mu\nu\rho\sigma} (D [U_\mu, U_\nu^\dagger]_- \bar{D}_{\rho\sigma} - D_{\rho\sigma} [U_\nu^\dagger, U_\mu]_- \bar{D}) \end{aligned}$$

³ The Λ_χ can be recognized as the typical scale of higher-energy modes. It always appears as a suppression factor ($\sim 1/\Lambda_\chi$) in a low-energy effective theory. This effect can be illustrated by integrating out the high-energy modes [70, 71, 89, 64].

$$\begin{aligned}
& -2(2\tilde{c}_2 + \tilde{c}_3)D^{\alpha\beta}\bar{D}_{\alpha\beta}\text{Tr}(U_\mu U^{\mu\dagger}) + 2\tilde{c}_3 D^{\alpha\beta}U_\mu U^{\mu\dagger}\bar{D}_{\alpha\beta} - \frac{(2\tilde{c}_4 + \tilde{c}_5)}{\dot{M}_{D^*}^2}\partial_\mu D^{\alpha\beta}\partial_\nu\bar{D}_{\alpha\beta}\text{Tr}[U^\mu, U^{\nu\dagger}]_+ \\
& + \frac{\tilde{c}_5}{\dot{M}_{D^*}^2}\partial_\mu D^{\alpha\beta}[U^\mu, U^{\nu\dagger}]_+\partial_\nu\bar{D}_{\alpha\beta} - 4\tilde{c}_6 D^{\mu\alpha}[U_\mu, U^{\nu\dagger}]_-\bar{D}_{\nu\alpha}.
\end{aligned} \tag{2.116}$$

We allowed a hyperfine difference between the $c_{4,5}$ and $\tilde{c}_{4,5}$ interactions in terms of the chiral-limit charmed-meson masses \dot{M}_D and \dot{M}_{D^*} . They tend to be identical with the asymptotic value M_0 in the heavy-quark limit. Substituting $U_\mu = \frac{i}{2f}\partial_\mu\Phi + O(\Phi^3)$, we can get

$$\begin{aligned}
\mathcal{L}_4^{(2)} &= \frac{2c_2 + c_3}{f^2}D\bar{D}\text{Tr}(\partial_\mu\Phi\partial^\mu\Phi) - \frac{c_3}{f^2}D\partial_\mu\Phi\partial^\mu\Phi\bar{D} + \frac{(2c_4 + c_5)}{2\dot{M}_D^2 f^2}\partial_\mu D\partial_\nu\bar{D}\text{Tr}[\partial^\mu\Phi, \partial^\nu\Phi]_+ \\
& - \frac{c_5}{2\dot{M}_D^2 f^2}\partial_\mu D[\partial^\mu\Phi, \partial^\nu\Phi]_+\partial_\nu\bar{D} + i\frac{c_6}{4f^2}\epsilon^{\mu\nu\rho\sigma}(D[\partial_\mu\Phi, \partial_\nu\Phi]_-\bar{D}_{\rho\sigma} - D_{\rho\sigma}[\partial_\nu\Phi, \partial_\mu\Phi]_-\bar{D}) \\
& - \frac{2\tilde{c}_2 + \tilde{c}_3}{2f^2}D^{\alpha\beta}\bar{D}_{\alpha\beta}\text{Tr}(\partial_\mu\Phi\partial^\mu\Phi) + \frac{\tilde{c}_3}{2f^2}D^{\alpha\beta}\partial_\mu\Phi\partial^\mu\Phi\bar{D}_{\alpha\beta} - \frac{(2\tilde{c}_4 + \tilde{c}_5)}{4\dot{M}_{D^*}^2 f^2}\partial_\mu D^{\alpha\beta}\partial_\nu\bar{D}_{\alpha\beta}\text{Tr}[\partial^\mu\Phi, \partial^\nu\Phi]_+ \\
& + \frac{\tilde{c}_5}{4\dot{M}_{D^*}^2 f^2}\partial_\mu D^{\alpha\beta}[\partial^\mu\Phi, \partial^\nu\Phi]_+\partial_\nu\bar{D}_{\alpha\beta} - \frac{\tilde{c}_6}{f^2}D^{\mu\alpha}[\partial_\mu\Phi, \partial^\nu\Phi]_-\bar{D}_{\nu\alpha}.
\end{aligned} \tag{2.117}$$

The c_i and \tilde{c}_i are identical if the heavy-quark symmetry is respected. One can confirm this fact by matching the Lagrangian (2.116) into the heavy-quark reduced form

$$\begin{aligned}
\mathcal{L}_{4,H}^{(2)} &= -2\frac{C_2}{\Lambda_\chi}\text{tr}_D(H\bar{H})\text{Tr}(U_\mu U^{\mu\dagger}) + 2\frac{C_3}{\Lambda_\chi}\text{tr}_D(HU_\mu U^{\mu\dagger}\bar{H}) - \frac{C_4}{\Lambda_\chi}v_\mu v_\nu\text{tr}_D(H\bar{H})\text{Tr}[U^\mu, U^{\nu\dagger}]_+ \\
& + \frac{C_5}{\Lambda_\chi}v_\mu v_\nu\text{tr}_D(H[U^\mu, U^{\nu\dagger}]_+\bar{H}) + i\frac{C_6}{\Lambda_\chi}\text{tr}_D(H\sigma_{\mu\nu}[U^\mu, U^{\nu\dagger}]_-\bar{H}),
\end{aligned} \tag{2.118}$$

and observe [29]

$$\begin{aligned}
2c_2 + c_3 &= 2\tilde{c}_2 + \tilde{c}_3 = \frac{M_0}{\Lambda_\chi}C_2, & 2c_4 + c_5 &= 2\tilde{c}_4 + \tilde{c}_5 = \frac{M_0}{\Lambda_\chi}C_4, \\
c_3 &= \tilde{c}_3 = \frac{M_0}{\Lambda_\chi}C_3, & c_5 &= \tilde{c}_5 = \frac{M_0}{\Lambda_\chi}C_5, & c_6 &= \tilde{c}_6 = \frac{M_0}{\Lambda_\chi}C_6.
\end{aligned} \tag{2.119}$$

The 4-point interactions (2.117) will contribute at N³LO by forming tadpole loops. The leading order heavy-meson scale dependence is emphasized by the factor M_0/Λ_χ . The chiral-symmetry respecting terms contribute to $O(Q^4)$ self-energy loop corrections. The heavy-quark correlation (2.119) are asserted in our forthcoming study of the self-energy chiral corrections. On the contrary, we will release the heavy-quark constraints between c_0, c_1 and \tilde{c}_0, \tilde{c}_1 (2.115). We will probe the detail of these conditions in the next chapter.

The possible NNLO (Q^3) counter terms are redundant under a suitable redefinition of open-charm meson fields [90, 91, 51]. And at N³LO there are several χ -SB counter terms involved in the self-energy corrections. They are stated as

$$\begin{aligned}
\mathcal{L}_\chi^{(4)} &= -d_1 D\chi_+^2\bar{D} - d_2 D\chi_+\bar{D}\text{Tr}(\chi_+) - d_3 D\bar{D}\text{Tr}(\chi_+^2) - d_4 D\bar{D}(\text{Tr}\chi_+)^2 \\
& + \frac{1}{2}\tilde{d}_1 D^{\mu\nu}\chi_+^2\bar{D}_{\mu\nu} + \frac{1}{2}\tilde{d}_2 D^{\mu\nu}\chi_+\bar{D}_{\mu\nu}\text{Tr}(\chi_+) + \frac{1}{2}\tilde{d}_3 D^{\mu\nu}\bar{D}_{\mu\nu}\text{Tr}(\chi_+^2) + \frac{1}{2}\tilde{d}_4 D^{\mu\nu}\bar{D}_{\mu\nu}(\text{Tr}\chi_+)^2.
\end{aligned} \tag{2.120}$$

The power suppressions from the chiral breaking scale $1/\Lambda_\chi^2$ are implicitly incorporated in to the coupling constants, ending up with dimension [m^{-2}] LECs d_i and \tilde{d}_i . The two-point counter terms read as

$$\mathcal{L}_\chi^{(4)} = -d_1 D\chi_0^2\bar{D} - d_2 D\chi_0\bar{D}\text{Tr}(\chi_0) - d_3 D\bar{D}\text{Tr}(\chi_0^2) - d_4 D\bar{D}(\text{Tr}\chi_0)^2$$

$$+ \frac{1}{2} \tilde{d}_1 D^{\mu\nu} \chi_0^2 \bar{D}_{\mu\nu} + \frac{1}{2} \tilde{d}_2 D^{\mu\nu} \chi_0 \bar{D}_{\mu\nu} \text{Tr}(\chi_0) + \frac{1}{2} \tilde{d}_3 D^{\mu\nu} \bar{D}_{\mu\nu} \text{Tr}(\chi_0^2) + \frac{1}{2} \tilde{d}_4 D^{\mu\nu} \bar{D}_{\mu\nu} (\text{Tr} \chi_0)^2. \quad (2.121)$$

The terms with more flavor traces get more suppressed with under the large N_C approximation (see Appendix C). But all of them are necessary in compensating the divergence of the chiral loop corrections of the charmed-meson self-energy. It is straightforward to construct the corresponding heavy-quark reduced terms. And the heavy-quark symmetry is implemented when the d_i 's are identified with \tilde{d}_i 's,

$$d_1 = \tilde{d}_1, \quad d_2 = \tilde{d}_2, \quad d_3 = \tilde{d}_3, \quad d_4 = \tilde{d}_4. \quad (2.122)$$

We will assert these correlations in our treatment of the chiral self-energy corrections for the open-charm mesons in the next chapter.

3 Chiral extrapolation for open-charm meson masses

In this chapter we will study the chiral corrections for the masses of pseudo-scalar and vector D meson states up to next-to-next-to-next-leading order ($N^3\text{LO}$, $O(Q^4)$). To this end, the one-loop effects from the chiral Lagrangian we introduced for D -meson fields in the previous chapter will be derived in the first section.

We should first discuss the power counting scheme. The power counting for systems with Goldstone boson only was already reviewed in this work. In a case where matter fields are involved, the power counting needs particular attention. If the conventional modified minimal-subtraction ($\overline{\text{MS}}$) scheme is employed in renormalizing the loops [73], derived from a relativistic chiral Lagrangian, power counting violating effects are observed. In contrast, a consistent power counting scheme is obtained within the heavy-hadron formalism. Here the heavy-meson propagator is proportional to $1/v \cdot k$, with $k \sim Q$. In turn the heavy-meson propagator is of chiral order Q^{-1} . For a given diagram with N_L loops including I_H (I_M) heavy meson (Goldstone boson) inner lines and N_n^H (N_{2n}^M) heavy-meson (pure Goldstone-boson) vertices of the n th ($2n$ th) order, the chiral order is given by [92, 53]

$$n_q = 4N_L - 2I_M - I_H + \sum_{n=1}^{\infty} 2nN_{2n}^M + \sum_{n=1}^{\infty} nN_n^B = 2N_L + I_N + 2 + \sum_{n=1}^{\infty} (2n-2)N_{2n}^M + \sum_{n=1}^{\infty} (n-2)N_n^H. \quad (3.1)$$

Here the topological relation $N_L = I_M + I_H - N_M - N_H + 1$ had been used in the last step.

Unfortunately, the heavy-hadron approach suffers from unphysical analytic properties of its Green's functions [93]. In this approach physical quantities are systematically expanded in powers of the inverse heavy-hadron masses. After this reduction, the analytic structure of the Green's functions such as the pole positions and the branch-cut behaviors is not consistent with the results obtained in the framework of a fully relativistic field theory [94, 54, 95]. Therefore, it is advantageous to go back to the covariant description where the micro-causality constraints of a local quantum field theory are manifest. To this end, different renormalization schemes are proposed in order to render the loop effects free from power-counting breaking effects. The first attempt is the infrared regularization [94]. The infrared contribution which is attributed to the chiral dynamics has been disentangled from the full loop correction. While this approach has great success, unphysical cuts contribute in dispersion-integral representation of loop expressions [95, 47]. It was realized that all the power counting breaking terms appear as some polynomials in powers of light quark masses or small momenta [96]. Thus the power counting breaking terms can be avoided by appropriate subtraction schemes, without harming the analytic property of the loop functions. Different subtraction schemes have been proposed, e.g. the chiral minimal subtraction method ($\chi\text{-}\overline{\text{MS}}$) [97, 22, 47] and the extended-on-mass-shell method (EOMS) [98, 99]. Both of the schemes protect the analytic structure of the chiral loop corrections. These schemes are supposed to give the same leading order contribution of a same loop, leaving out less important higher order differences.

Although both of these renormalization schemes have gained plausible success in the chiral extrapolation processes [43, 100], the chiral power counting of the covariant formalism deserves further classification. In the covariant ChPT, one may specify the starting chiral order of a certain loop using covariant ChPT, but in principle higher chiral order corrections contribute to the loop. A naive chiral expansion according to small m_Q/M_H (m_Q as the Goldstone-boson mass, M_H as the heavy hadron mass) is expected to disentangle different chiral orders. But this expansion essentially reduces the covariant form to the heavy-hadron form and, unsurprisingly, fails to converge in many applications. We will scrutinize this problem later in this chapter, in application of a modified version of the $\chi\text{-}\overline{\text{MS}}$ subtraction scheme [52]. To be specific, the chiral expansions for the bubble-loop corrections of the D -meson self-energy will be investigated in the second section of this chapter.

With well analyzed chiral corrections, we end up with D -meson mass formulae and higher chiral order uncertainties are under well control. The involved undetermined LECs will be determined according

to lattice data for the D -meson masses at various unphysical quark masses. We apply the finite-box correction proposed in [43] in the chiral loop integrals. We perform the fitting according to two lattice data sets, and compare the fitted LECs to previous studies. Detailed discussions about these issues will be performed in the last section of the chapter.

3.1 Chiral corrections for the masses of open-charm mesons up to $N^3\text{LO}$

In this section, we will study the chiral corrections for the open-charm meson masses up to next-to-next-to-next leading order ($N^3\text{LO}$). This is the chiral order Q^4 . A first numerical estimate of the NNLO chiral corrections will be provided in the end of this section.

3.1.1 Self-energies for the 0^- and 1^- open-charm mesons

The chiral Lagrangian generating the chiral corrections up to $O(Q^4)$ involve the kinetic terms (2.102, 2.103), the 3-point interaction terms (2.104) as well as order Q^2 and Q^4 counter terms, (2.112, 2.117) and (2.121). For later convenience we introduce the chiral-limit mass \dot{M}_H of an open-charm meson H with

$$\dot{M}_{H \in [0^-]} = M, \quad \dot{M}_{H \in [1^-]} = M + \Delta. \quad (3.2)$$

Based on the chiral Lagrangian given in the last section, we can calculate the polarization, $\Pi_H(p^2)$, for the pseudoscalar (D, D_s) and the vector (D^*, D_s^*) triplets states respectively. To the order Q^4 , the polarization can be sorted into the contributions from tree-level and the one-loop diagrams

$$\Pi_H = \Pi_H^{2-\chi} + \Pi_H^{4-\chi} + \Pi_H^{\text{loop}} + \Pi_H^{\text{tadpole}}, \quad (3.3)$$

where $\Pi_H^{(2)}$ is the tree-level contribution from the χ -SB counter terms at $O(Q^2)$ (2.112), and $\Pi_H^{4-\chi}$ represents the tree-level contributions from the χ -SB $O(Q^4)$ counter terms (2.121). The loop-level correction consists of bubble-loop contributions collected in Π_H^{loop} , counted as order Q^3 , and an order Q^4 tadpole-loop contributions Π_H^{tadpole} . The mass M_H is evaluated according to,

$$M_H^2 - \dot{M}_H^2 - \Pi_H(M_H^2) = 0. \quad (3.4)$$

where \dot{M}_H is the bare mass in the chiral limit as assigned in (3.2). By implementing the chiral corrections, the wave functions of the D -mesons receive a renormalization with $|H\rangle_r = \sqrt{Z_H}|H_0\rangle$. The wave-function renormalization factor Z_H is derived from the polarization tensor with,

$$Z_H - 1 = \left. \frac{\partial}{\partial p^2} \Pi_H^{\text{loop}}(p^2) \right|_{p^2=M_H^2} \quad (3.5)$$

If we have used the bare fields H_0 , the propagator of H_0 will experience a modification around the pole mass by,

$$S_{H_0} = \frac{Z_H}{p^2 - M_H^2 + i\epsilon} \quad (3.6)$$

Because of the wave-function renormalization Z_H , the bubble-loop correction will scale with the factor $Z_H Z_R$ if bare fields are used. If the deviation of Z_H from one is sufficiently small, one may neglect the contribution of Z_H . But actually, as we will see later, the Z_H factor is significantly larger than 1 for $H = D_s$ and $H = D_s^*$. Therefore, instead of using the bare fields we use the renormalized charmed-meson fields.

The merit of performing the field renormalization is that we can directly relate the imaginary part of the bubble-loop correction with the charmed-meson decay amplitudes at tree level via the optical theorem. This is crucial since the coupling constant g_p is extracted from the D^* decay width at tree level. This will be discussed in Sec.3.1.4. A renormalized charmed-meson field H_r is related with a bare field H_0 according to $H_r = H_0/\sqrt{Z_H}$, such that the normalization relation $\langle 0|H_r|H_r\rangle = \langle 0|H_0|H_0\rangle = 1$ holds. If we use the renormalized field H_r , the propagator is renormalized as

$$S_H^r = \frac{1}{p^2 - M_H^2 + i\epsilon}. \quad (3.7)$$

The bubble loop correction calculated in terms of the renormalized fields $\bar{\Pi}_H^{\text{loop}}$ is connected with the bare-field result Π_H^{loop} as

$$\bar{\Pi}_H^{\text{loop}} = Z_H \Pi_H^{\text{loop}}. \quad (3.8)$$

Now it is justified to match the renormalized coupling g_p with the D^* decay width at tree-level. We will suppress the label of r and implicitly imply all the quantities later on involved are renormalized. In terms of the renormalized fields, the mass formula (3.4) ends up with the following expression,

$$M_H^2 - \dot{M}_H^2 - \bar{\Pi}_H^{2-\chi} - \bar{\Pi}_H^{4-\chi} - \bar{\Pi}_H^{\text{tadpole}} - \bar{\Pi}_H^{\text{loop}}/Z_H = 0. \quad (3.9)$$

A self-consistent solution of this set of equations determines the D -meson masses.

The tree-level chiral corrections contribute at $O(Q^2)$ and $O(Q^4)$. The tree-level contributions are expressed as

$$\begin{aligned} \bar{\Pi}_D^{2-\chi} &= 2B_0(4c_0 - 2c_1)(m_s + 2m) + 4B_0c_1m, \\ \bar{\Pi}_{D_s}^{2-\chi} &= 2B_0(4c_0 - 2c_1)(m_s + 2m) + 4B_0c_1m_s, \\ \bar{\Pi}_{D^*}^{2-\chi} &= 2B_0(4\tilde{c}_0 - 2\tilde{c}_1)(m_s + 2m) + 4B_0\tilde{c}_1m, \\ \bar{\Pi}_{D_s^*}^{2-\chi} &= 2B_0(4\tilde{c}_0 - 2\tilde{c}_1)(m_s + 2m) + 4B_0\tilde{c}_1m_s. \end{aligned} \quad (3.10)$$

at $O(Q^2)$, and

$$\begin{aligned} \bar{\Pi}_D^{4-\chi} &= 4B_0^2(d_1 + 2d_2 + 2d_3 + 4d_4)m^2 + 4B_0^2(d_3 + d_4)m_s^2 + 4B_0^2(d_2 + 4d_4)mm_s, \\ \bar{\Pi}_{D_s}^{4-\chi} &= 4B_0^2(2d_3 + 4d_4)m^2 + 4B_0^2(d_1 + d_2 + d_3 + d_4)m_s^2 + 4B_0^2(2d_2 + 4d_4)mm_s, \\ \bar{\Pi}_{D^*}^{4-\chi} &= 4B_0^2(\tilde{d}_1 + 2\tilde{d}_2 + 2\tilde{d}_3 + 4\tilde{d}_4)m^2 + 4B_0^2(\tilde{d}_3 + \tilde{d}_4)m_s^2 + 4B_0^2(\tilde{d}_2 + 4\tilde{d}_4)mm_s, \\ \bar{\Pi}_{D_s^*}^{4-\chi} &= 4B_0^2(2\tilde{d}_3 + 4\tilde{d}_4)m^2 + 4B_0^2(\tilde{d}_1 + \tilde{d}_2 + \tilde{d}_3 + \tilde{d}_4)m_s^2 + 4B_0^2(2\tilde{d}_2 + 4\tilde{d}_4)mm_s. \end{aligned} \quad (3.11)$$

at $O(Q^4)$. The light-quark masses are related with the Goldstone-boson masses according to conventional ChPT. With the accuracy up to order Q^4 , the Goldstone-boson masses are expressed in terms of light quark masses as [14]

$$\begin{aligned} m_\pi^2 &= \frac{2B_0m}{f^2} \left\{ f^2 + \frac{1}{3}I_\pi - \frac{1}{6}I_\eta + 16B_0[(2m + m_s)(2L_6 - L_4) + m(2L_8 - L_5)] \right\}, \\ m_K^2 &= \frac{B_0(m + m_s)}{f^2} \left\{ f^2 + \frac{1}{3}I_\eta + 16B_0[(2m + m_s)(2L_6 - L_4) + \frac{1}{2}(m + m_s)(2L_8 - L_5)] \right\}, \\ m_\eta^2 &= \frac{2B_0(m + 2m_s)}{3f^2} \left\{ f^2 + I_K - \frac{2}{3}I_\eta + 16B_0[(2m + m_s)(2L_6 - L_4) + \frac{1}{3}(m + 2m_s)(2L_8 - L_5)] \right\} \end{aligned}$$

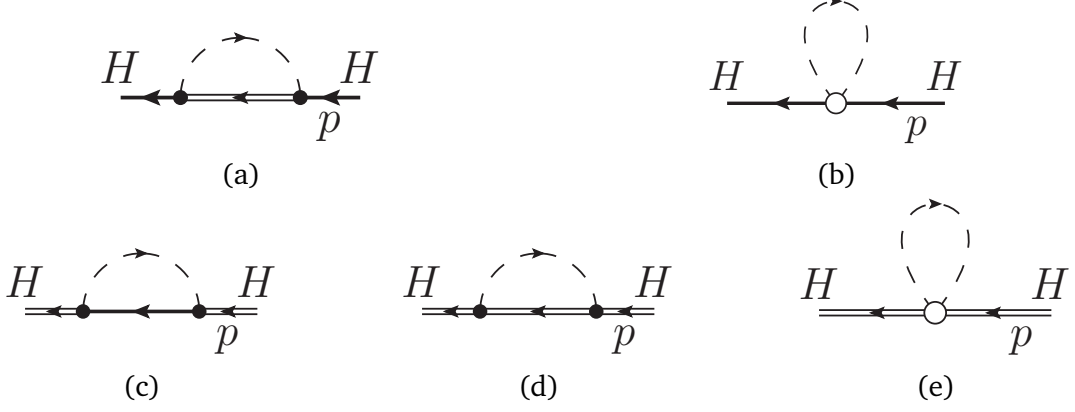


Figure 3.1.: Loop corrections for D -meson masses. The single line represents 0^- mesons D or D_s . The double line represents the 1^- mesons D^* or D_s^* . The Goldstone bosons are symbolized by the dashed line. The arrows show the directions of momenta.

$$+ \frac{2B_0 m}{f^2} \left[\frac{1}{6} I_\eta - \frac{1}{2} I_\pi + \frac{1}{3} I_K \right] + \frac{128 B_0^2 (m - m_s)^2}{9 f^2} (3L_7 + L_8), \quad (3.12)$$

where the empirical values of the LECs involved have been provided in Table II of Ref. [51].

The loop-level chiral corrections, as afore-mentioned, consists of bubble loops $\bar{\Pi}_H^{\text{loop}}$ and tadpole loops $\bar{\Pi}_H^{\text{tadpole}}$. We have shown the corresponding Feynman diagrams in Fig. 3.1.

Up to $N^3\text{LO}$, the masses of pseudo-scalar D -mesons receive contributions from bubble loops and tadpole loops shown as Fig. 3.1(a), (b). The bubble loops read as

$$\bar{\Pi}_{H \in [0^-]}^{\text{loop}}(p^2) = \sum_{Q \in [8]} \sum_{R \in [1^-]} \left(\frac{G_{QR}^{(H)}}{2f} \right)^2 \int \frac{d^d k}{(2\pi)^d} \frac{i \mu^{4-d}}{k^2 - m_Q^2 + i\epsilon} k_\mu k_\rho p_\nu p_\sigma S_R^{\mu\nu, \rho\sigma}(p-k). \quad (3.13)$$

And the tadpole loops read as

$$\bar{\Pi}_{H \in [0^-]}^{\text{tadpole}} = \sum_{Q \in [8]} \int \frac{d^d k}{(2\pi)^d} \frac{i \mu^{4-d}}{k^2 - m_Q^2 + i\epsilon} \left[\left(\frac{G_{HQ}^{(\chi)}}{4f^2} \right) - \sum_{Q \in [8]} \left(\frac{G_{HQ}^{(S)}}{4f^2} \right) k^2 - \sum_{Q \in [8]} \left(\frac{G_{HQ}^{(V)}}{4f^2} \right) (p \cdot k)^2 \right], \quad (3.14)$$

where $S_R^{\mu\nu, \rho\sigma}(p)$ is the open-charm vector meson propagator in the tensor field representation,

$$S_R^{\mu\nu, \rho\sigma}(p) = -\frac{1}{p^2 - M_R^2 + i\epsilon} \left[\frac{M_R^2 - p^2}{M_R^2} g^{\mu\rho} g^{\nu\sigma} + \frac{p^\nu p^\sigma}{M_R^2} g^{\mu\rho} - \frac{p^\nu p^\rho}{M_R^2} g^{\mu\sigma} - (\mu \leftrightarrow \nu) \right] \quad (3.15)$$

which is discussed in more detail in Appendix B. Using the Passarino-Veltman reduction techniques, the loop integral can be reduced into several basic integrals and reads

$$\begin{aligned} \bar{\Pi}_{H \in [0^-]}^{\text{loop}}(p^2) &= \sum_{Q \in [8]} \sum_{R \in [1^-]} \left(\frac{G_{QR}^{(H)}}{2f} \right)^2 \left[a_{QR}^{[1^-]}(p^2) I_R + b_{QR}^{[1^-]}(p^2) I_Q + c_{QR}^{[1^-]}(p^2) I_{QR}(p^2) \right], \\ a_{QR}^{[1^-]}(p^2) &= -\frac{1}{4} (p^2 - m_Q^2 + M_R^2), \quad b_{QR}^{[1^-]}(p^2) = -\frac{1}{4} (p^2 - M_R^2 + m_Q^2), \\ c_{QR}^{[1^-]}(p^2) &= -\frac{1}{4} (p^4 - 2(M_R^2 + m_Q^2) + (M_R^2 - m_Q^2)^2), \end{aligned} \quad (3.16)$$

$G_{\pi D^*}^{(D)} = 2\sqrt{3}g_P$	$G_{KD^*}^{(D_s)} = 4g_P$		
$G_{\eta D^*}^{(D)} = \frac{2}{\sqrt{3}}g_P$	$G_{\eta D_s^*}^{(D_s)} = \frac{4}{\sqrt{3}}g_P$		
$G_{\bar{K}D_s^*}^{(D)} = 2\sqrt{2}g_P$			
$G_{\pi D}^{(D^*)} = 2\sqrt{3}g_P$	$G_{KD}^{(D_s^*)} = 4g_P$	$G_{\pi D^*}^{(D^*)} = 2\sqrt{3}\tilde{g}_P$	$G_{KD^*}^{(D_s^*)} = 4\tilde{g}_P$
$G_{\eta D}^{(D^*)} = \frac{2}{\sqrt{3}}g_P$	$G_{\eta D_s}^{(D_s^*)} = \frac{4}{\sqrt{3}}g_P$	$G_{\eta D^*}^{(D^*)} = \frac{2}{\sqrt{3}}\tilde{g}_P$	$G_{\eta D_s^*}^{(D_s^*)} = \frac{4}{\sqrt{3}}\tilde{g}_P$
$G_{\bar{K}D_s}^{(D^*)} = 2\sqrt{2}g_P$		$G_{\bar{K}D_s^*}^{(D^*)} = 2\sqrt{2}\tilde{g}_P$	

Table 3.1.: The coefficients $G_{QR}^{(H)}$ appeared in the $H \in [0^-]$ and $H \in [1^-]$ bubble loops, defined with respect to isospin-strangeness states (see the next chapter).

and the tadpoles

$$\Pi_{H \in [0^-]}^{\text{tadpole}}(p^2) = \frac{1}{4f^2} \sum_{Q \in [8]} \left[G_{HQ}^{(\chi)} I_Q - G_{HQ}^{(S)} m_Q^2 I_Q - G_{HQ}^{(V)} p^2 I_Q^{(2)} \right]. \quad (3.17)$$

The scalar-loop integrals are defined as

$$\begin{aligned} I_Q &\equiv \int \frac{d^d k}{(2\pi)^d} \frac{i\mu^{4-d}}{k^2 - m_Q^2 + i\epsilon}, & I_R &\equiv \int \frac{d^d k}{(2\pi)^d} \frac{i\mu^{4-d}}{k^2 - M_R^2 + i\epsilon}, \\ I_Q^{(2)} &\equiv \int \frac{d^d k}{(2\pi)^d} \frac{i\mu^{4-d}}{k^2 - m_Q^2 + i\epsilon} \left(\frac{k \cdot p}{\sqrt{p}} \right)^2, \\ I_{QR}(p^2) &\equiv \int \frac{d^d k}{(2\pi)^d} \frac{-i\mu^{4-d}}{k^2 - m_Q^2 + i\epsilon} \frac{1}{(p-k)^2 - M_R^2 + i\epsilon}. \end{aligned} \quad (3.18)$$

In the infinite-volume limit $I_Q^{(2)}$ reduces to the scalar tadpole I_Q according to $I_Q^{(2)} \rightarrow \frac{m_Q^2}{d} I_Q$.

The coefficients $G_{QR}^{(H)}$ are listed in Table 3.1. The indices of Q and R refer to different isospin-strangeness states. Each of such states has a certain value of isospin and strangeness. The values of the coefficients $G_{HQ}^{(\chi)}$, $G_{HQ}^{(S)}$ and $G_{HQ}^{(V)}$ can be found in the Table 3.2.

In order to apply dimensional regularization, we have computed the loop integral (3.13) in an arbitrary space-time dimension d . Once having defined the theory in the dimension d , the boson fields carry as dimension $\frac{d}{2} - 1$. The renormalization-scale dependence (μ^{4-d}) in the loop integrals is introduced such that the loops possess the same dimension as in the real physical space ($d = 4$).

As pointed out before, the integral $\Pi_{H \in [0^-]}^{\text{loop}}$ contributes at order Q^3 if naive dimensional counting rules are applied. However, if dimensional regularization with the $\overline{\text{MS}}$ subtraction scheme is used, power counting violating terms of chiral order Q^0 and Q^2 arise in the result. As we mentioned earlier, we will use the χ - $\overline{\text{MS}}$ renormalization scheme in order to restore the power counting scheme. This subject will be discussed in the next section in more detail.

We proceed with open-charm vector meson masses. Similar to the pseudoscalar meson session, there is a NNLO bubble loop and N³LO tadpole loop contributions, shown in Fig.3.1(c),(d),(e). The 1-PI loop diagram for D^* propagator in the tensor representation can be written as a rank-4 tensor $\Pi^{\mu\nu\rho\sigma}(p^2)$. To be explicit, the bubble-loop diagrams Fig.3.1(c),(d) can be written as

$$\bar{\Pi}_{H \in [1^-]}^{\text{loop}; \mu\nu\rho\sigma}(p^2) = \sum_{Q \in [8]} \int \frac{d^d k}{(2\pi)^d} \frac{i\mu^{4-d}}{k^2 - m_Q^2 + i\epsilon} \left[\sum_{R \in [0^-]} \left(\frac{G_{QR}^{(H)}}{2f} \right)^2 k_\mu k_\rho p_\nu p_\sigma S_R(p-k) + \sum_{R \in [1^-]} \left(\frac{G_{QR}^{(H)}}{2f} \right)^2 \right]$$

H Q	$G_{HQ}^{(\chi)}$	$G_{HQ}^{(S)}$	$\check{M}_H^2 G_{HQ}^{(V)}$
D π	$-48(2c_0 - c_1)B_0m - 24c_1B_0m$	$24(2c_2 + c_3) - 12c_3$	$24(2c_4 + c_5) - 12c_5$
D K	$-32(2c_0 - c_1)B_0(m_s + m) - 8c_1B_0(m_s + m)$	$32(2c_2 + c_3) - 8c_3$	$32(2c_4 + c_5) - 8c_5$
D η	$-\frac{16}{3}(2c_0 - c_1)B_0(2m_s + m) - \frac{8}{3}c_1B_0m$	$8(2c_2 + c_3) - \frac{4}{3}c_3$	$8(2c_4 + c_5) - \frac{4}{3}c_5$
D_s π	$-48(2c_0 - c_1)B_0m$	$24(2c_2 + c_3)$	$24(2c_4 + c_5)$
D_s K	$-32(2c_0 - c_1)B_0(m_s + m) - 16c_1B_0(m_s + m)$	$32(2c_2 + c_3) - 16c_3$	$32(2c_4 + c_5) - 16c_5$
D_s η	$-\frac{16}{3}B_0(2m_s + m)(2c_0 - c_1) - \frac{32}{3}B_0m_s c_1$	$8(2c_2 + c_3) - \frac{16}{3}c_3$	$8(2c_4 + c_5) - \frac{16}{3}c_5$
D^* π	$-48(2\check{c}_0 - \check{c}_1)B_0m - 24\check{c}_1B_0m$	$24(2\check{c}_2 + \check{c}_3) - 12\check{c}_3$	$24(2\check{c}_4 + \check{c}_5) - 12\check{c}_5$
D^* K	$-32(2\check{c}_0 - \check{c}_1)B_0(m_s + m) - 8\check{c}_1B_0(m_s + m)$	$32(2\check{c}_2 + \check{c}_3) - 8\check{c}_3$	$32(2\check{c}_4 + \check{c}_5) - 8\check{c}_5$
D^* η	$-\frac{16}{3}(2\check{c}_0 - \check{c}_1)B_0(2m_s + m) - \frac{8}{3}\check{c}_1B_0m$	$8(2\check{c}_2 + \check{c}_3) - \frac{4}{3}\check{c}_3$	$8(2\check{c}_4 + \check{c}_5) - \frac{4}{3}\check{c}_5$
D_s^* π	$-48(2\check{c}_0 - \check{c}_1)B_0m$	$24(2\check{c}_2 + \check{c}_3)$	$24(2\check{c}_4 + \check{c}_5)$
D_s^* K	$-32(2\check{c}_0 - \check{c}_1)B_0(m_s + m) - 16\check{c}_1B_0(m_s + m)$	$32(2\check{c}_2 + \check{c}_3) - 16\check{c}_3$	$32(2\check{c}_4 + \check{c}_5) - 16\check{c}_5$
D_s^* η	$-\frac{16}{3}B_0(2m_s + m)(2\check{c}_0 - \check{c}_1) - \frac{32}{3}B_0m_s \check{c}_1$	$8(2\check{c}_2 + \check{c}_3) - \frac{16}{3}\check{c}_3$	$8(2\check{c}_4 + \check{c}_5) - \frac{16}{3}\check{c}_5$

Table 3.2.: Coefficients $G_{HQ}^{(\chi)}$, $G_{HQ}^{(S)}$ and $G_{HQ}^{(V)}$

$$\times \left(\frac{1}{4}\right)^2 \left(\epsilon_{\alpha\beta\xi\sigma} p_\rho + \epsilon_{\rho\beta\xi\sigma} (p-k)_\alpha \right) \left(\epsilon_{\gamma\delta\tau\nu} p_\mu + \epsilon_{\mu\delta\tau\nu} (p-k)_\gamma \right) k^\xi k^\tau S_R^{\alpha\beta,\gamma\delta} (p-k), \quad (3.19)$$

where the coefficients $G_{QR}^{(H\in[1^-])}$ can be found in Table 3.1. And the tadpole-loop diagram Fig. 3.1(c) reads

$$\begin{aligned} \bar{\Pi}_{H\in[1^-]}^{\text{tadpole};\mu\nu,\rho\sigma} = & -\frac{1}{2} \sum_{Q\in[8]} \int \frac{d^D k}{(2\pi)^D} \frac{i\mu^{4-D}}{k^2 - m_Q^2 + i\epsilon} \left[\left(\frac{G_{HQ}^{(\chi)}}{4f^2} \right) g_{\mu\rho} g_{\nu\sigma} - \left(\frac{G_{HQ}^{(S)}}{4f^2} \right) k^2 g_{\mu\rho} g_{\nu\sigma} \right. \\ & \left. - \left(\frac{G_{HQ}^{(V)}}{4f^2} \right) (p \cdot k)^2 g_{\mu\rho} g_{\nu\sigma} \right], \end{aligned} \quad (3.20)$$

where the coefficients involved can be found in Table 3.2.

The self-energy tensor $\Pi_{\mu\nu,\rho\sigma}(p^2)$ can be decomposed into a vector part and a tensor part,

$$\Pi_{\mu\nu,\rho\sigma}(p^2) = \Pi^V(p^2) \mathcal{Y}_{\mu\nu,\rho\sigma}^{(1)} + \Pi^T(p^2) \mathcal{Y}_{\mu\nu,\rho\sigma}^{(2)}, \quad (3.21)$$

where only the vector part Π^V contributes to the mass. In the conventional vector representation, this part can be projected by the transverse projector $\mathcal{Y}_{\mu\nu}^{(V)} = g_{\mu\nu} - p_\mu p_\nu / p^2$ (see e.g. [101, 102]). The projectors for the two components in the tensor representation $\mathcal{Y}_{\mu\nu,\rho\sigma}^{(1)}$ can readily be constructed. We recall from [29]

$$\mathcal{Y}_{\mu\nu,\rho\sigma}^{(1)} = \frac{1}{2p^2} (g_{\mu\rho} p_\nu p_\sigma - g_{\mu\sigma} p_\nu p_\rho - g_{\nu\rho} p_\mu p_\sigma + g_{\nu\sigma} p_\mu p_\rho), \quad (3.22)$$

$$\mathcal{Y}_{\mu\nu,\rho\sigma}^{(2)} = \frac{1}{2} \left[(g_{\mu\rho} g_{\nu\sigma} - g_{\nu\rho} g_{\mu\sigma}) - \frac{1}{p^2} (g_{\mu\rho} p_\nu p_\sigma - g_{\mu\sigma} p_\nu p_\rho - g_{\nu\rho} p_\mu p_\sigma + g_{\nu\sigma} p_\mu p_\rho) \right]. \quad (3.23)$$

They satisfy the projection relations

$$\mathcal{Y}_{\mu\nu,\rho\sigma}^{(i)} \mathcal{Y}^{(j)\rho\sigma}_{\alpha\beta} = \delta_{ij} \mathcal{Y}_{\mu\nu,\alpha\beta}^{(j)}. \quad (3.24)$$

We note the additional properties

$$\begin{aligned} \mathcal{Y}^{(1); \mu\nu,\rho\sigma} \mathcal{Y}_{\mu\nu,\rho\sigma}^{(1)} &= d-1, & \mathcal{Y}^{(2); \mu\nu,\rho\sigma} \mathcal{Y}_{\mu\nu,\rho\sigma}^{(2)} &= \frac{1}{2} (d^2 - 3d + 2), \\ \mathcal{Y}^{(1); \mu\nu,\rho\sigma} \mathcal{Y}_{\mu\nu,\rho\sigma}^{(2)} &= 0. \end{aligned} \quad (3.25)$$

We can decompose the (bare) propagator (3.15) in terms of the projectors

$$S_{\mu\nu,\rho\sigma}^0(p^2) = -\frac{2}{p^2 - \dot{M}_H^2 + i\epsilon} \left(\mathcal{Y}_{\mu\nu,\rho\sigma}^{(1)} - \frac{p^2 - \dot{M}_H^2}{\dot{M}_H^2} \mathcal{Y}_{\mu\nu,\rho\sigma}^{(2)} \right) \quad (3.26)$$

and observe that the self-energy tensor $\Pi_{\mu\nu,\rho\sigma}(p^2)$ contributes to the full propagator $S_{\mu\nu,\rho\sigma}(p^2)$ according to

$$S_{\mu\nu,\rho\sigma}^{\text{full}}(p^2) = -\frac{2}{p^2 - \dot{M}_H^2 + 2\Pi^V(p^2) + i\epsilon} \left(\mathcal{Y}_{\mu\nu,\rho\sigma}^{(1)} - \frac{p^2 - \dot{M}_H^2 + 2\Pi^V(p^2)}{\dot{M}_H^2 - 2\Pi^T(p^2)} \mathcal{Y}_{\mu\nu,\rho\sigma}^{(2)} \right), \quad (3.27)$$

The Π^V modifies the pole position of the vector meson. In the vicinity of this pole, the $\mathcal{Y}^{(2)}$ component disappears, which resembles the behavior of the bare propagator. The pole of the propagator (3.27) at $p^2 = 0$ should be canceled by requiring $\Pi^V(0) = \Pi^T(0)$. We can check that this condition is indeed fulfilled for the loop diagrams we are considering here. Since the hard scale \dot{M}_H^2 is always much larger than the chiral correction $2\Pi^T(p^2)$, the second term in (3.27) gives no additional pole structures. To this end, we identify with $-2\Pi^V$ the loop contribution to the polarization Π_H appearing in the mass formula (3.9)¹. $\Pi_{\mu\nu,\rho\sigma}$ with the projection operator $\mathcal{Y}_{\mu\nu,\rho\sigma}^{(1)}$, and obtain the loop corrections to the polarization Π_H with

$$\Pi_{H \in [1^-]}^{\text{loop}}(p^2) = \frac{-2}{d-1} \mathcal{Y}^{(1); \mu\nu,\rho\sigma} \Pi_{\mu\nu,\rho\sigma}^{\text{loop}}(p^2). \quad (3.28)$$

This leads to our result

$$\begin{aligned} \bar{\Pi}_{H \in [1^-]}^{\text{loop}}(p^2) &= \sum_{Q \in [8]} \sum_{R \in [0^-]} \left(\frac{G_{QR}^{(H)}}{2f} \right)^2 \left[a_{QR}^{[0^-]}(p^2) I_R + b_{QR}^{[0^-]}(p^2) I_Q + c_{QR}^{[0^-]}(p^2) I_{QR}(p^2) \right] \\ &+ \sum_{Q \in [8]} \sum_{R \in [1^-]} \left(\frac{G_{QR}^{(H)}}{2f} \right)^2 \left[b_{QR}^{[1^-]}(p^2) I_Q + a_{QR}^{[1^-]}(p^2) I_R + c_{QR}^{[1^-]}(p^2) I_{QR}(p^2) + d_{QR}^{[1^-]} I_Q^{(2)} \right], \\ a_{QR}^{[0^-]}(p^2) &= -\frac{1}{4(d-1)} (p^2 - m_Q^2 + M_R^2), & b_{QR}^{[0^-]}(p^2) &= -\frac{1}{4(d-1)} (p^2 - M_R^2 + m_Q^2), \\ c_{QR}^{[0^-]}(p^2) &= -\frac{1}{4(d-1)} (p^4 - 2(M_R^2 + m_Q^2) + (M_R^2 - m_Q^2)^2), \\ a_{QR}^{[1^-]}(p^2) &= -\frac{d^2 - 5d + 6}{16(d-1)M_R^2 p^2} (M_R^2 + p^2)^2 (p^2 - m_Q^2 + M_R^2), \\ b_{QR}^{[1^-]}(p^2) &= -\frac{d^2 - 5d + 6}{16(d-1)M_R^2 p^2} [p^6 - p^4((2d-5)m_Q^2 - M_R^2) \end{aligned}$$

¹ This result agrees with the result of the formalism in [103].

$$\begin{aligned}
& -p^2 \left(M_R^4 - 6m_Q^2 M_R^2 \right) + m_Q^2 M_R^4 - M_R^6 \Big], \\
c_{QR}^{[1^-]}(p^2) &= -\frac{d^2 - 5d + 6}{16(d-1)M_R^2} \frac{(M_R^2 + p^2)^2}{p^2} \left(p^4 - 2(M_R^2 + m_Q^2) + (M_R^2 - m_Q^2)^2 \right), \\
d_{QR}^{[1^-]}(p^2) &= \frac{d^2 - 5d + 6}{16(d-1)M_R^2} (4M_R^2 + 2p^2), \tag{3.29}
\end{aligned}$$

and

$$\bar{\Pi}_{H \in [1^-]}^{\text{tadpole}}(p^2) = \frac{1}{4f^2} \sum_{Q \in [8]} \left[G_{HQ}^{(\chi)} I_Q - G_{HQ}^{(S)} m_Q^2 I_Q - G_{HQ}^{(V)} p^2 I_Q^{(2)} \right]. \tag{3.30}$$

We note that for technical convenience we will assign $d \rightarrow 4$ in the coefficients of the scalar loops before performing the χ - $\overline{\text{MS}}$ renormalization, to be introduced in the next subsection. It is known that this leads to a finite renormalization of the counter terms in the chiral Lagrangian only. This is because a power of $d - 4$ may show up in the prefactor and cancels the divergence proportional to $1/(d - 4)$ in some of the corresponding scalar integrals. We do not follow up this finite renormalization in this work.

3.1.2 The χ - $\overline{\text{MS}}$ subtraction scheme

In the previous section, we detailed the sub-leading order corrections to the D meson masses. The one-loop integrals were evaluated by means of the Passarino-Veltman reduction approach. In this manner, all one-loops are expressed in terms of several scalar-loop functions I_Q , I_R , I_{QR} (which are referred to as Passarino-Veltman functions). As we mentioned before, the one-loop corrections suffer from power-counting violating terms. We employ the χ - $\overline{\text{MS}}$ scheme to renormalize the loop integrals in accordance with dimensional power counting rules. This subtraction scheme was proposed in Ref. [97, 47].

It is proven in Ref. [47] that any given one-loop integral (involving a single heavy particle line) is compatible with the power counting rules after a suitable renormalization of the Passarino-Veltman functions. It suffices to devise a subtraction scheme for the Passarino-Veltman functions such that they respect the dimensional counting rules. The important observation made was that only those Passarino-Veltman functions that diverge in the limit $d \rightarrow 4$ need to be modified. In turn, the χ - $\overline{\text{MS}}$ scheme specifies the subtraction terms for the divergent Passarino-Veltman functions as they appear in a one-loop calculation. These are the I_Q , I_R or I_{QR} functions, for which the χ - $\overline{\text{MS}}$ scheme is implemented by specifying the subtraction terms. In this work we use the particular form as suggested recently in [52]. We specify

$$\begin{aligned}
\delta I_Q &= \frac{m_Q^2}{16\pi^2} \left(-\frac{2}{4-d} + \gamma - 1 - \ln(4\pi) \right), \\
\delta I_R &= \frac{M_R^2}{16\pi^2} \left(-\frac{2}{4-d} + \gamma - 1 - \ln(4\pi) + \ln \left(\frac{M_R^2}{\mu^2} \right) \right), \\
\delta I_{QR} &= \frac{1 - \gamma_R^H}{16\pi^2} - \frac{I_R}{M_R^2}. \tag{3.31}
\end{aligned}$$

with

$$I_R = \delta I_R + \bar{I}_R, \quad I_Q = \delta I_Q + \bar{I}_Q, \quad I_{QR}(p^2) = \delta I_{QR} + \bar{I}_{QR}(p^2). \tag{3.32}$$

Here the renormalization of the function $I_{QR}(p^2)$ has been slightly modified from the original work [47] such that the ultraviolet divergence in I_{QR} is canceled by the hard-scalar tadpole I_R only [52]. In Ref.

[47] the renormalized the scalar bubble I_{QR} suffers from an artificial pole at $m_Q^2 = M_R^2$ [52]. With the assignment of (3.32), this problem has been avoided. Note the additional subtraction term $\gamma_R RH$, defined as

$$\gamma_R^H = - \lim_{\substack{m \rightarrow 0 \\ m_s \rightarrow 0}} \frac{M_R^2 - M_H^2}{M_H^2} \log \left| \frac{M_R^2 - M_H^2}{M_R^2} \right|. \quad (3.33)$$

According to the definition, this dimensionless quantity is only nonzero for the off-diagonal loops (where the external open-charm meson and the loop open-charm meson don't have the same spin). This subtraction leads to a vanishing \bar{I}_{QR} in the chiral limit.

We provide analytic expressions for the non-renormalized forms of the Passarino-Veltman integrals in Appendix D. The renormalized quantities \bar{I}_R , \bar{I}_Q and \bar{I}_{QR} we take from [52],

$$\begin{aligned} \bar{I}_R &= 0, & \bar{I}_Q &= \frac{m_Q^2}{16\pi^2} \log \left(\frac{m_Q^2}{\mu} \right), \\ \bar{I}_{QR}(p^2) &= \frac{1}{16\pi^2} \left[\gamma_R^H - \left(\frac{1}{2} + \frac{m_Q^2 - M_R^2}{2p^2} \right) \log \left(\frac{m_Q^2}{M_R^2} \right) \right. \\ &\quad \left. + \frac{p_{QR}}{\sqrt{p^2}} \left(\ln \left(1 - \frac{p^2 - 2p_{QR}\sqrt{p^2}}{m_Q^2 + M_R^2} \right) - \log \left(1 - \frac{p^2 + 2p_{QR}\sqrt{p^2}}{m_Q^2 + M_R^2} \right) \right) \right], \\ \text{with } p_{QR}^2 &= \frac{M_H^2}{4} - \frac{M_R^2 + m_Q^2}{2} + \frac{(M_R^2 - m_Q^2)^2}{4M_H^2}. \end{aligned} \quad (3.34)$$

We express the loop corrections employed in our forthcoming calculation in terms of the renormalized scalar-loop integrals \bar{I}_Q and \bar{I}_{QR} as

$$\begin{aligned} \bar{\Pi}_{H \in [0^-]}^{\text{loop}} &= \sum_{Q \in [8]} \sum_{R \in [1^-]} \left(\frac{G_{QR}^{(H)}}{2f} \right)^2 \left[-M_H^2 p_{QR}^2 \bar{I}_{QR} + \frac{1}{4} (M_R^2 - M_H^2) \frac{m_Q^2}{(4\pi)^2} \log \frac{m_Q^2}{M_R^2} + \alpha_{QR}^H \right], \\ \bar{\Pi}_{H \in [1^-]}^{\text{loop}} &= \sum_{Q \in [8]} \sum_{R \in [0^-]} \left(\frac{G_{QR}^{(H)}}{2f} \right)^2 \left[-\frac{1}{3} M_H^2 p_{QR}^2 \bar{I}_{QR} + \frac{1}{12} (M_R^2 - M_H^2) \frac{m_Q^2}{(4\pi)^2} \log \frac{m_Q^2}{M_R^2} + \alpha_{QR}^H \right] \\ &\quad + \sum_{Q \in [8]} \sum_{R \in [1^-]} \left(\frac{G_{QR}^{(H)}}{2f} \right)^2 \left\{ -\frac{(M_H^2 + M_R^2)^2}{6M_R^2} p_{QR}^2 \bar{I}_{QR} + \frac{(M_H^2 + M_R^2)^2}{24M_H^2 M_R^2} (M_R^2 - M_H^2) \frac{m_Q^2}{(4\pi)^2} \log \frac{m_Q^2}{M_R^2} \right\}, \end{aligned} \quad (3.35)$$

and

$$\bar{\Pi}_{H \in [0^-] \text{ or } [1^-]}^{\text{tadpole}} = \frac{1}{4f^2} \sum_{Q \in [8]} \left[G_{HQ}^{(\chi)} \bar{I}_Q - G_{HQ}^{(S)} m_Q^2 \bar{I}_Q - G_{HQ}^{(V)} M_H^2 \bar{I}_Q^{(2)} \right]. \quad (3.37)$$

Comparing with the un-renormalized expressions (3.16), (3.29), one may notice that there is yet an additional subtraction term $\alpha_{QR}^{(H)}$ added in the bubble loop corrections. They are defined as

$$\begin{aligned} \alpha_{QR}^{(H \in [0^-])} &= \frac{\alpha_1 \Delta^2}{32\pi^2} \left[(M_H^2 - M^2) \left(\frac{\Delta \partial}{\partial M} - \frac{\Delta \partial}{\partial \Delta} - \frac{M + \Delta}{M} \right) \right. \\ &\quad \left. + (M_R^2 - (M + \Delta)^2) \frac{M}{M + \Delta} \left(\frac{\Delta \partial}{\partial \Delta} + 1 \right) \right] \gamma_1 + \frac{\alpha_1 \gamma_2 \Delta M}{16\pi^2} m_Q^2, \end{aligned}$$

$$\alpha_{QR}^{(H \in [1^-])} = \frac{\tilde{\alpha}_1 \Delta^2}{96\pi^2} \left[(M_H^2 - (M + \Delta)^2) \frac{M}{M + \Delta} \left(\frac{\Delta \partial}{\partial \Delta} + 1 \right) + (M_R^2 - M^2) \left(\frac{\Delta \partial}{\partial M} - \frac{\Delta \partial}{\partial \Delta} - \frac{M + \Delta}{M} \right) \right] \tilde{\gamma}_1 + \frac{\tilde{\alpha}_1 \tilde{\gamma}_2 \Delta M}{48\pi^2} m_Q^2. \quad (3.38)$$

After implementing the subtractions (3.33) and (3.38), the bubble-loop contributions scale with power m_Q^4 in the chiral limit. In particular, the open-charm meson masses are not renormalized in the chiral limit. Thus, the bare masses M and $M + \Delta$ specify the pseudo-scalar and vector D meson masses at $m_u = m_d = m_s = 0$ respectively. Also the chiral corrections of the wave functions start from order m_Q^2 . According to this subtraction scheme, the wave function ends up with unity in the chiral limit,

$$\lim_{m, m_s \rightarrow 0} Z_H = 1. \quad (3.39)$$

More details will be discussed in Sec. 3.2.2.

We emphasize that our final expressions for the renormalized loop functions does not depend on the renormalization scale. Such a dependence is completely driven by the scalar tadpole terms \bar{I}_Q given the χ - $\overline{\text{MS}}$ framework. From the expressions for the un-renormalized loop functions one finds terms proportional to $m_Q^2 \bar{I}_Q$, which are not included in (3.36). This is justified because such terms can be absorbed into the available tadpole terms. The only contributions that require particular attention are proportional to $(M_R^2 - M_H^2) \bar{I}_Q$. The latter have been decomposed according to

$$(M_R^2 - M_H^2) \bar{I}_Q = (M_R^2 - M_H^2) \frac{m_Q^2}{(4\pi)^2} \log \frac{m_Q^2}{M_R^2} + \frac{M_R^2 - M_H^2}{M_R^2} m_Q^2 \bar{I}_R. \quad (3.40)$$

The first piece involves a chiral logarithm ($\sim \log m_Q$), which cancels the asymptotic chiral logarithmic at order m_Q^2 possessed by the scalar-bubble contribution \bar{I}_{QR} towards the chiral limit. We will make further discussions on this issue in Sec.3.2.2. The second piece has a scale dependence which scaling with a heavy scale M_R . This part is redundant in the χ - $\overline{\text{MS}}$ framework and therefore should be dropped. We can systematically absorb this contribution into the available counter terms according to the renormalization scheme (3.31).

In the next subsection, we will provide the expressions for the renormalization of the NLO LECs c_i , which aim to absorb the scalar-tadpole contributions at $O(m_Q^4)$ in the bubble loops. The LECs at N³LO, d_i , possess renormalization-scale dependence, such that the full chiral correction up to $O(Q^4)$ is renormalization scale free. We will also provide the renormalization of d_i in the next subsection.

3.1.3 Renormalization of the low energy constants

In the last subsection we have illustrated the forms of the loop corrections under a well defined subtraction scheme. We claimed that the scalar-tadpole contribution from the bubble loops proportional to $m_Q^2 \bar{I}_Q$ can be absorbed into the Q^4 tadpole loop contributions by a suitable renormalization of the c_i . Indeed we derive the following

$$\begin{aligned} c_2^r &= c_2 + \frac{1}{8} g_P^2, & c_3^r &= c_3 - \frac{1}{4} g_P^2, \\ \tilde{c}_2^r &= \tilde{c}_2 + \frac{1}{12} \tilde{g}_P^2 + \frac{1}{24} g_P^2, & \tilde{c}_3^r &= \tilde{c}_3 - \frac{1}{6} \tilde{g}_P^2 - \frac{1}{12} g_P^2, \\ \tilde{c}_4^r &= \tilde{c}_4 - \frac{1}{8} \tilde{g}_P^2, & \tilde{c}_5^r &= \tilde{c}_5 + \frac{1}{4} \tilde{g}_P^2, \end{aligned} \quad (3.41)$$

We end up with the bubble loop contributions (3.35) and (3.36), where $m_Q^2 \bar{I}_Q$ dropped.

H	$\bar{\Pi}_H^{(2-\chi)}/(2M_H)$	$\bar{\Pi}_H^{\text{loop}}/(2M_H)$	Z_H		with loop	tree level
D	4.7 MeV	-50.2 MeV	1.108	M	1907.4 MeV	1862.7 MeV
D_s	106.2 MeV	-65.5 MeV	1.418	Δ	191.7 MeV	141.3 MeV
D^*	5.0 MeV	-113.4 MeV	1.163	c_1	0.440	0.426
D_s^*	114.1 MeV	-166.1 MeV	1.643	\tilde{c}_1	0.508	0.469

Table 3.3.: The loop functions (3.35,3.36) are evaluated with the coupling constants $g_p = \tilde{g}_p \simeq 0.57$ and the physical isospin averaged meson masses. The large- N_c relations (3.45) are assumed.

Renormalization-scale dependence is involved in the $O(Q^4)$ tadpole contributions (3.37), which is readily eliminated by the running behavior of the LECs d 's at order Q^4 as

$$\mu^2 \frac{d}{d\mu^2} d_i^r = -\frac{1}{4} \frac{1}{(4\pi f)^2} \Gamma_{d_i}^{(1)} \quad (3.42)$$

for d_i^r . The coefficients $\Gamma_{d_i}^{(1)}$ are

$$\begin{aligned} \Gamma_{d_1}^{(1)} &= \frac{1}{6}(4c_1 + 12c_3 + 3c_5), \\ \Gamma_{d_2}^{(1)} &= \frac{1}{9}(44c_1 - 52c_3 - 13c_5), \\ \Gamma_{d_3}^{(1)} &= \frac{1}{18}(240c_0 - 84c_1 + 240c_2 + 68c_3 + 60c_4 + 17c_5), \\ \Gamma_{d_4}^{(1)} &= \frac{1}{27}(264c_0 - 132c_1 + 264c_2 + 140c_3 + 66c_4 + 35c_5). \end{aligned} \quad (3.43)$$

The \tilde{d}_i^r manifest the same behavior. We just read off $\Gamma_{\tilde{d}_i}^{(1)}$ out of the corresponding $\Gamma_{d_i}^{(1)}$ by simply replacing c_i with \tilde{c}_i .

3.1.4 Numerical estimate on the importance of the bubble-loop corrections

In this section we provide a first numerical estimate on how much does the bubble loop corrections $\bar{\Pi}_H^{\text{loop}}$ affect the D -meson masses. We make a comparison with the numerical contribution of the $O(Q^2)$ (NLO) chiral correction $\bar{\Pi}_H^{2-\chi}$ according to (3.9). For the time being, we switch off the $O(Q^4)$ ($N^3\text{LO}$) contributions, $\bar{\Pi}_H^{4-\chi} = \bar{\Pi}_H^{\text{tadpole}} = 0$. The free parameters include the chiral-limit masses M , Δ , the LECs c_0 , c_1 and \tilde{c}_0 , \tilde{c}_1 at NLO and g_p , \tilde{g}_p at NNLO. We assert the heavy-quark symmetry in our estimate for \tilde{g}_p . This constraint leads to $\tilde{g}_p = g_p$ as we have seen in the last chapter. The value of g_p is derived from the $D^* \rightarrow \pi D$ decay width, which leads to [29]

$$g_p = \tilde{g}_p \simeq 0.57. \quad (3.44)$$

We estimate the values of the leading-order masses M , Δ and NLO LECs c_0 , c_1 and \tilde{c}_0 , \tilde{c}_1 from the physical D -meson masses m_D , m_{D_s} , m_D^* and $m_{D_s}^*$. An average within each isospin multiplet is assumed with $M_D = 1.8672\text{GeV}$, $M_{D_s} = 1.9683\text{GeV}$ and $M_{D^*} = 2.0086\text{GeV}$, $M_{D_s^*} = 2.1121\text{GeV}$. In the estimation of the NLO LECs, we allow a violation of heavy quark symmetry but assume the large N_c limit. Under the large N_c limit, the following relations hold,

$$c_0 = \frac{1}{2}c_1, \quad \tilde{c}_0 = \frac{1}{2}\tilde{c}_1. \quad (3.45)$$

The fitted parameters are collected in the second last column of Tab. 3.3. In the third column, we show the size of the bubble-loop contribution $\bar{\Pi}_H^{\text{loop}}$. As a comparison, we list the size of the NLO corrections $\Pi_H^{2-\chi}$ as well. We conclude that the bubble-loop corrections are as important as the NLO corrections and should not be neglected. We also display the size of the wave-function renormalization factor Z_H in the fourth column. We find that the wave function factor significantly deviates from 1 for the strange D -mesons. To this end, the wave-function renormalization effects from loops are not negligible in our flavor SU(3) framework. We also compare with the parameters determined by switching off all loop effects (shown in the last column of Tab. 3.3). We observe that the inclusion of the bubble loop corrections reasonably changes the values of the low-energy parameters.

3.2 The convergence of chiral expansions on the loop corrections

This section will be dedicated to performing a chiral expansion for the loop corrections. It has been perceived for a long time that a conventional chiral expansion fails already at physical quark masses, in particular due to the considerable size of the physical strange quark mass. The convergence property of the chiral expansion has been extensively studied especially for baryons (readers are referred to Ref. [95] for a comprehensive review). For the flavor SU(2) baryon chiral effective theories, it was demonstrated the convergence domain is up to around 300 MeV for the pion mass if a conventional heavy-baryon expansion scheme is followed [104–106]. This poor convergence results in a bad performance in applying the expanded chiral series to QCD lattice data, because the masses of Goldstone bosons are in part much larger than their physical values (e.g. [107, 108]). In the realistic world, the smallness of the convergence domain may impede the use of flavor SU(3) chiral effective theories, since kaon and eta are as heavy as 500 MeV. The analysis of the chiral expansion of the flavor SU(3) baryonic framework shows poor convergence as well, in the calculation of different baryonic observables [48]. One may expect the convergence of the chiral series in the open-charm meson sector could be better than baryonic sector since the mass of D -meson is much heavier than the light baryons. But the existing works disagree with this expectation. In Ref. [50], a study on the values of decay constants of D mesons from LQCD has been performed in a flavor SU(3) framework. The chiral expanded ChPT results exhibit a much poorer performance in fitting the lattice data as compared with the full covariant ChPT results.

One might be content with using the full un-expanded relativistic formalism (see e.g. calculations [109, 110, 47, 51] for the baryon spectroscopy, [46, 111] for the baryon axial currents, [50, 100] for the open-charm meson decay constants). But the full relativistic chiral effective theories including massive hadrons suffer from model dependence, which is embodied by the choice of a renormalization scheme. Different renormalization schemes lead to different higher chiral order contributions. If the chiral series fails to converge, we must admit that the higher order renormalization-scheme dependence could be even dominant. Another problem is the uncontrolled scale dependence we have discussed before. If we adopt the full relativistic formalism, the renormalization-scale dependence will rise at each chiral order [112]. Unless we provide the full chiral series of the counter terms that compensates the scale dependence (which is practically not feasible), our result will suffer from an artificial scale dependence. In the Sec.3.1.3, we removed the higher order μ -dependent terms such that the finite counter terms up to $O(Q^4)$ can fully control the renormalization-scale dependence. Such a treatment will be less convincing if the corresponding μ -independent part is kept to all orders. A convergent chiral expansion strategy can significantly systematize computations based on the flavour SU(3) chiral Lagrangian.

In this section we focus on four different kinds of chiral expansion schemes. Three different assumptions are assigned on the largeness of the D -meson mass splittings in comparison with the Goldstone-boson masses, ending up with the distinct expansion strategies of the loop functions. We will observe that the three expansions work well within different ranges of Goldstone-boson masses. But all of them fail to converge uniformly for Goldstone-boson masses ranging from the chiral limit to physical kaon and eta masses. In the last, we applied a novel chiral expansion scheme developed recently for the chiral extrapolation of the baryon octet and decuplet masses [52]. We will see that this expansion scheme

properly works when the Goldstone-boson masses varies from the chiral limit to the size of physical kaon and eta masses.

3.2.1 The convergence behavior in the heavy-quark mass limit

In this subsection we probe the asymptotic domain where the Goldstone boson is heavier than the mass splitting between the D -mesons. When the charm quark mass M_Q is sufficiently heavy, the hyperfine mass splitting between the 0^- and the 1^- D -mesons becomes sufficiently small such that $M_H - M_R \ll m_Q$ holds, where H and R are D -mesons with different spins and m_Q is a Goldstone-boson mass. We introduce the notation $H \perp R$ to characterize this case. This result is derived from the heavy-quark effective theory, which shows that the heavy-meson spin splitting effect is suppressed by the heavy quark mass,

$$M_H - M_R \sim \frac{\Lambda_{\text{QCD}}}{M_Q}. \quad (3.46)$$

Therefore, for a sufficiently large heavy quark mass and a properly large Goldstone-boson mass, the ratio $M_H - M_R/m_Q$ may be counted with

$$\frac{M_H - M_R}{m_Q} \sim Q \quad \text{for } H \perp R. \quad (3.47)$$

For the case when H and R have the same spin, denoted as $H \parallel R$, the mass difference $M_H - M_R$ is derived from the chiral correction starting from $O(Q^2)$ which implies the same counting rule

$$\frac{M_H - M_R}{m_Q} \sim Q \quad \text{for } H \parallel R. \quad (3.48)$$

To this end, we can get the power counting assumption

$$\frac{M_H - M_R}{m_Q} \sim \frac{m_Q}{M_R} \sim \frac{m_Q}{M_H} \sim Q, \quad \frac{M_H - M_R}{M_H} \sim Q^2. \quad (3.49)$$

At the physical value of the charm quark mass, the typical size of $M_H - M_R$ is 200 MeV. Thus the counting scheme is justified for the heavier Goldstone bosons. For the pion, this counting scheme is not a good approximation. However, since the bubble-loop contributions gets larger when the Goldstone-boson mass increases the kaon and eta meson contributions dominate the size of the loop. Therefore this approximation is illustrative in understanding the convergence behavior of a flavor SU(3) chiral corrections. Accurate to $O(Q^5)$, the bubble-loops are readily expanded with

$$\begin{aligned} \bar{\Pi}_{H \in [0^-]}^{\text{loop}} &= \sum_{Q \in [8]} \sum_{R \in [1^-]} \left(\frac{G_{QR}^{(H)}}{2f} \right)^2 \left\{ \alpha_{QR}^H + X_{QR}^{(H)} \right. \\ &\quad \left. + \frac{\gamma_R^H}{16\pi^2} M_H^2 m_Q^2 \left[1 - \left(\frac{m_Q}{2M_H} - \frac{M_R - M_H}{m_Q} \right)^2 \right] \right\} + \mathcal{O}(Q^6), \\ \bar{\Pi}_{H \in [1^-]}^{\text{loop}} &= \frac{2}{3} \sum_{Q \in [8]} \sum_{R \in [1^-]} \left(\frac{G_{QR}^{(H)}}{2f} \right)^2 X_{QR}^{(H)} + \frac{1}{3} \sum_{Q \in [8]} \sum_{R \in [0^-]} \left(\frac{G_{QR}^{(H)}}{2f} \right)^2 \left\{ \alpha_{QR}^H + X_{QR}^{(H)} \right. \\ &\quad \left. + \frac{\gamma_R^H}{16\pi^2} M_H^2 m_Q^2 \left[1 - \left(\frac{m_Q}{2M_H} - \frac{M_R - M_H}{m_Q} \right)^2 \right] \right\} + \mathcal{O}(Q^6), \end{aligned}$$

H	$\bar{\Pi}_H^{\text{loop}}/(2M_H)$	$\bar{\Pi}_H^{\text{loop-3}}/(2M_H)$	$\bar{\Pi}_H^{\text{loop-4}}/(2M_H)$	$\bar{\Pi}_H^{\text{loop-5}}/(2M_H)$
D	-50.2 MeV	-38.7 MeV	-29.4 MeV	22.8 MeV
D_s	-65.5 MeV	-93.2 MeV	27.3 MeV	2.4 MeV
D^*	-113.4 MeV	-135.1 MeV	19.0 MeV	6.3 MeV
D_s^*	-166.1 MeV	-308.3 MeV	99.8 MeV	61.8 MeV

Table 3.4.: The decomposition of the bubbles according to (3.49). The parameters involved are given by Tab. 3.3.

$$\begin{aligned}
X_{QR}^H = & M_H^2 \frac{m_Q^2}{16\pi^2} \left(\frac{m_Q^2}{M_H^2} + 2 \frac{M_R - M_H}{M_H} \right) - M_H^2 \frac{m_Q^2}{32\pi^2} \left(\frac{m_Q^2}{M_H^2} - 3 \frac{M_R - M_H}{M_H} \right) \log \frac{m_Q^2}{M_R^2} \\
& + M_H \frac{m_Q^3}{16\pi^2} \left[-\pi + \frac{3\pi}{2} \left(\frac{m_Q}{2M_H} - \frac{M_R - M_H}{m_Q} \right)^2 \right].
\end{aligned} \tag{3.50}$$

The odd-order terms in X_{QR}^H originate from the non-regular part of the scalar bubble I_{QR} (see the appendix). We can read off the 3rd, 4th and 5th order contributions from the above expression. Numerical results are shown in Table 3.4. Here we use our first estimate for the low-energy parameters $c_{0,1}$ and $\tilde{c}_{0,1}$ as displayed in the second last column of Tab. 3.3. The normalization factor of $2M_H$ is applied in order to make the dimension of the loop to be $[m]$. While the summation up to the 5th order correction qualitatively agree with the full result, the convergence is not well controlled owing to the smallness of the pion mass. This fact is manifest especially in the case of the D meson, where the bubble with an intermediate pion state plays an important role.

By construction, the counting rule (3.49) fails in the chiral regime where the light-quark masses approach zero. This is illustrated by Fig.3.2, where we plot the bubble-loop $\bar{\Pi}_H$ as a function of the Goldstone-boson masses in the flavor limit, $m_\pi = m_K = m_\eta$. The D -meson masses $M_D = M_{D_s}$ and $M_{D^*} = M_{D_s^*}$ are obtained by self-consistently solving the set of equations (3.9). The light-quark masses are determined according to the GOR relation. The parameters displayed in the second last column of Tab. 3.3 are again used. The 3rd, 4th and 5th order corrections are plotted in dashed, dotted and dash-dotted lines, in comparison with the full result plotted in the solid black line. We also provided the 6th order correction as a reference, plotted in a thin dash-dotted line. We notice that the 5th order approximation agrees with the full term quite well when m_π gets larger than about 300 MeV. Especially, in the case of the D -meson [Fig. 3.2(a)], there is a bending effect of the full bubble at ~ 550 MeV. This behavior is well recovered by the large mutual cancellation effect between the $(M_R - M_H)^2$ and the $(M_R - M_H)$ terms in 5th order correction. We can observe that these terms arise from the expansion of the non-regular part of the bubble (3.50). On the contrary, there is no convergence, when approximating the chiral limit, even when the higher order correction are considered. We observe from Fig. 3.2 that the 6th order correction shows a logarithmic divergence in the extreme chiral regime where the Goldstone-boson mass is significantly smaller than the heavy-meson mass splitting, characterized by $\Delta \sim 200$ MeV. This logarithm is absent in the full \bar{I}_{QR} , it is unavoidable in the the given expansion scheme.

3.2.2 The convergence behavior in the light-quark mass limit

In the last subsection, we observed that the expansion according to the counting scheme $M_R - M_H/m_Q \sim Q$ respects the asymptotic domain well where the heavy-meson mass splitting is significantly smaller than the Goldstone boson mass. This is a good approximation in the limit when the heavy quark mass tends to infinity. In the case of physical charm quark mass, this is still a good approximation for the heavier Goldstone bosons kaon and eta. But this expansion doesn't fit for the loops involving the pion, because the

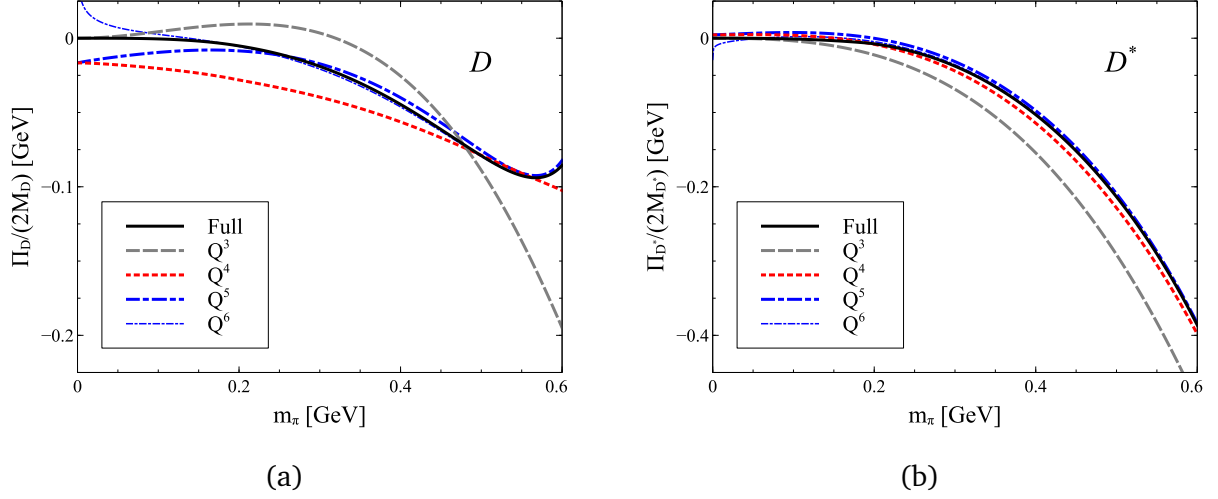


Figure 3.2.: The decomposed bubble loops $\bar{\Pi}_{D/D^*}^{\text{loop}}$ according to (3.49), as functions of the light quark masses.

pion mass locates in the extreme chiral regime where the Goldstone-boson mass is significantly smaller than the characteristic D -meson mass-splitting $\Delta \sim 200$ MeV. In this regime, a strict chiral expansion is a good approximation. The strict chiral expansion is performed according to the counting scheme

$$\frac{m_Q}{\Delta} \sim Q, \quad \frac{\Delta}{M} \sim Q^0. \quad (3.51)$$

The chiral-limit D meson mass M serves as hard scale, which we assume to be of similar size as the chiral symmetry breaking scale, Λ_χ , $M \sim \Lambda_\chi$. The physical masses of the D -mesons are expanded according to the chiral corrections,

$$M_{H \in [0^-]}^2 = M^2 + \Pi_H^{(2)} + \Pi_H^{(3)} + O(Q^4), \quad M_{H \in [1^-]}^2 = (M + \Delta)^2 + \Pi_H^{(2)} + \Pi_H^{(3)} + O(Q^4), \quad (3.52)$$

where $\Pi_H^{(n)}$ is the n -th order chiral correction of the D -meson mass. In turn the bubble loops are decomposed as

$$\bar{\Pi}_{H \in [0^-]}^{\text{loop-3}} = 0 \quad \bar{\Pi}_{H \in [1^-]}^{\text{loop-3}} = -\frac{2}{3} \sum_{Q \in [8]} \sum_{R \in [1^-]} \left(\frac{G_{QR}^H}{8\pi f} \right)^2 \pi m_Q^3 (M + \Delta), \quad (3.53)$$

at third order, and

$$\begin{aligned} \bar{\Pi}_{H \in [0^-]}^{\text{loop-4}} &= \sum_{Q \in [8]} \sum_{R \in [1^-]} \left(\frac{G_{QR}^H}{8\pi f} \right)^2 \left\{ \gamma_d^{(1)} m_Q^2 \Pi_R^{(2)} + \gamma_d^{(2)} m_Q^2 \Pi_H^{(2)} + \gamma_d^{(3)} \Pi_R^{(2)} \Pi_R^{(2)} + \gamma_d^{(4)} \Pi_H^{(2)} \Pi_H^{(2)} \right. \\ &\quad \left. + \gamma_d^{(5)} \Pi_R^{(2)} \Pi_H^{(2)} + \frac{M}{\Delta} m_Q^4 \left[(\alpha_2 \gamma_2 - \alpha_1 \gamma_4) + (\alpha_2 \gamma_3 - \alpha_1 \gamma_5) \log \frac{m_Q^2}{(M + \Delta)^2} \right] \right\}, \\ \bar{\Pi}_{H \in [1^-]}^{\text{loop-4}} &= \sum_{Q \in [8]} \sum_{R \in [0^-]} \left(\frac{G_{QR}^H}{8\pi f} \right)^2 \left\{ \tilde{\gamma}_d^{(1)} m_Q^2 \Pi_R^{(2)} + \tilde{\gamma}_d^{(2)} m_Q^2 \Pi_H^{(2)} + \tilde{\gamma}_d^{(3)} \Pi_R^{(2)} \Pi_R^{(2)} + \tilde{\gamma}_d^{(4)} \Pi_H^{(2)} \Pi_H^{(2)} \right. \\ &\quad \left. + \tilde{\gamma}_d^{(5)} \Pi_R^{(2)} \Pi_H^{(2)} + \frac{M}{\Delta} m_Q^4 \left[(\tilde{\alpha}_2 \tilde{\gamma}_2 - \tilde{\alpha}_1 \tilde{\gamma}_4) + (\tilde{\alpha}_2 \tilde{\gamma}_3 - \tilde{\alpha}_1 \tilde{\gamma}_5) \log \frac{m_Q^2}{M^2} \right] \right\} \end{aligned}$$

$$\begin{aligned}
& + \sum_{Q \in [8]} \sum_{R \in [1^-]} \left(\frac{G_{QR}^H}{8\pi f} \right)^2 \frac{2}{3} \left\{ m_Q^2 (m_Q^2 - \Pi_H^{(2)} + \Pi_R^{(2)}) \right. \\
& \left. - \frac{1}{4} (2m_Q^2 + 3\Pi_H^{(2)} - 3\Pi_R^{(2)}) m_Q^2 \log \frac{m_Q^2}{(M + \Delta)^2} \right\}, \tag{3.54}
\end{aligned}$$

at fourth order. We organize the prefactor of each term in terms of some dimensionless coefficients α_n , γ_n and $\tilde{\alpha}_n$, $\tilde{\gamma}_n$. They depend on the ratio Δ/M only. While the coefficients γ_n , $\tilde{\gamma}_n$ characterize the chiral expansion of the scalar bubble functions, the α_n , $\tilde{\alpha}_n$ result from a chiral expansion of the coefficients in front of the scalar loop functions. All such coefficients are provided in Appendix E. The fifth order contribution for the vector D -mesons read as

$$\begin{aligned}
\bar{\Pi}_{H \in [1^-]}^{\text{loop-5}} & = \sum_{Q \in [8]} \sum_{R \in [1^-]} \left(\frac{G_{QR}^{(H)}}{8\pi f} \right)^2 \frac{1}{12} \frac{\pi m_Q}{M + \Delta} \left\{ 3m_Q^4 + 2m_Q^2 (\Pi_H^{(2)} - 3\Pi_R^{(2)}) \right. \\
& \left. + 3(\Pi_H^{(2)} - \Pi_R^{(2)})^2 \right\} + \dots \tag{3.55}
\end{aligned}$$

where the dots stand for additional terms constructed from (3.54) by the replacement $\Pi^{(2)} \rightarrow \Pi^{(3)}$. The fifth order terms for the pseudo-scalar D -mesons are completely derived from (3.54) with the replacement $\Pi^{(2)} \rightarrow \Pi^{(3)}$.

The strict expanded forms are free from order m_Q^0 and m_Q^2 chiral logarithms of the form $\sim \log m_Q$ or $\sim m_Q^2 \log m_Q$. The potential $O(m_Q^0)$ chiral logarithm from the scalar-bubble (see (3.34)) is compensated by the chiral logarithm from the strict chiral expansion of the last term in (3.34)². A further cancellation mechanism prevents the contribution of a possible $m_Q^2 \log m_Q$ chiral logarithm. The contribution from the scalar tadpole contribution is proportional to α_4 (or $\tilde{\alpha}_4$). It is compensated by a corresponding term from the chiral expansion of the scalar-bubble, proportional to $\alpha_1 \gamma_3$ (or $\tilde{\alpha}_1 \tilde{\gamma}_3$) (see also Appendix E). Our claim follows from

$$\frac{1}{2} \alpha_4 = \alpha_1 \gamma_3, \quad \frac{1}{2} \tilde{\alpha}_4 = -\tilde{\alpha}_1 \tilde{\gamma}_3, \tag{3.56}$$

In the off-diagonal case, the convergence of the strict chiral expansion is seriously constrained by a threshold condition. For $H \in [0^-]$ and $R \in [1^-]$, as an example, the origin of the expansion is $M_H = M$, $M_R = M + \Delta$ and $m_Q = 0$. The convergence domain is restricted according to the location of the threshold condition $m_Q < |M_H - M_R|$. If we neglect the $O(m_Q^2)$ corrections for the D -meson masses, the convergence radius is characterized by the hyperfine-splitting between the D -mesons Δ ,

$$m_Q \lesssim \Delta. \tag{3.57}$$

Only within the strict chiral regime, where the Goldstone-boson masses are much smaller than the characteristic hyperfine-splitting scale Δ , such an expansion is applicable.

This highly restricted convergence behavior is depicted by plotting the bubble-loops $\bar{\Pi}_H$ as functions of the Goldstone-boson masses in the flavor limit, $m_\pi = m_K = m_\eta$, as we did in the last section. The D -meson masses are, again, obtained according to the self-consistent approach, using the same setup of the parameters as the plots of the last section. The plots have been given in Fig. 3.3. The gray vertical line indicates the location of Δ . We can observe that this expansion fails when the pion mass reaches Δ . This expansion is clearly not a good approximation for a flavor SU(3) description of the chiral corrections for the D -meson masses: the mass splitting scale Δ is as small as some of the Goldstone-boson masses.

² This correlation was broken in the expansion of the last section. In that case the $O(m_Q^0)$ chiral logarithm from the last term in (3.34) can only be obtained upon a summation of all odd-power components. The breaking of this correlation leads to the logarithmic divergence in the chiral limit from the 6th order correction according to the expansion of the last section.

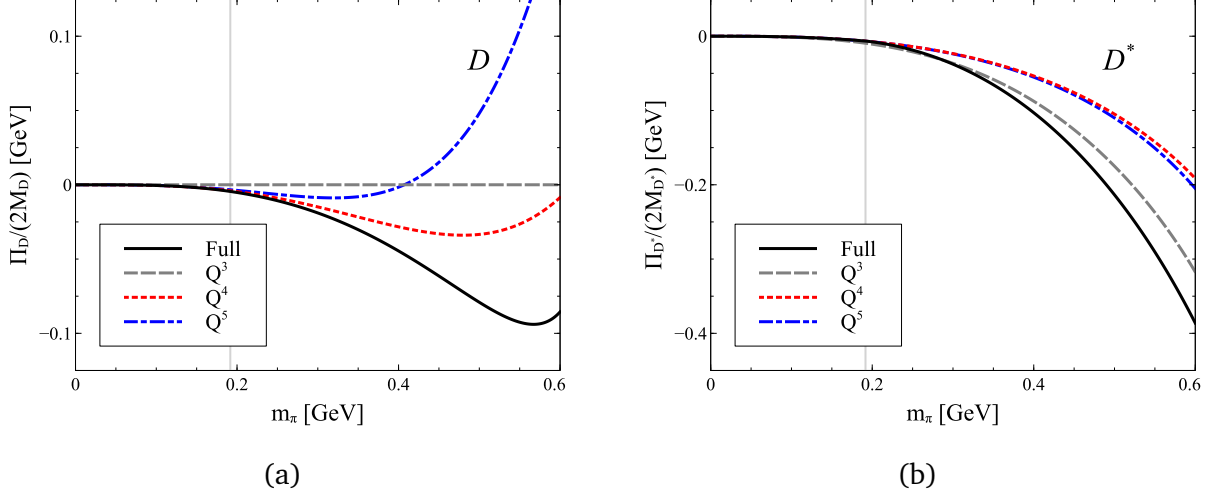


Figure 3.3.: The decomposed bubble loops $\Pi_{D/D^*}^{\text{loop}}$ according to (3.51), as functions of the light quark masses.

3.2.3 The convergence behavior in a small-scale expansion

In the last subsection we have seen that the convergence of a strict chiral expansion assuming $\Delta/M \sim Q^0$ is highly limited to the extreme chiral regime where the Goldstone-boson masses are much smaller than the D -meson hyperfine splitting Δ . An approach to improve the convergence behavior is to consider the hyperfine splitting as a soft scale with $\Delta \sim m_Q$. According to this we will use the following counting rules

$$\Delta \sim m_Q \sim Q, \quad \Delta_Q = \sqrt{\Delta^2 - m_Q^2} \sim Q. \quad (3.58)$$

This expansion scheme is referred to as a small-scale expansion (SSE) scheme [113–116]. The full bubble loops are accordingly expanded as

$$\begin{aligned} \bar{\Pi}_{H \in [0^-]}^{\text{loop}} &= \sum_{Q \in [8]} \sum_{R \in [1^-]} \left(\frac{G_{QR}^{(H)}}{2f} \right)^2 \frac{1}{16\pi^2} \left\{ -\frac{1}{2} M \Delta m_Q^2 \right. \\ &\quad + \frac{m_Q^2}{4} (-3\Delta^2 + 4m_Q^2 - 4\Pi_H + 4\Pi_R) - \frac{m_Q^2}{4} (2m_Q^2 + 3\Pi_H - 3\Pi_R) \log \frac{m_Q^2}{M^2} \\ &\quad + M \left[\left(\Delta_Q^2 - \frac{m_Q^2}{2} \right) + \frac{3\Delta}{2M} \left(\Delta_Q^2 - \Pi_H + \Pi_R - \frac{m_Q^2}{2} \right) \right] \left(2\Delta \log \frac{2\Delta}{M} - \Delta \log \frac{m_Q^2}{M^2} \right) \\ &\quad \left. - M \left(\Delta_Q^2 + \frac{3\Delta}{2M} (\Delta_Q^2 - \Pi_H + \Pi_R) \right) \Delta_Q \left(\log(\Delta + \Delta_Q) - \log(\Delta - \Delta_Q) \right) \right\} \\ \bar{\Pi}_{H \in [1^-]}^{\text{loop}} &= \sum_{Q \in [8]} \sum_{R \in [1^-]} \left(\frac{G_{QR}^{(H)}}{2f} \right)^2 \frac{1}{24\pi^2} \left\{ m_Q^2 (m_Q^2 - \Pi_H + \Pi_R) \right. \\ &\quad \left. - \frac{m_Q^2}{4} (2m_Q^2 + 3\Pi_H - 3\Pi_R) \log \frac{m_Q^2}{M^2} - \pi M m_Q^3 \left(1 + \frac{\Delta}{M} \right) \right\} \\ &\quad + \sum_{Q \in [8]} \sum_{R \in [0^-]} \left(\frac{G_{QR}^{(H)}}{2f} \right)^2 \frac{1}{48\pi^2} \left\{ \frac{1}{2} M \Delta m_Q^2 + \frac{m_Q^2}{4} (-\Delta^2 + 4m_Q^2 - 4\Pi_H + 4\Pi_R) \right. \\ &\quad \left. - \frac{m_Q^2}{4} (2m_Q^2 + 3\Pi_H - 3\Pi_R) \log \frac{m_Q^2}{M^2} \right\} \end{aligned}$$

H	$\bar{\Pi}_H^{\text{loop}}/(2M_H)$	$\bar{\Pi}_H^{\text{loop-3}}/(2M_H)$	$\bar{\Pi}_H^{\text{loop-4}}/(2M_H)$	$\bar{\Pi}_H^{\text{loop-5}}/(2M_H)$
D	-50.2 MeV	-67.7 MeV	15.0 MeV	-8.9 MeV
D_s	-65.6 MeV	-152.8 MeV	27.8 MeV	26.6 MeV
D^*	-113.4 MeV	-111.7 MeV	-57.1 MeV	18.6 MeV
D_s^*	-166.1 MeV	-252.0 MeV	84.3 MeV	-69.5 MeV

Table 3.5.: The decomposition of the bubbles according to (3.58). The parameters involved are given by Tab. 3.3.

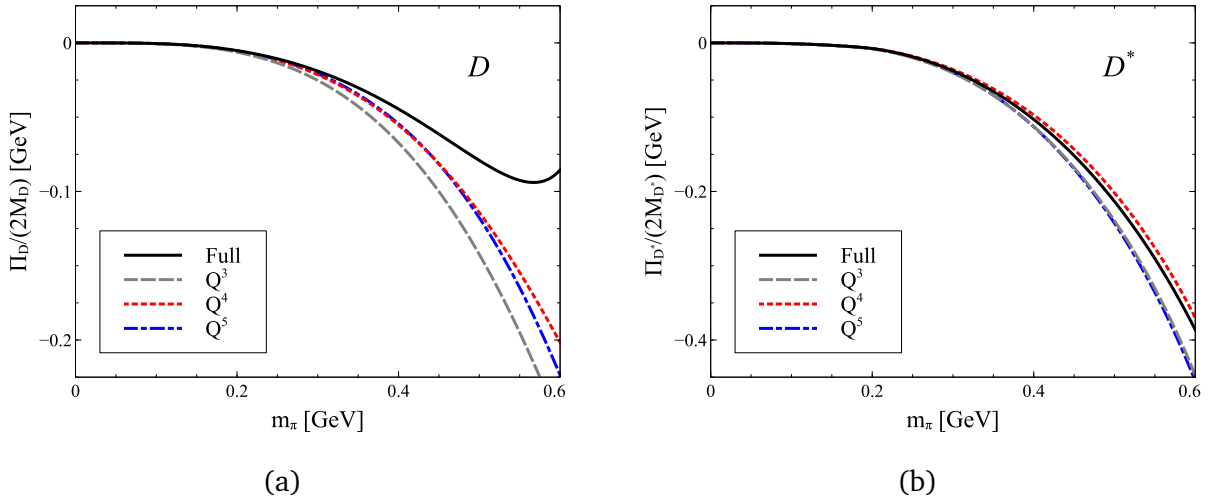


Figure 3.4.: The decomposed bubble loops $\Pi_{D/D^*}^{\text{loop}}$, according to (3.58), as functions of the light quark masses.

$$\begin{aligned}
& -M \left[\left(\Delta_Q^2 - \frac{m_Q^2}{2} \right) - \frac{\Delta}{2M} \left(\Delta_Q^2 - 3\Pi_H + 3\Pi_R - \frac{m_Q^2}{2} \right) \right] \left(2\Delta \log \frac{2\Delta}{M} - \Delta \log \frac{m_Q^2}{M^2} \right) \\
& + M \left[\Delta_Q^2 - \frac{\Delta}{2M} \left(\Delta_Q^2 - 3\Pi_H + 3\Pi_R \right) \right] \Delta_Q \left(\log(-\Delta - \Delta_Q) - \log(-\Delta + \Delta_Q) \right) \Bigg\}, \tag{3.59}
\end{aligned}$$

up to $O(Q^4)$. The fifth order correction is listed in Appendix E.

The numerical results up to the fifth order corrections are listed in Table 3.2.3. The convergence behavior is not as good as one might have expected. We further plot the expanded bubble loops according to the variable $m_\pi = m_K = m_\eta$ in the flavor limit, as we did in the previous two expansions. The plots are shown in Fig. 3.4. We observe that the convergence is improved when m_π is larger than Δ . But the expansion still manifests a poor convergence behavior when the Goldstone-boson mass is larger than about 300 MeV. The failure of the convergence is especially significant for the D meson case at around $m_\pi \sim 550$ MeV, where the full curve bends up. We recall that the expansion according to the first power-counting scenario (3.49) significantly recovers this bend at the 5th order, where a large cancellation between $(M_R - M_H)$ component and $(M_R - M_H)^2$ component from the non-regular part of the scalar-bubble took place. It is obvious that this expansion spoils the correlations between the $M_R - M_H$ components in the non-regular part.

3.2.4 A novel chiral-expansion pattern

Up to now we have investigated three different kinds of chiral expansion approaches on the bubble loop corrections. The first expansion allows a small heavy-meson mass-splitting $M_H - M_R/m_Q \sim Q$, which is justified at large Goldstone-boson masses $m_Q \sim m_K$. On the contrary, the second expansion, a strict chiral expansion regarding $m_Q/\Delta \sim Q$, works only when m_Q is much smaller than the characteristic mass splitting Δ . As a remedy, the third approach treats $\Delta \sim m_Q \sim Q$, and was expected to extend the convergence domain from the extreme chiral regime towards larger quark masses. But as we illustrated, this approach only qualitatively reproduce the trend of the full-loop behavior when the Goldstone-boson mass increases. Especially when the Goldstone-boson meson reaches the physical kaon mass, there is no convergence pattern observed.

In this section we aim to bridge the different expansion approaches, which work in different regimes of Goldstone-boson masses, into a uniformly convergent framework. It is an adaptation of the expansion scheme developed recently for the chiral extrapolation of the baryon octet and decuplet masses [52]. This scheme is supposed to interpolate the two extreme counting rules (3.49) and (3.51) into a novel counting rule

$$\begin{aligned} \frac{M_R - M_H}{m_Q} \sim Q, & \quad \frac{M_R - M_H}{M_H} \sim Q^2 & \quad \text{for } H \parallel R, \\ \frac{M_R - M_H}{m_Q} \sim Q^0, & \quad \frac{M_R - M_H \pm \Delta_H}{M_H} \sim Q^2 & \quad \text{for } H \perp R \\ \Delta_Q = \sqrt{(M_H - M_R)^2 - m_Q^2} \sim Q & \quad \text{with } \Delta_H = \Delta M_H \lim_{m_{u,d,s} \rightarrow 0} \frac{1}{M_H}, \end{aligned} \quad (3.60)$$

The driving idea behind this counting rule (3.60) is to formulate the expansion coefficients in terms of physical masses. A lot of comments have been made on the poor convergence of conventional chiral expansions [94, 54, 95, 117]. A significant source of such an unpleasant behavior is assigned to the butchering of the analytic structure as implied by the micro causality constraint of local quantum field theories. As a typical example of how unphysical analytic properties affect the convergence domain of a chiral expansion, we have already seen that the convergence domain of a strict chiral expansion is limited by an inappropriate treatment of a close-by threshold branch point (see Eq.(3.57), in Section 3.2.2). Keeping the physical masses in the expansion is of crucial importance in preserving critical analytic properties.

The threshold branch points constitute the most important analytic property of the bubble loop diagram. The threshold behavior of the scalar loop function is driven by the phase-space factor p_{QR} as introduced in (3.34). The phase space factor vanishes at $M_H^2 = (M_R \pm m_Q)^2$. We rewrite p_{QR} into

$$p_{QR}(M_H^2) = \frac{1}{2M_H} \Delta_Q \sqrt{(M_R + M_H)^2 - m_Q^2}, \quad (3.61)$$

where Δ_Q is defined according to (3.60). The factor Δ_Q vanishes at $(M_R - M_H)^2 = m_Q^2$ only, resulting in the branch point of the bubble loop at the normal threshold $M_H = M_R + m_Q$. Any expansion violating this correlation will fail to converge when the branch point is crossed by a variation of m_Q . The second zero point at $(M_R + M_H)^2 - m_Q^2$ in (3.61) is far from being reached by any physical values of m_Q . To this end, for the off-diagonal loops, we keep the exact structure Δ_Q in our novel expansion. For the diagonal loops, it always holds $M_H - M_R \ll m_Q$. In turn it would be justified to further expand Δ_Q in this case.

For an illustration of our expansion approach, it is convenient to express the loops in terms of the following dimensionless quantities [52]

$$d = \frac{M_R}{M_H} - 1, \quad x = \frac{m_Q}{M_H}. \quad (3.62)$$

with the physical masses M_H, M_R and m_Q . The counting scheme (3.60) can be expressed in terms of d and x as

$$\begin{aligned} \frac{d}{x} &\sim Q, & x &\sim Q, & d &\sim Q^2, & \text{for } H \parallel R, \\ \frac{d}{x} &\sim Q^0, & x &\sim Q, & d - d_0 &\sim Q^2 & \text{for } H \perp R, \\ x_d = \sqrt{d^2 - x^2} &\sim Q, & \text{with } d_0 &= \lim_{m_{u,d,s} \rightarrow 0} d. \end{aligned} \quad (3.63)$$

The scalar bubble \bar{I}_{QR} is readily expanded accordingly

$$\begin{aligned} (4\pi)^2 \bar{I}_{QR} &= \gamma_H^R + f_1^{(d)}(x^2) f_0^{(d)}(x^2) \\ &\quad - d(2+d) \log \frac{2(1+d)}{2+d} + \sum_{k=1}^{\infty} x^{2k} \frac{\delta_{2k}^{(d)}}{d^{2k-1}} \\ &\quad + d(2+d) \log \frac{x}{1+d} + \sum_{k=1}^{\infty} x^{2k} \frac{\delta_{2k+1}^{(d)}}{d^{2k-1}} \log \frac{x^2}{(1+d)^2}. \end{aligned} \quad (3.64)$$

where,

$$\begin{aligned} f_0^{(d)} &= x_d \left(\log(d + x_d) - \log(d - x_d) \right), \\ f_1^{(d)} &= 1 + \frac{d}{2} - \frac{x^2}{2(2+d)} - \frac{1}{16} \frac{x^4}{(2+d)^3} + O(x^6). \end{aligned} \quad (3.65)$$

The $\delta_i^{(d)}$ s up to $i = 5$ can be read off from the definition of δ_i in Appendix E by performing the substitution $M \rightarrow 1$, $\Delta \rightarrow d$. The expression (3.64) is valid for all the $d > 0$, $d < 0$ and $d = 0$. The expansion (3.64) is analytic at $d = 0$, no pole structure or branch point shows up at this point. In (3.64) no assumption on the size of d was made yet. Therefore the full realization of the counting rules (3.63) may require further expansions. All coefficients $\delta_k^{(d)}$ are analytic functions in d with branch points at $d = -1$ and $d = -2$ only. In the limit $d \rightarrow 0$ they all approach a finite value with $\delta_{2k}^{(d)} \sim \delta_{2k+1}^{(d)} \sim d^{2k-1}$.

The scalar bubble is expanded along three structures, the threshold-respecting part ($\sim f_0^{(d)}$), the chiral logarithm part (the third line in Eq.(3.64)) and the polynomial part (the second line in Eq.(3.64)). According to Ref. [52], there is an intricate cancellation mechanism between these three terms when x departs from zero. The general expansion approach is nicely illustrated by the particular case $d = 0$ (see Ref. [52]). In the limit $d = 0$, which is reached by the condition $M_H = M_R$, the function $f_0^{(d)}$ is simplified to

$$f_0^{(d=0)}(x^2) = -\pi \sqrt{x^2}. \quad (3.66)$$

The full expansion (3.64) is reduced to

$$\begin{aligned} (4\pi)^2 \bar{I}_{QR}^{(d=0)} &= - \left(1 - \frac{1}{8} x^2 - \frac{1}{128} x^4 + O(x^6) \right) \pi \sqrt{x^2} \\ &\quad + \left(1 - \frac{1}{12} x^2 - \frac{1}{120} x^4 + O(x^6) \right) x^2 - x^2 \log x. \end{aligned} \quad (3.67)$$

It is observed in [52], that there is a significant cancellation between the leading order contribution $f_0^{(d)}(x^2)$, $-\pi \sqrt{x^2}$, and the leading order polynomial contribution x^2 as well as the chiral logarithm

$x^2 \log x^2$. Therefore we group together the $-\pi \sqrt{x^2}$ and the terms $\sim x^2$ to form the leading order term for $\bar{I}_{QR}^{(d=0)}$,

$$(4\pi)^2 \bar{I}_{QR}^{(d=0)} [O(Q)] = -\pi \sqrt{x^2} + x^2 - x^2 \log x. \quad (3.68)$$

The n -th order contribution of $\bar{I}_{QR}^{(d=0)}$ is determined by picking up the n -th term from the two brackets in front of the two terms $\pi \sqrt{x^2}$ and x^2 in (3.67). It was proven in Ref. [52] that such an expansion converges rapidly for $|x| < 2 + d$, a surprisingly large convergence domain.

In the off-diagonal case, a significantly sized d may be encountered. In this case, another scale is necessarily involved, which is the chiral-limit mass difference Δ . The chiral expansion around this scale has been arranged according to the counting scheme $d - d_0 \sim Q^2$ from Eq.(3.63). Note that strict consistency with the chiral domain at $x < d_0$ requires to consider $d_0 \sim Q^0$. In the off-diagonal case, we meet two terms that are proportional to the mass difference d , which are the first terms in the second and third line of Eq.(3.64) respectively. We follow the counting rule (3.63) to consider them as $O(Q)$. If we replaced those linear terms with $d \rightarrow d_0$ at leading order we would obtain contributions of order Q^0 at $x < d_0$. Moreover the chiral logarithm terms proportional to $d \log x$ would not be canceled properly in the chiral regime. This is seen from the following expansion

$$f_0^{(d)} \rightarrow -d \log \frac{x^2}{4d^2} + \frac{x^2}{2d} \left(\log \frac{x^2}{4d^2} - 1 \right) + O(x^4). \quad (3.69)$$

By substituting the above expression into (3.64), a full cancellation between the chiral logarithm proportional to d has been implemented when x approaches the chiral limit.

We are prepared to recall the leading order contributions of the full scalar-bubble at $d \neq 0$. It is emphasized that the full $f_0^{(d)}$ has to be kept in order not to butcher the critical analytic property of the loop function. Consistency with the chiral domain requires the presence of some linear terms in d . Altogether we find,

$$(4\pi)^2 \bar{I}_{QR} [O(Q)] = \gamma_H^R + \left(1 + \frac{d_0}{2} \right) f_0^{(d)}(x^2) - d(2 + d_0) \log \frac{2(1 + d_0)}{2 + d_0} + \frac{\delta_2^{(d_0)}}{d_0} x^2 \\ + d(2 + d_0) \log \frac{x}{1 + d} + \frac{\delta_3^{(d_0)}}{d_0} x^2 \log \frac{x^2}{(1 + d)^2}. \quad (3.70)$$

The order Q^2 contribution is the $O(d - d_0)$ correction of the leading order term. The $O(Q^3)$ term consists of the $O[(d - d_0)^2]$ correction of the leading order term, and the once x^2 power higher correction of the leading order term. According to [52], an M_R dependence in the logarithm has been kept, because this is the natural structure generated in loop diagrams.

3.2.4.1 The third order chiral correction of the one-loop self energy

Having reviewed the chiral expansion scheme for the scalar bubble, we are ready to perform the chiral expansion for the full bubble functions as they are needed in the D meson polarization tensors. We derive the order Q^3 and Q^4 chiral corrections in this subsection. The $O(Q^5)$ terms are presented in Appendix E.

For the diagonal-diagram bubble-loop contribution, when H and R come from the same spin multiplet, the $O(Q^3)$ contribution reads,

$$\Pi_{H \in [1^-]}^{(3-\chi)} = M_H \sum_{Q \in [8], R \in [1^-]} \left(\frac{G_{QR}^{(H)}}{4\pi f} \right)^2 \frac{1}{6} \left\{ \frac{m_Q^2}{M_H} \left(1 - \log \frac{m_Q}{M_R} \right) - \pi m_Q \right\} (m_Q^2 - (M_R - M_H)^2), \quad (3.71)$$

Note that such a diagonal contribution appears for the $[1^-]$ meson loop corrections only. The correlation amongst the m_Q and m_Q^2 in the scalar bubble as shown in Eq.(3.68) has been respected. We keep the factor $m_Q^2 - (M_R - M_H)^2$ in front of the LO scalar bubble contribution derived from the phase space factor $d^2 - x^2$. The overall scale M_H , which is the typical mass scale of the chiral corrections of a charmed-meson polarization tensor, is pulled out.

So far with the diagonal contributions, we consider the $O(Q^3)$ off-diagonal bubble contributions to both the pseudo-scalar and vector charmed-meson masses. The off-diagonal contribution accounts for the full $O(Q^3)$ chiral correction of the pseudo-scalar meson self-energy,

$$\begin{aligned} \Pi_{H \in [0^-]}^{(3)} = & \sum_{Q \in [8], R \in [1^-]} \left(\frac{1}{4\pi f} G_{QR}^{(H)} \right)^2 \frac{\alpha_1}{4} \left\{ \delta_7 \Delta M m_Q^2 + \delta_6 \Delta^2 M (M_R - M_H - \Delta_H) \right. \\ & + M_H \left[\Delta_Q^2 (\gamma_1 \Delta_H - \delta_1 (M_R - M_H)) \right. \\ & - \frac{2M + \Delta}{2M} \left((M_R - M_H) \left(\Delta_Q^2 - \frac{m_Q^2}{2} \right) \log \frac{m_Q^2}{M_R^2} \right. \\ & \left. \left. + \Delta_Q^3 \left[\log (M_R - M_H + \Delta_Q) - \log (M_R - M_H - \Delta_Q) \right] \right) \right] \\ & \left. \left. + \frac{m_Q^2}{\Delta_H} \left(-\delta_2 \Delta_Q^2 + \delta_3 m_Q^2 \log \frac{m_Q^2}{M_R^2} \right) \right] \right\}, \end{aligned} \quad (3.72)$$

where the coefficients γ_i , δ_i and α_i are provided in Appendix E.

The phase-space factor Δ_Q^2 in front of the scalar bubble is kept. In the extreme chiral regime, the chiral logarithms at powers m_Q^0 and m_Q^2 must vanish, as a result of chiral Ward identities. The cancellation at power m_Q^0 is implemented as a consequence of the scalar-bubble expansion (3.68). In contrast, a possible chiral logarithm at power m_Q^2 is absent owing to an interplay of the scalar bubble and the scalar tadpole using the identity (3.56). The expansion of the scalar-tadpole contribution is organized to preserve this cancellation. We point at the importance the δ_6 term in (3.72). It ensures that wave-function factor vanishes in the chiral limit

$$\lim_{m, m_s \rightarrow 0} \frac{\partial}{\partial M_H^2} \bar{\Pi}_H^{\text{loop-3}} = 0. \quad (3.73)$$

We note that this is a property that is also satisfied by the full loop expression.

According to the same approach, the off-diagonal contribution of the $O(Q^3)$ charmed vector-meson self-energy chiral correction is well determined. We collect the full $O(Q^3)$ chiral correction for the charmed vector-meson self-energy as

$$\begin{aligned} \Pi_{H \in [1^-]}^{(3)} = & \Pi_{H \in [1^-]}^{3-\chi} + \sum_{Q \in [8], R \in [0^-]} \left(\frac{G_{QR}^{(H)}}{4\pi f} \right)^2 \frac{\tilde{\alpha}_1}{12} \left\{ \tilde{\delta}_7 \Delta M m_Q^2 - \tilde{\delta}_6 \Delta^2 M (M_R - M_H + \Delta_H) \right. \\ & + M_H \frac{M}{M + \Delta} \left[\Delta_Q^2 (\tilde{\gamma}_1 \Delta_H - \tilde{\delta}_1 (M_H - M_R)) \right. \\ & + \frac{M(2M + \Delta)}{2(M + \Delta)^2} \left((M_H - M_R) \left(\Delta_Q^2 - \frac{m_Q^2}{2} \right) \log \frac{m_Q^2}{M_R^2} \right. \\ & \left. \left. + \Delta_Q^3 \left[\log (M_R - M_H - \Delta_Q) - \log (M_R - M_H + \Delta_Q) \right] \right) \right] \\ & \left. \left. + \frac{m_Q^2}{\Delta_H} \left(-\tilde{\delta}_2 \Delta_Q^2 + \tilde{\delta}_3 m_Q^2 \log \frac{m_Q^2}{M_R^2} \right) \right] \right\}, \end{aligned} \quad (3.74)$$

The coefficients $\tilde{\delta}_i$, $\tilde{\delta}_i$ and $\tilde{\alpha}_1$ are provided in Appendix E. We recall Eq.(3.71) for the diagonal contribution $\Pi_H^{3-\chi}$. The chiral expanded form at this order provides us a subtraction-scheme independent expectation of the $O(Q^3)$ covariant bubble-loop chiral correction [52].

We proceed and provide the order Q^4 corrections. The explicit $O(Q^4)$ contribution from an off-diagonal bubble loop comes from the $(d - d_0)$ correction of the $O(Q^3)$ contribution, noticing $(d - d_0) \sim Q$. In comparison, we assert the power counting for the diagonal case with $d \sim Q^2$. Therefore, the $O(Q^4)$ diagonal bubble-loop contribution mainly consists of $d x^2$ terms. These terms experienced a strong cancellation with the non-analytical contribution ($\sim \pi d x^2 \sqrt{x}$). We incorporate this cancellation at this order [52].

We collect $O(Q^4)$ bubble-loop chiral corrections as

$$\begin{aligned} \bar{\Pi}_{H \in [0^-]}^{\text{loop-4}} = & \sum_{Q \in [8], R \in [1^-]} \left(\frac{G_{QR}^{(H)}}{4\pi f} \right)^2 \left\{ -\frac{1}{4} \alpha_1 M \Delta^2 \delta_6 + \frac{M_H}{4} \left[\alpha_1 \Delta^2 \frac{\partial \Delta \gamma_1}{\partial \Delta} + \Delta_Q^2 \beta_4 \right. \right. \\ & - \Delta_Q^2 \beta_5 \frac{M_R - M_H}{\Delta_H} - \frac{\beta_1}{\Delta_H} \left((M_R - M_H) \left(\Delta_Q^2 - \frac{m_Q^2}{2} \right) \log \frac{m_Q^2}{M_R^2} \right. \\ & \left. \left. + \Delta_Q^3 \left[\log(M_R - M_H + \Delta_Q) - \log(M_R - M_H - \Delta_Q) \right] \right) \right. \\ & \left. \left. + \frac{m_Q^2}{\Delta_H^2} \left(-\beta_1 \Delta_Q^2 + \beta_3 m_Q^2 \log \frac{m_Q^2}{M_R^2} \right) \right\} (M_R - M_H - \Delta_H), \end{aligned} \quad (3.75)$$

$$\begin{aligned} \bar{\Pi}_{H \in [1^-]}^{\text{loop-4}} = & \sum_{\substack{Q \in [8] \\ R \in [1^-]}} \left(\frac{G_{QR}^{(H)}}{4\pi f} \right)^2 \frac{M_H}{3} \left\{ \left(-\frac{3\pi m_Q}{4 M_H} + 1 + \frac{1}{2} \log \frac{m_Q^2}{M_R^2} \right) (m_Q^2 - (M_R - M_H)^2) \right. \\ & \left. + \frac{m_Q^2}{4} \log \frac{m_Q^2}{M_R^2} \right\} (M_R - M_H) \\ & + \sum_{\substack{Q \in [8] \\ R \in [0^-]}} \left(\frac{G_{QR}^{(H)}}{4\pi f} \right)^2 \left\{ \frac{1}{12} \beta_1 M \Delta^2 \tilde{\delta}_6 + \frac{M_H}{12} \left[-\beta_1 \Delta^2 \frac{\partial \Delta \delta_1}{\partial \Delta} - \tilde{\beta}_1 \Delta_Q^2 \right. \right. \\ & \left. \left. + \tilde{\beta}_2 \Delta_Q^2 \frac{M_H - M_R}{\Delta_H} - \frac{\tilde{\beta}_1}{\Delta_H} \left((M_H - M_R) \left(\Delta_Q^2 - \frac{m_Q^2}{2} \right) \log \frac{m_Q^2}{M_R^2} \right. \right. \right. \\ & \left. \left. + \Delta_Q^3 \left[\log(M_R - M_H - \Delta_Q) - \log(M_R - M_H + \Delta_Q) \right] \right) \right. \\ & \left. \left. - \frac{m_Q^2}{\Delta_H^2} \left(-\tilde{\beta}_2 \Delta_Q^2 + \tilde{\beta}_3 m_Q^2 \log \frac{m_Q^2}{M_R^2} \right) \right\} (M_R - M_H + \Delta_H). \end{aligned} \quad (3.76)$$

The requirement of the vanishing $O(m_Q^0)$ wave-function correction leads to the δ_6 and $\tilde{\delta}_6$ terms, such that

$$\lim_{m, m_s \rightarrow 0} \frac{\partial}{\partial M_H^2} \bar{\Pi}_H^{\text{loop-4}} = 0. \quad (3.77)$$

We notice they completely cancel out the counter part in $O(Q^3)$ corrections that added by the requirement of the vanishing $O(m_Q^0)$ wave-function correction.

3.2.4.2 The convergence behavior of the expansion

In this subsection we probe the numerical implications of the novel expansion we worked out in this chapter. Following the same approach as we did in the previous expansions, the numerical estimate of

H	$\bar{\Pi}_H^{\text{loop}}/(2M_H)$	$\bar{\Pi}_H^{\text{loop-3}}/(2M_H)$	$\bar{\Pi}_H^{\text{loop-4}}/(2M_H)$	$\bar{\Pi}_H^{\text{loop-5}}/(2M_H)$
D	-50.2 MeV	-48.5 MeV	-2.8 MeV	1.1 MeV
D_s	-65.6 MeV	-88.3 MeV	20.1 MeV	2.9 MeV
D^*	-113.4 MeV	-99.5 MeV	-17.1 MeV	3.1 MeV
D_s^*	-166.1 MeV	-197.5 MeV	26.3 MeV	6.6 MeV

Table 3.6.: The decomposition of the bubbles according to (3.60). The parameters involved are given by Tab. 3.3.

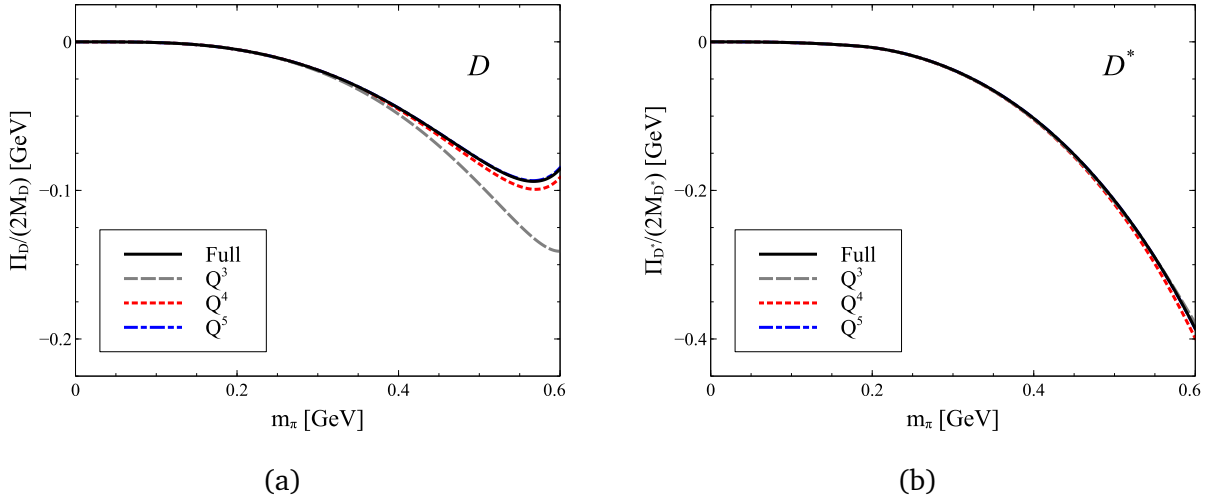


Figure 3.5.: The decomposed bubble loops $\bar{\Pi}_{D/D^*}^{\text{loop}}$, according to (3.60), as functions of the light quark masses.

the expanded contributions are listed in Tab. 3.6. The evaluation is taken at physical values of D -meson masses. Again, we use our first estimate for the low-energy parameters $c_{0,1}$ and $\tilde{c}_{0,1}$ as displayed in the second last column of Tab. 3.3. We observe that there is a good convergence behavior for all four open-charm mesons. The $O(Q^5)$ corrections are always as small as a few MeV. The total error of the expansion up to $O(Q^5)$ correction is well controlled within the MeV level, about 1%.

We further demonstrate the convergence behavior by plotting the loops $\bar{\Pi}_H$ as functions of the flavor-limit masses $m_\pi = m_K = m_\eta$. The self-consistent approach has been applied to determine $M_D = M_{D_s}$ and $M_{D^*} = M_{D_s^*}$ as we did before. The plots are shown in Fig. 3.5. The convergence of the expansion is manifest uniformly with a Goldstone-boson mass varying from the chiral limit to as large as 600 MeV. The improvement is especially significant in the case of D meson [Fig. 3.5(a)]. As we discussed in the previous sections, there is a large correlation amongst terms in the non-analytic structure, resulting in a bending at ~ 550 MeV. We observe from Fig. 3.5(a) that this effect has been well described with the inclusion of the $O(Q^4)$ correction.

From the demonstrations above, we conclude that our novel expansion approach is indeed a systematic convergent approach for the D -mesons. And up to $O(Q^4)$, the order we are considering, the decomposition has a well controlled error at the level of a few MeV. A full control of the accuracy at the scale of few MeV is feasible upon a complete inclusion of Q^5 chiral corrections. This would involve a class of two-loop diagrams.

3.3 Chiral Extrapolation

In the last sections, we scrutinized chiral mass formula for the pseudoscalar and vector D -mesons up to chiral order Q^4 . The results depend on the poorly known LECs c_i and d_i of the chiral Lagrangian, which we will attempt to determine from lattice QCD simulations of the D meson masses (for a recent review, see [118]). The lattice QCD approach has been intensively applied in the study of D -meson masses so that there exists a significant data set for D -meson masses at various (unphysical) Goldstone-boson masses. Once we determined the LECs in our mass formula, the D -meson masses can be computed at any values for the up, down and strange quark masses, sufficiently small as to justify the application of the chiral extrapolation. In this section, we will fit the LECs to lattice data. We first make a review regarding to the current status of lattice simulations of the D -meson masses, and provide the lattice data considered in our fits.

3.3.1 Lattice simulations for open-charm meson masses

Since 2007, the European Twisted Mass collaboration (ETMC) generated lattice configurations based on twisted-mass formalism [119–122]. The early configurations involved only u , d sea quarks ($N_f = 2$). Recently, an improvement of the configurations have been made including both s and c sea quarks [123–125]. Based on these configurations, Kalinowski et.al. provided the up-to-date most comprehensive simulation for all the 0^- and 1^- D -meson masses [40, 126].

There are works providing D -meson masses based on FNAL/MILC AsqTad configurations as well. These configurations were generated by Fermilab and MILC collaborations [127]. The u , d and s sea quarks have been implemented according to AsqTad formalism, which is an improved staggered-fermion formalism [128]. HPQCD collaboration have applied the FNAL/MILC AsqTad configurations for extensive studies of open-charm physics (e.g. Refs. [35, 129, 130]). Evaluations of D -meson masses can be found from some of the works [131–133, 130]. Full relativistic description of the valence charm quark has been implemented in these works, in terms of highly improved staggered-quark formalism [134]. The FNAL/MILC AsqTad configurations have also been adopted by LHP collaboration in [135]. This work entails valence charm quark using Fermilab approach to study the DK scattering process. Values of m_{D/D_s} are provide in this work.

Besides the works mentioned above, there are more works on open-charm meson masses. In a work by Mohler et.al. [41, 37], simulation of 0^- and 1^- D -meson masses have been performed using PACS-CS configurations [136]. The configurations contain $N_f = 2 + 1$ dynamical quarks with improved Wilson fermion formalism. The valence charm quark was implemented according to Fermilab approach [137, 138].

In this thesis we will mainly focus on analyzing the data given by ETMC and PACS-CS [40, 41]. In the rest of this subsection, we make a detailed discussion on processing the raw data from these two works.

3.3.1.1 The lattice data from ETMC

In this work, we employ the ETMC results provided by M. Kalinowski and M. Wagner, the authors of Ref. [40], as a main resource of data in the fitting. Details of the involved ensembles are listed in Tables 3.7, 3.8, and the corresponding D -meson masses are in Tables F.1, F.2 in Appendix F. For each ensemble, the D -meson masses are computed at two different values of the charm valence-quark mass μ_c . Two different discretization modes have been applied according to the twisted-mass action. For each ensemble at a given μ_c , two different sets of the D -meson masses have been computed according to two different discretization schemes, labeled with (\pm, \mp) and (\pm, \pm) . We take the center value of the masses from the results according to (\pm, \mp) discretization. The difference between the (\pm, \mp) and (\pm, \pm) results measures the discretization error of the computation. We assign such difference, averaged over

am_π	am_K	$a[\text{fm}]$	$N_S^3 \times N_T$	$a\mu_c$	discr.	aM_{η_c}	$aM_{J/\psi}$
0.1240(4)	0.2512(3)	0.0885	$32^3 \times 64$	0.2772	(\pm, \mp)	1.3869(1)	1.4649(3)
				0.2270	(\pm, \mp)	1.2241(2)	1.3042(4)
				0.2772	(\pm, \pm)	1.4180(3)	1.4569(3)
				0.2270	(\pm, \pm)	1.2522(2)	1.2973(3)
0.1412(3)	0.2569(3)	0.0885	$32^3 \times 64$	0.2768	(\pm, \mp)	1.3859(1)	1.4636(3)
				0.2389	(\pm, \mp)	1.2642(1)	1.3430(3)
				0.2768	(\pm, \pm)	1.4171(1)	1.4556(2)
				0.2389	(\pm, \pm)	1.2929(2)	1.3360(3)
0.1440(6)	0.2589(4)	0.0885	$24^3 \times 48$	0.2768	(\pm, \mp)	1.3863(2)	1.4645(4)
				0.2389	(\pm, \mp)	1.2645(2)	1.3442(5)
				0.2768	(\pm, \pm)	1.4178(3)	1.4564(3)
				0.2389	(\pm, \pm)	1.2936(3)	1.3370(4)
0.1988(3)	0.2764(3)	0.0885	$24^3 \times 48$	0.2929	(\pm, \mp)	1.4273(2)	1.5069(4)
				0.2299	(\pm, \mp)	1.2353(2)	1.3172(5)
				0.2929	(\pm, \pm)	1.4600(2)	1.4981(3)
				0.2299	(\pm, \pm)	1.2646(2)	1.3103(4)

Table 3.7.: Ensembles involved in ETMC results, provided by the authors of Ref. [40]. The results correspond to $\beta = 1.90$.

two different m_c 's for each ensemble, as the systematic error of the result. The error given at each (\pm, \mp) calculation is assigned to be the statistic error of the result. The lattice spacing serves as a free parameter in our fitting program.

We linearly interpolate the heavy meson masses M_H (open-charm or charmonium) in accordance with the valence charm-quark mass μ_c as

$$aM_H = \alpha_H + \beta_H a\mu_c. \quad (3.78)$$

The coefficients α_H and β_H are determined by aM_H at two given values of $a\mu_c$ from Tables E.1, E.2 in Appendix F. The $a\mu_c$ can be tuned to fit the physical value of the charmonium mass M_{η_c} or $M_{J/\psi}$. The lattice results of M_{η_c} and $M_{J/\psi}$ are taken from the configurations with the lightest pion mass at each lattice spacing given in Tables 3.7, 3.8. As an illustration, the interpolations of M_{η_c} and $M_{J/\psi}$ at $a = 0.0619\text{fm}$ have been shown in Fig. 3.6. From Fig. 3.6, we observe that the resulting $a\mu_c$ depends on whether M_{η_c} or $M_{J/\psi}$ has been fitted. As a result, a D -meson mass aM_H is interpolated to two different values corresponding to the $a\mu_c$ tuned in such two ways. Table 3.9 lists the D -meson masses interpolated according to the M_{η_c} fitting. The values M_{η_c} are listed in the last column. The M_{η_c} in the first rows of each lattice spacing correspond to the physical M_{η_c} with a 's given in Table 3.7. The M_{η_c} at other configurations have been obtained by the same interpolation process as applied to the D -meson masses. We observe that M_{η_c} doesn't have significant variation according to m_π , as one expected. Table 3.10 lists the D -meson masses interpolated according to the $M_{J/\psi}$ fitting. Following the same process obtaining M_{η_c} 's in Table 3.9, we provide the interpolated $M_{J/\psi}$ here for each ensemble. No significant change of $M_{J/\psi}$ according to m_π shows up either. We can observe that the two different fittings lead to a significant change of a D -meson mass. To this end, we allow a variation of $a\mu_c$ in Eq.(3.78) at each lattice scale to take account of this uncertainty. They are fitted collectively to the D -meson masses.

am_π	am_K	$a[fm]$	$N_S^3 \times N_T$	$a\mu_c$	discr.	aM_{η_c}	$aM_{J/\Psi}$
0.1074(5)	0.2133(4)	0.0815	$32^3 \times 64$	0.2230	(\pm, \mp)	1.3194(2)	1.3835(4)
				0.1727	(\pm, \mp)	1.1567(2)	1.2233(4)
				0.2230	(\pm, \pm)	1.3418(3)	1.3778(3)
				0.1727	(\pm, \pm)	1.1766(3)	1.2182(4)
0.1549(2)	0.2279(2)	0.0815	$32^3 \times 64$	0.2230	(\pm, \mp)	1.3251(1)	1.3903(2)
				0.1727	(\pm, \mp)	1.1573(1)	1.2253(2)
				0.2230	(\pm, \pm)	1.3480(1)	1.3844(2)
				0.1727	(\pm, \pm)	1.1779(1)	1.2202(2)
0.1935(4)	0.2430(4)	0.0815	$24^3 \times 48$	0.2230	(\pm, \mp)	1.3179(3)	1.3837(4)
				0.1727	(\pm, \mp)	1.1582(3)	1.2273(4)
				0.2230	(\pm, \pm)	1.3408(3)	1.3775(4)
				0.1727	(\pm, \pm)	1.1791(3)	1.2218(5)
0.0703(4)	0.1697(3)	0.0619	$48^3 \times 96$	0.2230	(\pm, \mp)	1.0595(2)	1.1006(3)
				0.1919	(\pm, \mp)	0.9570(2)	1.0003(4)
				0.2230	(\pm, \pm)	1.0683(2)	1.0985(3)
				0.1919	(\pm, \pm)	0.9653(2)	0.9984(4)
0.0806(3)	0.1738(5)	0.0619	$48^3 \times 96$	0.2227	(\pm, \mp)	1.0579(2)	1.0989(4)
				0.1727	(\pm, \mp)	0.8915(2)	0.9364(5)
				0.2227	(\pm, \pm)	1.0668(2)	1.0967(4)
				0.1727	(\pm, \pm)	0.8996(2)	0.9345(5)
0.0975(3)	0.1768(3)	0.0619	$48^3 \times 96$	0.2230	(\pm, \mp)	1.0591(1)	1.1002(3)
				0.1727	(\pm, \mp)	0.8919(1)	0.9370(3)
				0.2230	(\pm, \pm)	1.0679(2)	1.0980(2)
				0.1727	(\pm, \pm)	0.8999(2)	0.9350(3)

Table 3.8.: Ensembles involved in ETMC results, provided by the authors of Ref. [40](continued). The $a = 0.0815$ fm results correspond to $\beta = 1.95$. The $a = 0.0619$ fm results correspond to $\beta = 2.10$.

am_π	am_K	aM_D	aM_{D_s}	aM_{D^*}	$aM_{D_s^*}$	aM_{η_c}
0.1240(4)	0.2512(3)	0.8677(181)	0.9114(206)	0.9506(28)	0.9953(45)	1.3370(296)
0.1412(3)	0.2569(3)	0.8708(168)	0.9132(208)	0.9511(41)	0.9949(45)	1.3379(299)
0.1440(6)	0.2589(4)	0.8714(159)	0.9137(208)	0.9545(24)	0.9990(45)	1.3382(302)
0.1988(3)	0.2764(3)	0.8753(184)	0.9102(219)	0.9627(60)	0.9980(66)	1.3325(310)
0.1074(5)	0.2133(4)	0.7946(122)	0.8263(147)	0.8664(44)	0.9001(34)	1.2312(212)
0.1549(2)	0.2279(2)	0.8004(128)	0.8291(144)	0.8777(47)	0.9049(39)	1.2342(217)
0.1935(4)	0.2430(4)	0.8039(148)	0.8278(151)	0.8840(38)	0.9059(41)	1.2314(219)
0.0703(4)	0.1697(3)	0.5947(52)	0.6279(56)	0.6506(86)	0.6809(28)	0.9351(85)
0.0806(3)	0.1738(5)	0.5949(64)	0.6277(57)	0.6546(26)	0.6803(11)	0.9332(85)
0.0975(3)	0.1768(3)	0.5955(50)	0.6271(57)	0.6526(28)	0.6804(15)	0.9335(84)

Table 3.9.: Interpolated masses for D -mesons and η_c . The valence charm-quark mass is fitted to physical M_{η_c} . The first, second and third block in the table corresponds to β values of 1.90, 1.95 and 2.10 respectively.

am_π	am_K	aM_D	aM_{D_s}	aM_{D^*}	$aM_{D_s^*}$	$aM_{J/\psi}$
0.1240(4)	0.2512(3)	0.8514(181)	0.8953(206)	0.9356(28)	0.9806(45)	1.3890(75)
0.1412(3)	0.2569(3)	0.8544(168)	0.8972(208)	0.9363(41)	0.9802(45)	1.3895(75)
0.1440(6)	0.2589(4)	0.8552(159)	0.8978(208)	0.9403(23)	0.9844(45)	1.3906(77)
0.1988(3)	0.2764(3)	0.8599(184)	0.8950(219)	0.9487(60)	0.9841(66)	1.3882(79)
0.1074(5)	0.2133(4)	0.7840(122)	0.8159(147)	0.8568(44)	0.8905(34)	1.2791(55)
0.1549(2)	0.2279(2)	0.7895(128)	0.8183(144)	0.8678(47)	0.8950(39)	1.2828(55)
0.1935(4)	0.2430(4)	0.7934(148)	0.8175(151)	0.8745(38)	0.8965(41)	1.2818(58)
0.0703(4)	0.1697(3)	0.5905(52)	0.6236(56)	0.6466(86)	0.6770(28)	0.9715(20)
0.0806(3)	0.1738(5)	0.5906(64)	0.6234(57)	0.6506(26)	0.6763(11)	0.9697(21)
0.0975(3)	0.1768(3)	0.5913(50)	0.6229(57)	0.6486(28)	0.6764(15)	0.9703(21)

Table 3.10.: Interpolated masses for D -mesons and J/ψ . The valence charm-quark mass is fitted to physical $M_{J/\psi}$. The first, second and third block in the table corresponds to β values of 1.90, 1.95 and 2.10 respectively.

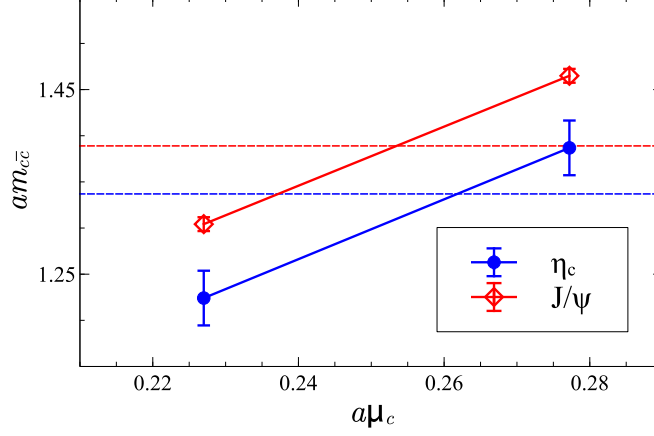


Figure 3.6.: The interpolation of charmonium masses to determine μ_c , at $a = 0.885$. The ensemble is chosen with $am_\pi = 0.1240$. The physical values of M_{η_c} and $M_{J/\psi}$ are indicated by the dashed lines.

$N_S^3 \times N_T$	am_π	am_K	aE_D	aE_{D_s}	aE_{D^*}	$aE_{D_s^*}$
$a = 0.0907(13)\text{fm}$						
$32^3 \times 64$	0.18903(79)	0.29190(67)	0.79580(61)	0.84000(36)	0.86327(99)	0.90429(60)
$32^3 \times 64$	0.17671(129)	0.26729(110)		0.82848(40)		0.89015(69)
$32^3 \times 64$	0.13593(140)	0.27282(103)	0.78798(82)	0.83929(26)	0.85776(122)	0.90429(43)
$32^3 \times 64$	0.07162(299)	0.25454(97)	0.77646(119)	0.83149(34)	0.83656(189)	0.89268(59)

Table 3.11.: The energy levels for $D_{(s)}$, $D_{(s)}^*$ mesons by Mohler et.al. [41]. The ensemble was given by PACS-CS. The results for the light meson spectrum had been cited from [136].

3.3.1.2 The lattice data from PACS-CS

In this work, we employ the lattice results from Mohler and Woloshyn [41] as another major resource of data in the fitting. We list the results in Table 3.11. The PACS-CS configurations have been used in this work. The Fermilab approach is employed in implementing the valence charm-quark [137, 138]. In the Fermilab approach, heavy-quark mass dependent counter terms are added in the heavy-quark action to systematically remove discretization effects. The valence charm-quark mass dependence is parameterized by a hopping parameter κ_c , which is tuned to match the average of the physical kinematic D -meson masses³. As a result, the energy obtained for a charmed meson E_H in Table 3.11 is not directly recognized as the masses M_H , an overall offset between M_H and E_H is allowed. We allow such offsets in our fitting. The lattice spacing is necessary in fitting the hopping parameter. We show the lattice spacing adopted in Ref. [41] in Table 3.11.

3.3.2 Fitting the D -meson chiral mass formula to lattice data

In this subsection we present the results of an analysis of the lattice data sets on D -meson masses. I would like to acknowledge my supervisor Prof. Dr. Matthias Lutz for providing the results of two typical fits of the chiral mass formulae as developed in this work. The GENEVA framework, an evolutionary

³ The kinematic mass refers to the mass appearing in the (non-relativistic) kinematic energy term.

minimization algorithm, was set up on the computing cluster at GSI where in the client server model fits were obtained with 400 clients working on a population of typical sizes of up to 3200. Data from different lattice groups were considered as presented in the last subsection.

Our main purpose is to determine the LECs involved in the chiral mass formula. As we discussed, we keep the heavy-quark correlations between the LECs contributing to Q^3 and Q^4 chiral corrections. The resulting identities (2.110),(2.119) and (2.122) are respected in our final fitting. We collect them here as

$$\begin{aligned} \tilde{g}_P &= g_P, \\ \tilde{c}_2 &= c_2, & \tilde{c}_3 &= c_3, & \tilde{c}_4 &= c_4, & \tilde{c}_5 &= c_5, \\ \tilde{d}_1 &= d_1, & \tilde{d}_2 &= d_2, & \tilde{d}_3 &= d_3, & \tilde{d}_4 &= d_4. \end{aligned} \quad (3.79)$$

The g_P is determined from $D^* \rightarrow D\pi$ decay width, reading as $|g_P| = 0.57$ [29]. The LECs $c_0, \tilde{c}_0, c_1, \tilde{c}_1$, are determined from the empirical D -meson masses at the physical Goldstone-boson masses. We employ the large N_C approximation for a further reduction of the LECs according to

$$c_2 = -\frac{c_3}{2}, \quad c_4 = -\frac{c_5}{2}. \quad (3.80)$$

We end up with the 8 low energy constants to be fitted to the lattice data set on the D -meson masses

$$M, \Delta, c_3, c_5, d_1, d_2, d_3, d_4. \quad (3.81)$$

Besides these low energy constants, additional free parameters are involved. This includes the mass of the valence c -quark masses, as we explained in the last section. The set of the parameters are determined by minimizing the χ^2/N with N data points. At a large enough volume of data, a good fitting will have a typical $\chi^2/N \sim 1$ provided that both the extrapolation formulae and the data set are free from any flaws. We determine the χ^2 according to [43] as

$$\chi^2 = \sum_{i=1}^N \left(\frac{M_i^{\text{lattice}} - M_i^{\chi\text{ET}}}{\Delta M_i} \right)^2, \quad (3.82)$$

provided the errors, ΔM_i , from different lattice sets are independent. Correlated errors may originate from the uncertainty of determining the lattice scale a [139–141, 43]. As discussed in Ref. [43], this correlation can be implemented by including the lattice scales as free parameters to be fitted to physical D -meson masses. According to this treatment, the error consists of uncorrelated statistical, systematical and theoretical errors according to

$$(\Delta M_i)^2 = (\Delta M_i^{\text{statistical}})^2 + (\Delta M_i^{\text{systematic}})^2 + (\Delta M_i^{\text{theoretical}})^2. \quad (3.83)$$

We take the interpolated statistical error for the ETMC data, as interpreted in the last subsection. The statistical error for the PACS data is taken directly from Table 3.7. The systematical errors are estimated from the typical size of discretization effects. For the ETMC data such an error is taken from the splitting between D meson masses evaluated in two discretization modes, as we explained in the last subsection. As a result, we can read off the statistical and systematical errors for ETMC, $\sqrt{(\Delta M_i^{\text{statistical}})^2 + (\Delta M_i^{\text{systematic}})^2}$, from Tables 3.9 and 3.10 for the M_{η_c} and $M_{J/\psi}$ fits respectively. An average over the two fits is taken. For the PACS data, we neglect the discretization effect since it is highly suppressed in the Fermilab approach. The theoretical error refers to a residual uncertainty of the $N^3\text{LO}$ chiral extrapolation. We estimate this error to be $\sim 5\text{MeV}$, according to the characteristic size of the 5th order contribution in our chiral expansion scenario as illustrated in Sec.3.2.4.

	Fit 1	Fit 2	Lattice result
f_0 [GeV]	0.0924		
μ [GeV]	0.77		
g_P	0.57		
$L_4 - 2L_6$	-0.109×10^{-3}		
$L_5 - 2L_8$	0.086×10^{-3}		
$L_8 + 3L_7$	-0.175×10^{-3}		
a_{PACS} [fm]	0.0907	0.0897	0.0907(13) [41]
$a_{\text{ETM}}^{\beta=2.10}$ [fm]	0.0885	0.0924	0.0885(36) [126]
$a_{\text{ETMC}}^{\beta=1.95}$ [fm]	0.0815	0.0856	0.0815(30) [126]
$a_{\text{ETMC}}^{\beta=1.90}$ [fm]	0.0619	0.0675	0.0619(18) [126]

Table 3.12.: Parameters involved in the fittings.

We report on two fits at given values of f , $L_4 - 2L_6$, $L_5 - 2L_8$, $L_8 + 3L_7$ and g_P according to Table 3.12. In the Fit 1, the lattice scales are fixed to be the values provided by the lattice groups. In the Fit 2, all the lattice scales are considered as free parameters. In such a way, the lattice spacing a for each β is determined by our global fit, where the empirical masses of the 4 D -mesons are considered as additional constraints. We show the resulting lattice scales in Table 3.12. The corresponding low energy coefficients are listed in Table 3.13.

We observe that the fitting of lattice scales lowers the χ^2 significantly as shown in Table 3.13. In Table 3.14 we specify the χ^2/N for the lattice data sets at each lattice scale. In the fitting to PACS data, if we fit the lattice scale as given in the paper, the χ^2/N is significantly reduced to a reasonable value. In both the cases, the χ^2/N for the ETMC data are smaller than 1. It might be attributed to an overestimate of the systematic errors or it may reflect that not all low-energy parameters are determined sufficiently well by the considered data set. By reducing the systematic error from discretization effects, one may enlarge the values of χ^2/N .

We observe that while all the scales of LECs are in agreement with the naturalness assumption, the explicit values may sensitively depend on the choice of lattice scale. One of the most interesting observation is that the low energy constants c_2 to c_5 have opposite signs in Fit 1 and Fit 2. As the LECs c_2 to c_5 are highly involved in unitary chiral effective approaches at NLO, it is useful to compare the values in these fittings with the results obtained in previous works. The comparison is referred to the next subsection.

3.3.3 Comparison of the values of LECs from different works

In previous studies on open-charm mesonic systems, the role of the LECs c_i have been extensively discussed. In this subsection, we compare our first results for the LECs with the predictions from other works.

In Table 3.15 we compare the results with previous works of our group, using unitary chiral effective approaches. The work [28] scrutinized the existence of the open-charm sextet resonance via two body scattering processes between an open-charm meson and a Goldstone boson. The work [29] probed the radiative and isospin-violating decays of open-charm resonances. The c_1 and \tilde{c}_1 are obtained according to the physical mass differences of the 0^- and 1^- D -mesons in these two papers. The LECs c_0 , $c_2 + c_4$ and $c_3 + c_5$ in Ref. [28] are obtained to match the physical masses and widths of $D_{s1}(2460)$ and $D_1(2420)$.

	Fit 1	Fit 2
$M[\text{GeV}]$	1.8505	1.7988
$\Delta[\text{GeV}]$	0.1372	0.1400
$c_0[\text{GeV}^0]$	0.1278	0.2750
$\tilde{c}_0[\text{GeV}^0]$	0.1972	0.3480
$c_1[\text{GeV}^0]$	0.2696	0.3744
$\tilde{c}_1[\text{GeV}^0]$	0.2840	0.3913
$c_2[\text{GeV}^0]$	0.0820	-0.0447
$c_3[\text{GeV}^0]$	-0.1640	0.0893
$c_4[\text{GeV}^0]$	0.0136	-0.2079
$c_5[\text{GeV}^0]$	-0.0272	0.4157
$d_1[\text{GeV}^{-2}]$	0.3509	0.3594
$d_2[\text{GeV}^{-2}]$	0.1874	0.5643
$d_3[\text{GeV}^{-2}]$	0.5028	0.7226
$d_4[\text{GeV}^{-2}]$	0.5181	0.0559
χ^2/N	1.392	0.772

Table 3.13.: LECs determined according to two different fitting methods, see the context.

χ^2/N	Total	PACS	ETMC($\beta = 2.10$)	ETMC($\beta = 1.95$)	ETMC($\beta = 1.90$)
Fit 1	1.392	2.771	0.670	0.922	0.983
Fit 2	0.772	1.480	0.563	0.615	0.265

Table 3.14.: The values of χ^2/N in the fittings.

	Fit 1	Fit 2	[28]	[29]
c_0	0.1278	0.2750	0.95	0.22
\tilde{c}_0	0.1972	0.3480	0.95	0.23
c_1	0.2696	0.3744	0.45	0.44
\tilde{c}_1	0.2840	0.3913	0.45	0.47
$c_2 + c_4$	0.0956	-0.2525	-1.64	-0.6
$c_3 + c_5$	-0.1912	0.5050	1.6	1.2

Table 3.15.: Comparison of the values of LECs from the two fits in this work with the results from works by Hofmann and Lutz [28], Lutz and Soyeur [29] using unitary approaches.

	Fit 1	Fit 2	HM(PKU) [142]	HM(TUM) [144]	Cov.(TUM) [144]
c_0	0.1278	0.2750	—	0.229	0.229
c_1	0.1972	0.3480	0.45	0.428	0.428
c_4	0.0136	-0.2079	—	—	2.16 ± 0.86
c_5	-0.0272	0.4157	—	—	-7.35 ± 1.56
$c_3 + c_5$	-0.1912	0.5050	3.46	-0.334 ± 0.034	0.252 ± 0.142
$2c_2 + c_3 + 2c_4 + c_5$	0	0	$2.40 - (4c_0 - 2c_1)$	0.024 ± 0.012	0.306 ± 0.070

Table 3.16.: Comparison of the values of LECs provided in this work with those from various fits using NLO perturbative approaches provided by Liu et.al (PKU) [142] and Altenbuchinger et.al (TUM) [144]

In [29], the large N_c approximation has been assumed according to (3.80). The parameter $c_3 + c_5$ or $\tilde{c}_3 + \tilde{c}_5$ was tuned to optimally match the physical values of $D_{s0}^*(2317)$ and $D_{s1}(2460)$ in [29].

More recently, progress in QCD lattice models makes it possible to extract the LECs from numerical simulations of scattering lengths between a D -meson and a Goldstone-boson. We discuss the results fitting to lattice scattering lengths from various groups in the following. All their values of the LEC are recalled according to the convention of our group.

In Table 3.16 we list the the scattering lengths from a perturbative calculation. The heavy-meson effective approach was applied by Liu et.al [142]. Because of the limited lattice data set, only part of c_i 's are determined in this work (Ref. [143]). We recall their values in the 4th column of Table 3.16. More recent results are provided by [144], based on a more comprehensive set of lattice data [135]. The fits are conducted either in the heavy-meson approximation or in full relativistic formalism. The results are listed in the 5th and 6th column respectively.

Unitarization approaches have been applied in the computation of the lattice scattering lengths in [27, 28, 145, 30, 135, 144, 146, 147]. Predictions for all scattering length were made prior to the availability of any lattice data in [27, 28]. In these works all coupled-channel scattering amplitude are shown in particular at the threshold points. We present the results of fits to lattice data from LHPC [135] in Tables 3.17, 3.18. In Table 3.17, the NLO fittings from Munich group are presented [31]. In this work, the unitarization was implemented according to three different approaches. One of them is the heavy-meson approach, denoted by "HM", and two of them are in covariant formalism, denoted by "HQS" proposed in the same work and " χ BS(3)" proposed by Lutz et.al [22] respectively. In Table 3.18 we list the NLO and NNLO fittings from Bonn-Jülich group [135, 147]. The results from Bonn-Jülich group adopted an approximation of Bethe-Salpeter formalism proposed in [25].

	Fit 1	Fit 2	NLO HQS	NLO χ BS(3)	NLO HM
c_0	0.1278	0.2750		0.229	
c_1	0.2696	0.3744		0.428	
c_2	0.0820	-0.0447	-1.90 ± 0.62	-0.720 ± 0.451	-4.59 ± 0.67
c_3	-0.1640	0.0893	3.86 ± 1.20	2.13 ± 0.84	—
c_4	0.0136	-0.2079	1.82 ± 0.62	0.620 ± 0.449	—
c_5	-0.0272	0.4157	-3.84 ± 1.20	-2.12 ± 0.84	—
$c_3 + c_5$	-0.1912	0.5050	0.022 ± 0.062	0.0074 ± 0.0680	18.90 ± 1.20
$2c_2 + c_3 + 2c_4 + c_5$	0	0	-0.136 ± 0.042	-0.192 ± 0.038	9.72 ± 0.60

Table 3.17.: Comparison of the values of LECs provided in this work with the NLO fits provided by Al-tenbuchinger et.al. [31], using different unitarization approaches.

	Fit 1	Fit 2	NLO B-J [135]	NNLO B-J [147]
c_0	0.1278	0.2750	0.217	0.2219
c_1	0.2696	0.3744	0.42	0.4266
c_2	0.0820	-0.0447	-1.97 ± 0.45	-1.54 ± 0.93
c_3	-0.1640	0.0893	4.14 ± 0.85	5.60 ± 1.74
$\frac{\bar{M}_D^2}{M^2} c_4$	0.0146	-0.2362	1.79 ± 0.45	1.74 ± 0.91
$\frac{\bar{M}_D^2}{M^2} c_5$	-0.0292	0.4724	-3.88 ± 0.84	-5.20 ± 1.71
$c_3 + \frac{\bar{M}_D^2}{M^2} c_5$	-0.1932	0.5617	0.26 ± 0.10	0.40 ± 0.31
$2c_2 + c_3 + \frac{\bar{M}_D^2}{M^2} (2c_4 + c_5)$	0	0	-0.10 ± 0.06	0.80 ± 0.10

Table 3.18.: Comparison of the values of LECs provided in this work with the NLO and NNLO UChPT fits by Bonn-Jülich group [135, 147], where $\bar{M}_D^2 = 1.9175\text{GeV}$.

From the tables above, we observe that the values of c_0 and c_1 are in agreement with previous results. This is so since all such fits determined c_0 and c_1 from the D -meson masses at tree-level like it was done previously in Ref. [28, 29]. The open-charm scattering lengths involve other c 's, most prominently the combination $c_3 + c_5$. According to [28, 29], the contribution of $c_3 + c_5$ is crucial for the resonances $D_{s0}^*(2317)$ and $D_{s1}(2460)$ but also for the possible existence of resonance states with exotic quantum numbers.

Our Fit 2 is in qualitative agreement with the previous works by Lutz et.al. [29] for $c_3 + c_5$ (see Table 3.15), which was fitted to the masses of $D_{s0}^*(2317)$ and $D_{s1}(2460)$ only. Comparing with the results from fits to the lattice scattering lengths (Tables 3.16, 3.18, 3.17), we observe that the Fit 2 is always roughly compatible with the covariant ChPT approaches (either perturbative or unitarized) at least regarding to the parameter combination $c_3 + c_5$ ⁴. In contrast our Fit 1, predicts an opposite sign for the combination $c_3 + c_5$, as is also the case in the scattering length study of the Munich group based on χ PT in the heavy-meson expansion approach (see Table 3.16). We note that also only moderate deviations from the leading order large N_C relations have been observed in Tables 3.16-3.18. A convenient measure for this is the combination $2c_2 + c_3 + 2c_4 + c_5$ which vanishes in the large- N_C limit. Here we exclude scenarios with unnaturally large LECs.

Next we will study the role of further QCD lattice data and then also relax on the large N_C relations. The quality of such fits will be scrutinized by an evaluation of the scattering lengths in different coupled-channel unitarization schemes.

⁴ For the Bonn-Jülich results, we compare the combination $c_3 + \frac{\bar{M}_D^2}{M^2}c_5$ for convenience, because of their convention. But the factor $\frac{\bar{M}_D^2}{M^2}$ is close to 1.

4 Summary

In this thesis, we have calculated chiral corrections for the pseudoscalar and vector D -meson masses. The chiral corrections have been derived up to order Q^4 ($N^3\text{LO}$). We employed a covariant flavor $SU(3)$ ChPT formalism for the chiral loop contributions. By matching the covariant formalism to a heavy-quark reduced formalism, we obtained correlations between LECs of the covariant chiral Lagrangian.

The loop contributions as given by the relativistic Lagrangian suffer from chiral power-counting breaking terms if evaluated in the conventional $\overline{\text{MS}}$ scheme [73]. We used a modified version of the χ - $\overline{\text{MS}}$ subtraction scheme proposed by [97, 47, 52]. It is based on a minimal subtraction of the scalar loop integrals in the Passarino-Veltman reduction scheme. We scrutinized the convergence behavior of the chiral expansion according to four different power counting schemes. The first expansion scenario is motivated by the heavy-quark symmetry but also is formulated in terms of the physical meson masses. The expansion is well convergent for large masses of the Goldstone-bosons but fails in the chiral limit. The second expansion scenario considered is the strict chiral expansion scheme. In contrast to the first scheme the second one is faithful at small quark masses but the expansion fails badly when the Goldstone-boson masses get as large as the kaon mass. As our third case, we investigated a conventional small-scale expansion, where the D - D^* mass splitting in the chiral limit and the Goldstone boson masses are assumed to be of similar size. This expansion still fails when the Goldstone bosons are as heavy as the kaon. Eventually we considered a novel expansion scheme which was proposed recently in [52]. According to this approach, the power counting rests on the values of the physical meson masses. As a consequence it uniformly converges from the chiral limit up to pion and kaon masses as large as 600 MeV. The size of the $N^4\text{LO}$ terms are estimated to be smaller than about 5 MeV in such a scheme.

First explorative applications to some QCD lattice data sets were reported on. We consider the D mesons as computed for various choices of the light quark masses. For the purpose of fitting the lattice data, finite volume corrections in the loop functions were properly taken into account. The physical meson masses are kept inside all loop integrals. We used data sets based on configurations of the ETM collaboration and PACS-CS group [42, 41], where we are grateful to the group of Marc Wagner for providing to us unpublished results on the D meson masses. In our explorative fittings, large N_C constraints have been assumed such that only 8 LECs are involved to fit 56 lattice data points. The isospin average of the physical D meson masses from the PDG are always reproduced exactly. It was illustrated that a good reproduction of the data set is possible. Further more detailed studies that consider lattice data from further lattice groups are needed to arrive at a unique set of the LECs.

Given an established set of such LECs it is possible to return to the open-charm scalar and axial-vector resonances as they are part of the physics program of PANDA at FAIR.

A Conventions

This appendix is devoted to collect the conventions we have used in this thesis. The Levi-Civita tensor is given by,

$$\epsilon^{\mu\nu\rho\sigma} = \begin{cases} +1, & \text{if } (\mu, \nu, \rho, \sigma) \text{ are even permutations of } (0, 1, 2, 3); \\ -1, & \text{if } (\mu, \nu, \rho, \sigma) \text{ are odd permutations of } (0, 1, 2, 3); \\ 0, & \text{other cases.} \end{cases} \quad (\text{A.1})$$

The Pauli matrices are written as,

$$\sigma_1 = \begin{pmatrix} 0 & 1 \\ 1 & 0 \end{pmatrix}, \quad \sigma_2 = \begin{pmatrix} 0 & -i \\ i & 0 \end{pmatrix}, \quad \sigma_3 = \begin{pmatrix} 1 & 0 \\ 0 & -1 \end{pmatrix}. \quad (\text{A.2})$$

The Gell-Mann matrices are given by,

$$\begin{aligned} \lambda_1 &= \begin{pmatrix} 0 & 1 & 0 \\ 1 & 0 & 0 \\ 0 & 0 & 0 \end{pmatrix}, & \lambda_2 &= \begin{pmatrix} 0 & -i & 0 \\ i & 0 & 0 \\ 0 & 0 & 0 \end{pmatrix}, & \lambda_3 &= \begin{pmatrix} 1 & 0 & 0 \\ 0 & -1 & 0 \\ 0 & 0 & 0 \end{pmatrix}, \\ \lambda_4 &= \begin{pmatrix} 0 & 0 & 1 \\ 0 & 0 & 0 \\ 1 & 0 & 0 \end{pmatrix}, & \lambda_5 &= \begin{pmatrix} 0 & 0 & -i \\ 0 & 0 & 0 \\ i & 0 & 0 \end{pmatrix}, & \lambda_6 &= \begin{pmatrix} 0 & 0 & 0 \\ 0 & 0 & 1 \\ 0 & 1 & 0 \end{pmatrix}, \\ \lambda_7 &= \begin{pmatrix} 0 & 0 & 0 \\ 0 & 0 & -i \\ 0 & i & 0 \end{pmatrix}, & \lambda_8 &= \frac{1}{\sqrt{3}} \begin{pmatrix} 1 & 0 & 0 \\ 0 & 1 & 0 \\ 0 & 0 & -2 \end{pmatrix}. \end{aligned} \quad (\text{A.3})$$

In addition, we define λ_0 as $\lambda_0 = \sqrt{2/3} \text{diag}\{1, 1, 1\}$.

B Vector versus tensor representations for vector particles

In the normal vector representation, a vector field V^μ is normalized as (see e.g. [70, 148]),

$$\langle 0|V^\mu(0)|p, \lambda\rangle = \epsilon^\mu(p, \lambda), \quad (\text{B.1})$$

where V^μ is the field operator, p, λ are the momentum and helicity of the state, and ϵ is the polarization vector. A free massive vector field satisfies the Lagrangian,

$$\mathcal{L} = -\frac{1}{4}F_{\mu\nu}F^{\mu\nu} + m^2V_\mu V^\mu, \quad (\text{B.2})$$

where the antisymmetric field strength is defined $F_{\mu\nu} = \partial_\mu V_\nu - \partial_\nu V_\mu$. The Lagrangian results in the equation of motion for a massive vector field,

$$\partial_\mu F^{\mu\nu} + m^2V^\mu = 0, \quad (\text{B.3})$$

which indicates the Lorentz condition,

$$\partial_\mu V^\mu = 0. \quad (\text{B.4})$$

Therefore only 3 space-like polarization vectors of an on-shell massive vector particle are independent. The polarization vectors satisfy the relation,

$$\sum_{\lambda=1}^3 \epsilon^\mu(\lambda)\epsilon^\nu(\lambda) = -g^{\mu\nu} + \frac{p^\mu p^\nu}{m^2}. \quad (\text{B.5})$$

The work of Ref. [70, 71] introduced the tensor representation of vector field $V^{\mu\nu}$, satisfying the normalization,

$$\langle 0|V^{\mu\nu}|p, \lambda\rangle = \epsilon^{\mu\nu}(p, \lambda) = \frac{i}{m}(p^\mu \epsilon^\nu(p, \lambda) - p^\nu \epsilon^\mu(p, \lambda)). \quad (\text{B.6})$$

The kinetic Lagrangian of a vector particle in the tensor representation reads [70, 71],

$$\mathcal{L} = -\partial^\mu V_{\mu\rho} \partial_\nu V^{\nu\rho} + \frac{1}{2}m^2 V_{\mu\nu} V^{\mu\nu} \quad (\text{B.7})$$

From the Lagrangian, one can get the equation of motion,

$$\partial^\mu \partial_\rho V^{\rho\nu} - \partial^\nu \partial_\rho V^{\rho\mu} + m^2 V^{\mu\nu} = 0 \quad (\text{B.8})$$

and the free propagator,

$$\begin{aligned} \langle 0|T[V^{\mu\nu}(x)V^{\rho\sigma}(y)]|0\rangle &= \int \frac{d^4p}{(2\pi)^4} e^{-i(x-y)\cdot p} iS^{\mu\nu, \rho\sigma}(p) \\ S^{\mu\nu, \rho\sigma}(p) &= -\frac{1}{m^2} \frac{1}{p^2 - m^2 + i\epsilon} [(m^2 - p^2)g^{\mu\rho} g^{\nu\sigma} + g^{\mu\rho} p^\nu p^\sigma - g^{\mu\sigma} p^\nu p^\rho - (\mu \leftrightarrow \nu)] \end{aligned} \quad (\text{B.9})$$

After multiplying $\epsilon_{\mu\nu\alpha\beta} \partial^\alpha$ to the equation of motion, one can obtain the relation,

$$\epsilon_{\mu\nu\alpha\beta} \partial^\alpha V^{\mu\nu} = 0, \quad (\text{B.10})$$

which is the Lorentz condition for tensor representation fields. This equation superficially gives 4 constraints on $V^{\mu\nu}$ meson. But because $\partial^\beta (\epsilon_{\mu\nu\alpha\beta} \partial^\alpha V^{\mu\nu}) \equiv 0$, only 3 constraints are independent. Noticing there are in general only 6 freedoms for an antisymmetric tensor, $V^{\mu\nu}$ has 3 independent degrees of freedom.

C Large N_C approximation

The large N_C approximation is a perturbative method to study QCD by assuming the number of colors N_C is considerably large. It was first pointed by 't Hooft [149], that physical quantities of a $SU(N_C)$ gauge theory can be expanded in a power series of $1/N_C$. The large N_C approximation shed insights of many features of QCD, though in reality $N_C = 3$, which is not so large (for reviews see e.g. [150, 151, 72]).

In the large N_C approach, the coupling constant of QCD has the behavior $g \sim 1/\sqrt{N_C}$ in order to keep $g^2 N_C \sim O(N_C^0)$ ¹. Quark and gluon propagators are depicted according to Fig. C.1. The solid lines represent the type of the color, while the arrows denote the flows of color charges. The double line notation describes a gluon in appearance of the direct product of N_C and \bar{N}_C . The direct product $N_C \otimes N_C$ serves as an adjoint representation of $U(N_C)$ symmetry rather than $SU(N_C)$. To get the correct representation for $SU(N_C)$, an color-singlet gluon component should be subtracted. But it has been shown (e.g. [151]), effects of the extra color-singlet gluon contribute at $1/N^2$ order, which is out of our concern.



Figure C.1.: Propagators of quark (left) and gluon (right) in large N_C notation.

From every closed color contour, there comes an N_C factor. This is attributed to the summation of colors. Using the rules above, we can find Feynman diagrams for a certain process can be sorted systematically in terms of $1/N_C$. The following conclusions can be drawn [72],

1. the leading order diagrams are planar diagrams possessing a minimal number of quark loops² ;
2. every additional quark loop gives rise a suppression of order N_C^{-1} ;
3. every non-planar gluon propagator is suppressed by N_C^{-2} .



Figure C.2.: Two leading order single-quark loops: (a) is a quark loop without gluons. (b) is a quark loop with a number of gluons connected in a planary way.

¹ It was shown by 't Hooft [149], unless $g^2 N_C$ is independent from N_C , the color-loop diagrams in large N_C limit will either remain to a trivial colorful diagram or diverge with arbitrary powers of N_C by adding more color loops. A discussion on g using the renormalization group equation gives the same behavior (see e.g. [151, 152]).

² A non-planar diagram is a diagram that have some internal lines crossing over each other when one manages to draw it in a plane.

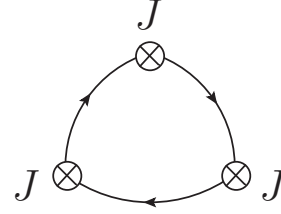
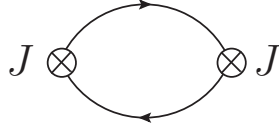


Figure C.3.: Diagram of two currents condensate. **Figure C.4.:** Diagram of three currents condensate.

So if one adds an arbitrary number of planar gluon loops to a certain diagram, the N_C -order will not change. For example, Fig. C.2(b) has the same order as Fig. C.2(a). In the following, we will investigate the constituent $\bar{q}q$ meson states $|n\rangle$, which have non-vanishing overlaps with quark-antiquark currents,

$$\langle 0|J(0)|n\rangle \neq 0, \quad \text{where, } J(x) = \bar{q}\Gamma q(x), \quad (\text{C.1})$$

Γ is a combination of Dirac gamma matrices. It is shown in Ref. [150], that in the large N_C limit, $J(x)$ can only couple with $\bar{q}q$ single-meson states. As Fig. C.2 depicted, it is convenient to study pure quark loops to get the large N_C behaviors of $\bar{q}q$ mesons.

A single $\bar{q}q$ meson propagator can be generated from a quark loop self interaction,

$$\langle J(x)J(0)\rangle, \quad (\text{C.2})$$

as illustrated in Fig. C.3. in the leading $1/N_C$ order. So $\langle J^\dagger(x)J(0)\rangle \sim N_C$. Since $J(x)$ can only couple with single-meson states in large N_C limit, $\langle J^\dagger(x)J(0)\rangle$ can be decomposed into a sequence of single-meson pole terms in momentum space,

$$\langle J(k)J(-k)\rangle = \sum_n \frac{|\langle 0|J|n\rangle|^2}{k^2 - m_n^2}. \quad (\text{C.3})$$

The summation runs over possible intermediate meson states with masses m_n . Since k^2 is independent from N_C , $\langle 0|J|n\rangle \sim \sqrt{N_C}$, and the meson masses behave as $m_n \sim N_C^0$ [150]. The wave functions $\langle 0|J|n\rangle$ are proportional to the decay constants of mesons. From Eq.(2.13) in Chapter 2, the pseudoscalar meson decay constant has the relation,

$$\langle 0|\partial_\mu A_m^\mu(0)|P_n\rangle = if_p m_p^2 \delta_{mn}, \quad (\text{C.4})$$

the pseudo scalar meson decay constant f_p is of order $f_p \sim N_C^{1/2}$.

The n-point meson vertices V_n are derived from n-current condensates (see Ref. [150]). For instance, in the large N_C limit, the 3-current condensate is dominated by single-meson poles,

$$\langle J(k_1)J(k_2)J(k_3)\rangle \sim \sum_{l,m,n} \frac{\langle 0|J|l\rangle}{k_1^2 - m_l^2} \frac{\langle 0|J|m\rangle}{k_2^2 - m_m^2} \frac{\langle 0|J|n\rangle}{k_3^2 - m_n^2} V_3 + \sum_{m,n} \langle 0|J|mn\rangle \frac{\langle 0|J|m\rangle}{k_2^2 - m_m^2} \frac{\langle 0|J|n\rangle}{k_3^2 - m_n^2}. \quad (\text{C.5})$$



Figure C.5.: Decay process of a meson. (a) is OZI suppressed. (b) is OZI allowed.

The 3-point single quark-loop diagram contributes to the leading $1/N_C$ order, which is depicted in Fig. C.4. It is of order N_C . The second term of Eq.(C.5) is proportional to a two-meson creation process. Since $\langle 0|J|n\rangle \sim N_C^{1/2}$, the matrix element of J annihilating a two-meson state, $\langle 0|J|mn\rangle$, is of order N_C^0 . It is $N_C^{-1/2}$ suppressed comparing to $\langle 0|J|n\rangle$. This fact is consistent with the statement that J is coupled mainly to single-meson states in the large N_C limit. The first term of (C.5) gives the large N_C scaling of the 3-point meson vertex V_3 ,

$$N_C^{-1/2}, \quad (\text{C.6})$$

while $\langle 0|J|n\rangle$ is of order $\sqrt{N_C}$. Generally, an n -point vertex has the order [153, 150],

$$N_C^{1-n/2}. \quad (\text{C.7})$$

From this scaling rule one can get that, when N_C tends to infinity, interactions between quark-antiquark mesons are switched off and they become stable.

The large N_C approximation can also interpret the OZI rule (see e.g. [72]). The quark disconnected decay amplitude (Fig. C.5(a)) is N_C^{-1} suppressed comparing to the quark connected decay amplitude (Fig. C.5(b)), since the quark disconnected diagrams have at least one more quark loop than the quark connected ones. Regarding to the effective chiral Lagrangian, we observe that a flavor trace can be interpreted as a quark loop. Therefore, the one more flavor trace will contribute a N_C^{-1} for the corresponding interaction. As an example, in the NLO chiral Lagrangian (2.117),

$$\begin{aligned} \mathcal{L}_4^{(2)} = & \frac{2c_2 + c_3}{f^2} D\bar{D}\text{Tr}(\partial_\mu\Phi\partial^\mu\Phi) - \frac{c_3}{f^2} D\partial_\mu\Phi\partial^\mu\Phi\bar{D} + \frac{(2c_4 + c_5)}{2\dot{M}_D^2 f^2} \partial_\mu D\partial_\nu\bar{D}\text{Tr}[\partial^\mu\Phi, \partial^\nu\Phi]_+ \\ & - \frac{c_5}{2\dot{M}_D^2 f^2} \partial_\mu D[\partial^\mu\Phi, \partial^\nu\Phi]_+ \partial_\nu\bar{D} + i\frac{c_6}{4f^2} \epsilon^{\mu\nu\rho\sigma} (D[\partial_\mu\Phi, \partial_\nu\Phi]_- \bar{D}_{\rho\sigma} - D_{\rho\sigma}[\partial_\nu\Phi, \partial_\mu\Phi]_- \bar{D}) \\ & - \frac{2\tilde{c}_2 + \tilde{c}_3}{2f^2} D^{\alpha\beta}\bar{D}_{\alpha\beta}\text{Tr}(\partial_\mu\Phi\partial^\mu\Phi) + \frac{\tilde{c}_3}{2f^2} D^{\alpha\beta}\partial_\mu\Phi\partial^\mu\Phi\bar{D}_{\alpha\beta} - \frac{(2\tilde{c}_4 + \tilde{c}_5)}{4\dot{M}_{D^*}^2 f^2} \partial_\mu D^{\alpha\beta}\partial_\nu\bar{D}_{\alpha\beta}\text{Tr}[\partial^\mu\Phi, \partial^\nu\Phi]_+ \\ & + \frac{\tilde{c}_5}{4\dot{M}_{D^*}^2 f^2} \partial_\mu D^{\alpha\beta}[\partial^\mu\Phi, \partial^\nu\Phi]_+ \partial_\nu\bar{D}_{\alpha\beta} - \frac{\tilde{c}_6}{f^2} D^{\mu\alpha}[\partial_\mu\Phi, \partial^\nu\Phi]_- \bar{D}_{\nu\alpha}, \end{aligned} \quad (\text{C.8})$$

the interactions with a flavor trace are suppressed by N_C^{-1} comparing to the interactions with no traces. This fact implies the following relations in the large- N_C limit

$$\begin{aligned} 2c_2 + c_3 &= 0, & 2c_4 + c_5 &= 0, \\ 2\tilde{c}_2 + \tilde{c}_3 &= 0, & 2\tilde{c}_4 + \tilde{c}_5 &= 0. \end{aligned} \quad (\text{C.9})$$

D Passarino-Veltman Integrals

According to the Passarino-Veltman reduction approach, the one-loop integrals can be decomposed into some master integrals. In our calculations, there are two such integrals involved,

$$I_i \equiv i\mu^{-\epsilon} \int \frac{d^{4+\epsilon}k}{(2\pi)^{4+\epsilon}} \frac{1}{k^2 - m_i^2 + i0^+}, \quad (\text{D.1})$$

$$I_{ij}(p^2) \equiv -i\mu^{-\epsilon} \int \frac{d^{4+\epsilon}k}{(2\pi)^{4+\epsilon}} \frac{1}{(k^2 - m_i^2 + i0^+)((k-p)^2 - m_j^2 + i0^+)}, \quad (\text{D.2})$$

where $\epsilon = d - 4$ and d is the dimension of the space-time. Other integrals might arise from our results under the reduction process, having the form,

$$I_\beta \equiv \int \frac{d^{4+\epsilon}k}{(2\pi)^{4+\epsilon}} (k^2)^{\beta-1}, \quad \beta = 0, 1, 2, \dots \quad (\text{D.3})$$

Under the dimensional regularization, they are assigned to be 0 according to 't Hooft-Veltman conjecture [154], In our loop calculations, we invoke the two integrals I_i and I_{ij} by assigning i, j to be either Q or R. In the physics world, the integrals are evaluated under the limit $d \rightarrow 4$.

D.1 Passarino-Veltman integrals in an infinite volume

In the infinite volume limit $V \rightarrow R^3$ of the continuum, the Passarino-Veltman integrals are divergent continuous integrals in the limit $\epsilon \rightarrow 0$. We use dimensional regularization to regularize the divergence and obtain

$$\begin{aligned} I_i &= \frac{m_i^2}{16\pi^2} \Gamma\left(-\frac{\epsilon}{2} - 1\right) \left(\frac{m_i^2}{4\pi\mu^2}\right)^{\epsilon/2} \\ &= \frac{m_i^2}{16\pi^2} \left[\frac{2}{\epsilon} + \gamma - 1 - \ln(4\pi) + \ln\left(\frac{m_i^2}{\mu^2}\right) + O(\epsilon) \right]. \end{aligned} \quad (\text{D.4})$$

The first term diverges in the physical limit $\epsilon \rightarrow 4$.

Using the Feynman parameterization, we can evaluate the second master integral, the scalar bubble I_{ij} , as

$$\begin{aligned} I_{ij}(p^2) &= -\frac{I_i - I_j}{m_i^2 - m_j^2} + \frac{1}{16\pi^2} \left\{ 1 + \frac{1}{2} \left(\frac{m_i^2 + m_j^2}{m_i^2 - m_j^2} - \frac{m_i^2 - m_j^2}{p^2} \right) \ln\left(\frac{m_i^2}{m_j^2}\right) \right. \\ &\quad \left. + \frac{p_{ij}(p^2)}{\sqrt{p^2}} \left[\ln\left(1 - \frac{p^2 - 2p_{ij}(p^2)\sqrt{p^2}}{m_i^2 + m_j^2}\right) - \ln\left(1 - \frac{p^2 + 2p_{ij}(p^2)\sqrt{p^2}}{m_i^2 + m_j^2}\right) \right] \right\}, \\ p_{ij}^2(p^2) &= \frac{p^2}{4} - \frac{m_i^2 + m_j^2}{2} + \frac{(m_i^2 - m_j^2)^2}{4p^2}, \end{aligned} \quad (\text{D.5})$$

where $-(I_i - I_j)/(m_i^2 - m_j^2)$ is identical to $I_{ij}(0)$. All the divergences of I_{ij} have been sorted into this term. According to Eq.(D.4), we can get the relation

$$\epsilon I_{ij}(p^2) = -\frac{1}{8\pi^2}. \quad (\text{D.6})$$

The product $4p^2 p_{ij}^2$ is known as Källén function $\lambda(p^2, m_i^2, m_j^2)$,

$$\lambda(x, y, z) = x^2 + y^2 + z^2 - 2xy - 2yz - 2zx. \quad (\text{D.7})$$

It is symmetric under an arbitrary permutation of p^2 , m_i^2 and m_j^2 . The imaginary part of the scalar bubble reads as

$$\text{Im } I_{ij}(p^2) = \frac{p_{ij}}{8\pi\sqrt{p^2}} \Theta(p^2 - (m_i + m_j)^2). \quad (\text{D.8})$$

It serves as the spectral function generating the spectral representation of the scalar bubble via the once subtracted dispersion relation

$$I_{ij}(p^2) = -\frac{I_i - I_j}{m_i^2 - m_j^2} + \int_{(m_i+m_j)^2}^{\infty} \frac{ds}{8\pi^2 s^{1/2}} \frac{p^2 p_{ij}(s)}{s - p^2}. \quad (\text{D.9})$$

We assign $i, j = Q, R$ in the above Passarino-Veltman integrals and obtain the scalar-loop functions I_Q , I_R and I_{QR} in this work. The infinite-volume results for these scalar-loop integrals under the χ - $\overline{\text{MS}}$ scheme are obtained by applying the subtractions Eq.(3.31).

D.2 Finite-volume corrections

In this work, finite-volume effects have been taken into account in the loop corrections of the D -meson self-energies. The finite-volume effects of the chiral effective theories have been extensively studied in literatures [155, 156, 140, 157]. To implement the finite-volume effects, it is sufficient to perform Passarino-Veltman reduction and apply the finite-volume corrections on the Passarino-Veltman integrals [43]. The finite-volume corrections of the Passarino-Veltman integrals involved in this work have been given in [43]. The results are listed below.

The finite-volume corrections denoted as $\Delta I \equiv I^V - I^{V \rightarrow \infty}$ for the corresponding scalar-loop integral I . The Goldstone-boson scalar-tadpole integral experiences the finite-volume correction as

$$\Delta \bar{I}_Q = \frac{1}{4\pi^2} \sum_{\vec{n} \in \mathbb{Z}^3}^{\vec{n} \neq 0} \frac{m_Q}{|\vec{x}_n|} K_1(m_Q |\vec{x}_n|), \quad \text{with} \quad \vec{x}_n = L\vec{n}. \quad (\text{D.10})$$

on top of the infinite-volume integral with χ - $\overline{\text{MS}}$ scheme (3.34). The function $K_n(x)$ is the modified Bessel function of the second kind. Special cares have been taken on the tadpoles $I_Q^{(2)}$,

$$I_Q^{(2)} = \int \frac{d^{4+\epsilon} k}{(2\pi)^{4+\epsilon}} \frac{i\mu^{-\epsilon}}{k^2 - m_i^2 + i0^+} \left(\frac{k \cdot p}{\sqrt{p^2}} \right)^2 \quad (\text{D.11})$$

The finite-volume correction reads,

$$\Delta \bar{I}_Q^{(2)} = -\frac{1}{4\pi^2} \sum_{\vec{n} \in \mathbb{Z}^3}^{\vec{n} \neq 0} \frac{m_Q^2}{|\vec{x}_n|^2} K_2(m_Q |\vec{x}_n|). \quad (\text{D.12})$$

on top of the infinite-volume relation $\bar{I}_Q^{(2)}(V \rightarrow \infty) = \frac{1}{4} m_Q^2 \bar{I}_Q$.

The heavy-light scalar bubble \bar{I}_{QR} experiences a finite-volume correction as well. For sub-threshold conditions $|p^2| < m_Q + M_R$, it reads

$$\Delta \bar{I}_{QR} - \frac{\Delta \bar{I}_Q}{M_R^2 - m_Q^2} = \frac{1}{8\pi^2} \sum_{\vec{n} \in \mathbb{Z}^3}^{\vec{n} \neq 0} \left(\int_0^1 dz K_0(|x_n| \mu(z)) - \frac{2m_Q K_1(m_Q |\vec{x}_n|)}{|\vec{x}_n| (M_R^2 - m_Q^2)} \right),$$

$$\text{with } \mu^2(z) = zM_R^2 + (1-z)m_Q^2 - (1-z)zp^2, \quad \vec{x}_n = L\vec{n}. \quad (\text{D.13})$$

In the beyond-threshold regime, the finite-volume correction reads

$$\begin{aligned} \Delta I_{QR} = & -i \frac{P_{QR}}{8\pi\sqrt{p^2}} + \frac{1}{8\pi^2 L \sqrt{p^2}} Z_{00}\left(1, \frac{L^2}{4\pi^2} P_{QR}^2\right) \\ & + \frac{1}{2\pi^2} \text{Re} \sum_{\vec{n} \in \mathbb{Z}^3}^{\vec{n} \neq 0} \int_0^\infty d\lambda \frac{\lambda}{|\vec{x}_n|} e^{-\lambda|\vec{x}_n|/\sqrt{2}} e^{i\lambda|\vec{x}_n|/\sqrt{2}} f(\lambda^2) \end{aligned}$$

with,

$$f(\lambda^2) = \frac{1}{2} \frac{1}{E_Q E_R (E_Q + E_R)} \frac{p^2}{(E_Q + E_R)^2 - p^2},$$

$$E_Q = \sqrt{m_Q^2 + i\lambda^2}, \quad E_R = \sqrt{M_R^2 + i\lambda^2}. \quad (\text{D.14})$$

The Lüscher's zeta function [158, 159] has been included, defined as

$$Z_{00}(1, k^2) = \sqrt{\pi^3} \sum_{\vec{n} \in \mathbb{Z}^3}^{\vec{n} \neq 0} \int_0^1 \frac{dt}{\sqrt{t^3}} e^{tk^2} + \sum_{\vec{n} \in \mathbb{Z}^3}^{\vec{n} \neq |k|} \frac{e^{-\vec{n} \cdot k^2}}{\vec{n}^2 - k^2} + \sqrt{\pi^3} \left\{ -2 + \int_0^1 \frac{dt}{\sqrt{t^3}} (e^{tk^2} - 1) \right\}. \quad (\text{D.15})$$

E Chiral expansions

E.1 Basic definitions

In the process of the chiral expansion Sec. 3.2.4, the following kinematic functions are introduced for convenience. For the 0^- D -meson masses, the following functions are involved

$$\begin{aligned}
\alpha_1 &= \frac{(2M + \Delta)^2}{4M^2}, & \alpha_2 &= \frac{2M^2 + 2\Delta M + \Delta^2}{2M^2}, & \alpha_3 &= 1, \\
\gamma_1 &= \frac{2M + \Delta}{M} \log \frac{\Delta(2M + \Delta)}{(M + \Delta)^2}, \\
\gamma_2 &= -\frac{2M^2 + 2\Delta M + \Delta^2}{M(M + 2\Delta)} \log \frac{\Delta(2M + \Delta)}{(M + \Delta)^2} - \frac{M}{M + 2\Delta}, & \gamma_3 &= \frac{M}{2M + \Delta}, \\
\gamma_4 &= -2 \frac{M(M + \Delta)^2}{(2M + \Delta)^3} \log \frac{\Delta(2M + \Delta)}{(M + \Delta)^2} + \frac{M^3}{2(2M + \Delta)^3}, & \gamma_5 &= \frac{M(M + \Delta)^2}{(2M + \Delta)^3}, \\
\delta_1 &= \gamma_1 - \frac{2M + \Delta}{M} \log \frac{2\Delta}{(M + \Delta)}, \\
\delta_2 &= \gamma_2 + \frac{2M^2 + 2\Delta M + \Delta^2}{M(M + 2\Delta)} \log \frac{2\Delta}{M^2} + \frac{2M + \Delta}{4M} \\
&\quad + 2(\tilde{\gamma}_3 - \gamma_3) \log \frac{M + \Delta}{M}, \\
\delta_3 &= \gamma_3 - \frac{2M^2 + 2\Delta M + \Delta^2}{(2M + \Delta)^3}, & \delta_5 &= 0, \\
\delta_4 &= \gamma_4 + \frac{2M(M + \Delta)^2}{(2M + \Delta)^3} \log \frac{2\Delta}{M} \\
&\quad - \frac{4M^2 + \Delta(4M + 5\Delta)}{32M(2M + \Delta)} + 2(\delta_5 - \gamma_5) \log \frac{M + \Delta}{M}, \\
\delta_6 &= \frac{2M + \Delta}{2M} \frac{\partial}{\partial \Delta} \frac{2M\Delta}{2M + \Delta} (\gamma_1 - \delta_1) + \gamma_1, & \delta_7 &= \gamma_2 + \frac{1}{2}(\gamma_1 - \delta_1) \frac{\Delta^2}{(2M + \Delta)^2}, \\
\beta_1 &= \Delta \frac{\partial}{\partial \Delta} \alpha_1 \frac{2M + \Delta}{2M}, \\
\beta_2 &= \Delta^2 \frac{\partial}{\partial \Delta} \frac{\alpha_1 \delta_2}{\Delta}, & \beta_3 &= \Delta^2 \frac{\partial}{\partial \Delta} \frac{\alpha_1 \delta_3}{\Delta}, \\
\beta_4 &= \Delta \gamma_1 \frac{\partial}{\partial \Delta} \alpha_1, & \beta_5 &= \Delta \frac{\partial}{\partial \Delta} \alpha_1 \delta_1, \\
\beta_6 &= \frac{\Delta^2 \partial^2}{\partial \Delta \partial \Delta} \left(\alpha_1 \frac{2M + \Delta}{2M} \right), & \beta_7 &= \Delta \frac{\Delta^2 \partial^2}{\partial \Delta \partial \Delta} \frac{\alpha_1 \delta_2}{\Delta} \\
\beta_8 &= \Delta \frac{\Delta^2 \partial^2}{\partial \Delta \partial \Delta} \frac{\alpha_1 \delta_3}{\Delta}, & \beta_9 &= \gamma_1 \frac{\Delta^2 \partial^2}{\partial \Delta \partial \Delta} \alpha_1, \\
\beta_{10} &= \frac{\Delta^2 \partial^2}{\partial \Delta \partial \Delta} \alpha_1 \delta_1, & \beta_{11} &= -\frac{1}{4} \alpha_1 \frac{M}{2M + \Delta} + (\alpha_1 - \alpha_2) \frac{(2M + \Delta)M}{2\Delta^2}. \tag{E.1}
\end{aligned}$$

For the 1^- D -meson masses, the following functions are involved

$$\begin{aligned}
\tilde{\alpha}_1 &= \frac{(2M + \Delta)^2}{4M^2}, & \tilde{\alpha}_2 &= \frac{2M^2 + 2\Delta M + \Delta^2}{2M^2}, & \tilde{\alpha}_3 &= 1, \\
\tilde{\gamma}_1 &= -\frac{M(2M + \Delta)}{(M + \Delta)^2} \log \frac{\Delta(2M + \Delta)}{M^2}, \\
\tilde{\gamma}_2 &= \frac{M}{2M + \Delta} + M \frac{2M^2 + 2\Delta M + \Delta^2}{(2M + \Delta)(M + \Delta)^2} \log \frac{\Delta(2M + \Delta)}{M^2}, \\
\tilde{\gamma}_3 &= -\frac{M}{2M + \Delta}, \\
\tilde{\gamma}_4 &= -\frac{M(M + \Delta)^2}{2(2M + \Delta)^3} + \frac{2M^3}{(2M + \Delta)^3} \log \frac{\Delta(2M + \Delta)}{M^2}, \\
\tilde{\gamma}_5 &= -\frac{M^3}{(2M + \Delta)^3}. \\
\tilde{\delta}_1 &= \tilde{\gamma}_1 + \frac{M(2M + \Delta)}{(M + \Delta)^2} \log \frac{2\Delta}{M} \\
\tilde{\delta}_2 &= \tilde{\gamma}_2 - \frac{M(2M^2 + 2\Delta M + \Delta^2)}{(M + \Delta)(M + \Delta)^2} \log \frac{2\Delta}{M + \Delta} \\
&\quad - \frac{M(2M + \Delta)}{4(M + \Delta)^2} - 2(\tilde{\delta}_3 - \tilde{\gamma}_3) \log \frac{M + \Delta}{M}, \\
\tilde{\delta}_3 &= \tilde{\gamma}_3 + \frac{M(2M^2 + 2\Delta M + \Delta^2)}{2(M + \Delta)^2(2M + \Delta)}, & \tilde{\delta}_5 &= 0, \\
\tilde{\delta}_4 &= \tilde{\gamma}_4 - \frac{2M^3}{(2M + \Delta)^3} \log \frac{2\Delta}{M + \Delta} \\
&\quad + \frac{M(4M^2 + 4\Delta M + 5\Delta^2)}{32(M + \Delta)^2(2M + \Delta)} - 2(\tilde{\delta}_5 - \tilde{\gamma}_5) \log \frac{M + \Delta}{M}, \\
\tilde{\delta}_6 &= \frac{2M + \Delta}{2M} \frac{\partial}{\partial \Delta} \frac{2(M + \Delta)}{2M + \Delta} \Delta (\tilde{\gamma}_1 - \tilde{\delta}_1) + \tilde{\gamma}_1, & \tilde{\delta}_7 &= \tilde{\gamma}_2 + \frac{1}{2} (\tilde{\gamma}_1 - \tilde{\delta}_1) \frac{\Delta^2}{(2M + \Delta)^2}, \\
\tilde{\beta}_1 &= \frac{M + \Delta}{M} \frac{\Delta}{\partial \Delta} \frac{\partial}{\partial \Delta} \tilde{\alpha}_1 \frac{(2M + \Delta)M^2}{2(M + \Delta)^3}, \\
\tilde{\beta}_2 &= \Delta^2 \frac{\partial}{\partial \Delta} \frac{\tilde{\alpha}_1 \tilde{\delta}_2}{\Delta}, & \tilde{\beta}_3 &= \Delta^2 \frac{\partial}{\partial \Delta} \frac{\tilde{\alpha}_1 \tilde{\delta}_3}{\Delta}, \\
\tilde{\beta}_4 &= \frac{\Delta}{M} \frac{(M + \Delta)^2}{M} \tilde{\gamma}_1 \frac{\partial}{\partial \Delta} \frac{M^2 \tilde{\alpha}_1}{(M + \Delta)^2}, & \tilde{\beta}_5 &= \frac{M + \Delta}{M} \frac{\Delta}{\partial \Delta} \frac{\partial}{\partial \Delta} \frac{\tilde{\alpha}_1 \tilde{\delta}_1 M}{M + \Delta}, \\
\tilde{\beta}_6 &= D_{\Delta\Delta} \frac{(2M + \Delta)M^2}{2(M + \Delta)^3} \tilde{\alpha}_1, & \tilde{\beta}_7 &= \frac{\Delta}{M + \Delta} D_{\Delta\Delta} \frac{M}{\Delta} \tilde{\alpha}_1 \tilde{\delta}_2, \\
\tilde{\beta}_8 &= \frac{\Delta}{M + \Delta} D_{\Delta\Delta} \frac{M}{\Delta} \tilde{\alpha}_1 \tilde{\delta}_3, & \tilde{\beta}_9 &= \tilde{\delta}_1 \frac{M + \Delta}{M} D_{\Delta\Delta} \frac{M^2}{(M + \Delta)^2} \tilde{\alpha}_1, \\
\tilde{\beta}_{10} &= D_{\Delta\Delta} \frac{M}{M + \Delta} \tilde{\alpha}_1 \tilde{\delta}_1, & \tilde{\beta}_{11} &= -\frac{1}{4} \tilde{\alpha}_1 \frac{M}{2M + \Delta} + (\tilde{\alpha}_1 - \tilde{\alpha}_2) \frac{(2M + \Delta)M}{2\Delta^2}. \tag{E.2}
\end{aligned}$$

The followings are the kinematic functions involved in the strict chiral expansion Sec. 3.2.2.

$$\gamma_d^{(1)} = \frac{M}{2(M + \Delta)} \left[\frac{\partial}{\partial \Delta} (\alpha_2 \Delta \gamma_1 - \alpha_1 \Delta \gamma_2) - \Delta \gamma_1 \frac{\partial \alpha_2}{\partial \Delta} \right],$$

$$\begin{aligned}
\gamma_d^{(2)} &= \frac{\Delta}{2M} \left[\frac{\partial}{\partial M} (\alpha_2 M \gamma_1 - \alpha_1 M \gamma_2) - \frac{1}{M} \gamma_1 \frac{\partial}{\partial M} (\alpha_2 M^2) \right] - \frac{M+\Delta}{M} \gamma_d^{(1)}, \\
\gamma_d^{(3)} &= -\frac{M}{4(M+\Delta)^2} \left(\frac{\partial \alpha_1 \Delta^2}{\partial \Delta} \right) \left(\frac{\partial \gamma_1 \Delta}{\partial \Delta} \right) - \frac{\alpha_1 \Delta^2 M}{4(M+\Delta)} \frac{\partial}{\partial \Delta} \left[\frac{1}{2(M+\Delta)} \left(\frac{\partial \gamma_1 \Delta}{\partial \Delta} \right) \right], \\
\gamma_d^{(4)} &= -\frac{1}{8M^2} \left(\frac{\partial}{\partial M} - \frac{\partial}{\partial \Delta} \right)^2 (\alpha_1 M \Delta^3 \gamma_1) + \frac{\gamma_1 \Delta}{8M^3} \left(\frac{\partial}{\partial M} - \frac{\partial}{\partial \Delta} \right)^2 (\alpha_1 M^2 \Delta^2) \\
&\quad + \frac{1}{8M^3} \left(\frac{\partial}{\partial M} - \frac{\partial}{\partial \Delta} \right) (\alpha_1 M \Delta^3 \gamma_1) - \frac{\gamma_1 \Delta}{8M^4} \left(\frac{\partial}{\partial M} - \frac{\partial}{\partial \Delta} \right) (\alpha_1 M^2 \Delta^2), \\
\gamma_d^{(5)} &= -\frac{1}{2M} \frac{\partial}{\partial M} \frac{1}{2(M+\Delta)} \frac{\partial}{\partial \Delta} (\alpha_1 M \Delta^3 \gamma_1) \\
&\quad + \frac{\gamma_1 \Delta}{2M^2} \frac{\partial}{\partial M} \frac{1}{2(M+\Delta)} \frac{\partial}{\partial \Delta} (\alpha_1 M^2 \Delta^2) - 2 \frac{M+\Delta}{M} \gamma_d^{(3)}, \tag{E.3}
\end{aligned}$$

and

$$\begin{aligned}
\tilde{\gamma}_d^{(1)} &= \frac{\Delta}{6M} \left[\frac{\partial}{\partial M} (\tilde{\alpha}_2 M \tilde{\gamma}_1 - \tilde{\alpha}_1 M \tilde{\gamma}_2) - \frac{1}{M} \tilde{\gamma}_1 \frac{\partial}{\partial M} (\tilde{\alpha}_2 M^2) \right] - \frac{M+\Delta}{M} \tilde{\gamma}_d^{(2)}, \\
\tilde{\gamma}_d^{(2)} &= \frac{M}{6(M+\Delta)} \left[\frac{\partial}{\partial \Delta} (\tilde{\alpha}_2 \Delta \tilde{\gamma}_1 - \tilde{\alpha}_1 \Delta \tilde{\gamma}_2) - \Delta \tilde{\gamma}_1 \frac{\partial}{\partial \Delta} \tilde{\alpha}_2 \right], \\
\tilde{\gamma}_d^{(3)} &= -\frac{1}{24M^2} \left(\frac{\partial}{\partial M} - \frac{\partial}{\partial \Delta} \right)^2 (\tilde{\alpha}_1 M \Delta^3 \tilde{\gamma}_1) + \frac{\tilde{\gamma}_1 \Delta}{24M^3} \left(\frac{\partial}{\partial M} - \frac{\partial}{\partial \Delta} \right)^2 (\tilde{\alpha}_1 M^2 \Delta^2) \\
&\quad + \frac{1}{24M^3} \left(\frac{\partial}{\partial M} - \frac{\partial}{\partial \Delta} \right) (\tilde{\alpha}_1 M \Delta^3 \tilde{\gamma}_1) - \frac{\tilde{\gamma}_1 \Delta}{24M^4} \left(\frac{\partial}{\partial M} - \frac{\partial}{\partial \Delta} \right) (\tilde{\alpha}_1 M^2 \Delta^2), \\
\tilde{\gamma}_d^{(4)} &= -\frac{M}{12(M+\Delta)^2} \left(\frac{\partial \tilde{\alpha}_1 \Delta^2}{\partial \Delta} \right) \left(\frac{\partial \tilde{\gamma}_1 \Delta}{\partial \Delta} \right) - \frac{\tilde{\alpha}_1 \Delta^2 M}{12(M+\Delta)} \frac{\partial}{\partial \Delta} \left[\frac{1}{2(M+\Delta)} \left(\frac{\partial \tilde{\gamma}_1 \Delta}{\partial \Delta} \right) \right], \\
\tilde{\gamma}_d^{(5)} &= -\frac{1}{6M} \frac{\partial}{\partial M} \frac{1}{2(M+\Delta)} \frac{\partial}{\partial \Delta} (\tilde{\alpha}_1 M \Delta^3 \tilde{\gamma}_1) \\
&\quad + \frac{\tilde{\gamma}_1 \Delta}{6M^2} \frac{\partial}{\partial M} \frac{1}{2(M+\Delta)} \frac{\partial}{\partial \Delta} (\tilde{\alpha}_1 M^2 \Delta^2) - 2 \frac{M+\Delta}{M} \tilde{\gamma}_d^{(4)}. \tag{E.4}
\end{aligned}$$

E.2 $O(Q^5)$ results according to the small-scale expansion scheme

Here we provide the fifth-order moments of the D -meson bubble-loop contributions according to the small-scale expansion (Sec. 3.2.3). The 5-th order correction for the pseudoscalar D -mesons is

$$\begin{aligned}
\bar{\Pi}_{H \in [0^-]}^{\text{loop-5}} &= \sum_{Q \in [8]} \sum_{R \in [1^-]} \left(\frac{G_{QR}^{(H)}}{8\pi f} \right)^2 \left\{ \frac{\Delta}{2M} \left[m_Q^4 + 2m_Q^2 (2\Pi_H^{(2)} - \Pi_R^{(2)}) + (\Pi_H - \Pi_R)^2 \right] \log \frac{m_Q^2}{M^2} \right. \\
&\quad \left. + \frac{\Delta}{8M} \left[14m_Q^4 - m_Q^2 (3\Delta^2 - 16\Pi_H^{(2)} + 36\Pi_R^{(2)}) + 10(\Pi_H - \Pi_R)^2 \right] \right. \\
&\quad \left. - \frac{\Delta_Q}{8M} \left(\log(\Delta + \Delta_Q) - \log(\Delta - \Delta_Q) \right) \left[6\Delta_Q^4 + 4\Delta_Q^2 (3\Pi_R^{(2)} - 5\Pi_H^{(2)}) \right. \right. \\
&\quad \left. \left. + 6(\Pi_H^{(2)} - \Pi_R^{(2)})^2 + 3m_Q^2 \left(\Delta_Q^2 + 2(\Pi_R^{(2)} - 3\Pi_H^{(2)}) + \frac{(\Pi_H^{(2)} - \Pi_R^{(2)})^2}{\Delta_Q^2} \right) \right] \right\}
\end{aligned}$$

$$\begin{aligned}
& + \frac{\Delta}{4M} \left[3\Delta_Q^4 - 2m_Q^4 - 2(\Delta^2 + m_Q^2)(\Pi_H^{(2)} + \Pi_R^{(2)}) \right. \\
& \quad \left. + (8\Delta^2 + \Pi_R^{(2)} - \Pi_H^{(2)})(\Pi_R^{(2)} - \Pi_H^{(2)}) \right] \log \frac{m_Q^2}{4\Delta^2} \Big\}. \tag{E.5}
\end{aligned}$$

The 5-th order correction for the vector D -mesons is

$$\begin{aligned}
\bar{\Pi}_{H \in [1^-]}^{\text{loop-5}} &= \sum_{Q \in [8]} \sum_{R \in [1^-]} \left(\frac{G_{QR}^{(H)}}{4\pi f} \right)^2 \frac{1}{12} \left\{ 4\Delta m_Q (2m_Q^2 - 3\Pi_R^{(2)} + 3\Pi_H^{(2)}) \right. \\
& \quad \left. + \pi \left[3m_Q^4 + 2m_Q^2(\Pi_H^{(2)} - 3\Pi_R^{(2)}) + 3(\Pi_R^{(2)} - \Pi_H^{(2)})^2 \right] \right\} \\
& + \sum_{Q \in [8]} \sum_{R \in [0^-]} \left(\frac{G_{QR}^{(H)}}{4\pi f} \right)^2 \frac{1}{3} \left\{ \frac{\Delta}{2M} \left(m_Q^4 + 2m_Q^2(2\Pi_H^{(2)} - \Pi_R^{(2)}) + (\Pi_H - \Pi_R)^2 \right) \log \frac{m_Q^2}{M^2} \right. \\
& \quad \left. + \frac{\Delta}{8M} \left[-6m_Q^4 + m_Q^2(3\Delta^2 - 4\Pi_H^{(2)} + 24\Pi_R^{(2)}) - 10(\Pi_H^{(2)} - \Pi_R^{(2)})^2 \right] \right. \\
& \quad \left. + \frac{\Delta_Q}{8M} \left(\log(-\Delta - \Delta_Q) - \log(-\Delta + \Delta_Q) \right) \left[6\Delta_Q^4 + 4\Delta_Q^2(3\Pi_R^{(2)} - 5\Pi_H^{(2)}) \right. \right. \\
& \quad \left. \left. + 6(\Pi_H^{(2)} - \Pi_R^{(2)})^2 + 3m_Q^2 \left(\Delta_Q^2 + 2(\Pi_R^{(2)} - 3\Pi_H^{(2)}) + \frac{(\Pi_H^{(2)} - \Pi_R^{(2)})^2}{\Delta_Q^2} \right) \right] \right. \\
& \quad \left. + \frac{\Delta}{4M} \left[3\Delta_Q^4 - 2m_Q^4 - 2(\Delta^2 + m_Q^2)(\Pi_H^{(2)} + \Pi_R^{(2)}) \right. \right. \\
& \quad \left. \left. + (8\Delta^2 + \Pi_R^{(2)} - \Pi_H^{(2)})(\Pi_R^{(2)} - \Pi_H^{(2)}) \right] \log \frac{m_Q^2}{4\Delta^2} \right\}. \tag{E.6}
\end{aligned}$$

E.3 $O(Q^5)$ results according to the novel chiral expansion scheme

The fifth-order contribution of the pseudo-scalar charmed meson self energy is provided as

$$\begin{aligned}
\Pi_{H \in [0^-]}^{5\text{-loop}} &= \sum_{\substack{Q \in [8] \\ R \in [1^-]}} \left(\frac{m_Q}{4\pi f} G_{QR}^{(H)} \right)^2 \left\{ -\frac{\alpha_1}{4} \frac{M^2}{2M + \Delta} \frac{\Delta^3}{4M^2} \log \frac{4\Delta^2}{(M + \Delta)^2} \right. \\
& \quad \left. + \frac{\alpha_1}{8} \frac{\Delta^2}{m_Q^2} (M_R - M_H - \Delta_H)^2 \frac{M}{M + \Delta} \frac{\partial}{\partial \Delta} (\gamma_1 \Delta) \right. \\
& \quad \left. + \frac{M_H}{4} \left[(\alpha_1 - \alpha_2) \left(\frac{2M + \Delta}{2M} \frac{m_Q^2}{\Delta_H^2} (M_R - M_H) \log \frac{m_Q^2}{M_R^2} - (\delta_1 - \gamma_1) \frac{\Delta_Q^2}{\Delta_H} \right. \right. \right. \\
& \quad \left. \left. - \delta_1 \frac{\Delta_Q^2}{\Delta_H^2} (M_R - M_H - \Delta_H) \right) - \frac{\beta_{11}}{M_H^2} \left((M_R - M_H)^3 \log \frac{m_Q^2}{M_R^2} \right. \right. \\
& \quad \left. \left. + \Delta_Q^3 \left[\log(M_R - M_H + \Delta_Q) - \log(M_R - M_H - \Delta_Q) \right] \right) \right. \\
& \quad \left. + \frac{m_Q^2 \Delta_Q^2}{\Delta_H^3} \left((\alpha_2 - \alpha_1) \left(\delta_2 + \delta_3 \log \frac{m_Q^2}{M_R^2} \right) - \alpha_1 \left(\delta_4 + \delta_5 \log \frac{m_Q^2}{M_R^2} \right) \right) \right] \\
& \quad \left. + \frac{M_H}{8} (M_R - M_H - \Delta_H)^2 \left[\beta_9 \frac{\Delta_Q^2}{m_Q^2 \Delta_H} - \beta_{10} \frac{\Delta_Q^2}{m_Q^2 \Delta_H^2} (M_R - M_B) \right] \right\}
\end{aligned}$$

$$\begin{aligned}
& -\frac{\beta_6}{m_Q^2 \Delta_H^2} \left((M_R - M_H) \left(\Delta_Q^2 - \frac{m_Q^2}{2} \right) \log \frac{m_Q^2}{M_R^2} \right. \\
& \quad \left. + \Delta_Q^3 \left[\log(M_R - M_H + \Delta_Q) - \log(M_R - M_H - \Delta_Q) \right] \right) \\
& \quad \left. + \left(-\beta_7 \frac{\Delta_Q^2}{\Delta_H^3} + \beta_8 \frac{m_Q^2}{\Delta_H^3} \log \frac{m_Q^2}{M_R^2} \right) \right] \Bigg\}, \tag{E.7}
\end{aligned}$$

The fifth-order contribution of the vector charmed meson self energy reads

$$\begin{aligned}
\Pi_{H \in [1^-]}^{5\text{-loop}} = & \sum_{\substack{Q \in [8] \\ R \in [1^-]}} \left(\frac{m_{QR}}{4\pi f} G_{QR}^{(H)} \right)^2 \frac{1}{3} \left\{ \frac{3\pi}{16} \frac{m_Q^3}{M_H} - \frac{m_Q^4}{M_H^2} \left(\frac{1}{6} - \frac{1}{8} \log \frac{m_Q}{M_R} \right) \right. \\
& \left. + (M_R - M_H)^2 \left(\frac{\pi}{4} \frac{M_H}{m_Q} + 1 + \frac{3}{2} \log \frac{m_Q}{M_R} \right) \right\} \\
& + \sum_{\substack{Q \in [8] \\ R \in [0^-]}} \left(\frac{m_Q}{4\pi f} G_{QR}^{(H)} \right)^2 \left\{ \frac{\tilde{\alpha}_1}{12} \frac{M^2}{(2M + \Delta)} \frac{\Delta^3}{4(M + \Delta)^2} \log \frac{4\Delta^2}{M^2} \right. \\
& \quad - \frac{\tilde{\alpha}_1}{24} \frac{\Delta^2}{m_Q^2} (M_R - M_H - \Delta_H)^2 \frac{M + \Delta}{M} \frac{\partial}{\partial \Delta} (\tilde{\gamma}_1 \Delta) \\
& \quad + \frac{M_H}{12} \frac{M}{M + \Delta} \left[-(\tilde{\alpha}_1 - \tilde{\alpha}_2) \left(\frac{M(2M + \Delta)}{2(M + \Delta)^2} \frac{m_Q^2}{\Delta_H^2} (M_H - M_R) \log \frac{m_Q^2}{M_R^2} \right. \right. \\
& \quad \left. \left. + (\tilde{\delta}_1 - \tilde{\gamma}_1) \frac{\Delta_Q^2}{\Delta_H} - \tilde{\delta}_1 \frac{\Delta_Q^2}{\Delta_H^2} (M_R - M_H + \Delta_H) \right) + \frac{\tilde{\beta}_{11}}{M_H^2} \left((M_H - M_R)^3 \log \frac{m_Q^2}{M_R^2} \right. \right. \\
& \quad \left. \left. + \Delta_Q^3 \left[\log(M_R - M_H - \Delta_Q) - \log(M_R - M_H + \Delta_Q) \right] \right) \right] \\
& \quad + \frac{m_Q^2 \Delta_Q^2}{\Delta_H^3} \left((\tilde{\alpha}_2 - \tilde{\alpha}_1) \left(\tilde{\delta}_2 + \tilde{\delta}_3 \log \frac{m_Q^2}{M_R^2} \right) - \beta_1 \left(\tilde{\delta}_4 + \tilde{\delta}_5 \log \frac{m_Q^2}{M_R^2} \right) \right) \Bigg\} \\
& + \frac{M_H}{24} (M_R - M_H - \Delta_H)^2 \left[\tilde{\beta}_9 \frac{\Delta_Q^2}{m_Q^2 \Delta_H} - \tilde{\beta}_{10} \frac{\Delta_Q^2}{m_Q^2 \Delta_H^2} (M_H - M_R) \right. \\
& \quad \left. + \frac{\tilde{\beta}_6}{m_Q^2 \Delta_H^2} \left((M_H - M_R) \left(\Delta_Q^2 - \frac{m_Q^2}{2} \right) \log \frac{m_Q^2}{M_R^2} \right. \right. \\
& \quad \left. \left. + \Delta_Q^3 \left[\log(M_R - M_H - \Delta_Q) - \log(M_R - M_H + \Delta_Q) \right] \right) \right] \\
& \quad \left. + \left(-\tilde{\beta}_7 \frac{\Delta_Q^2}{\Delta_H^3} + \tilde{\beta}_8 \frac{m_Q^2}{\Delta_H^3} \log \frac{m_Q^2}{M_R^2} \right) \right] \Bigg\}, \tag{E.8}
\end{aligned}$$

with $m_{QR}^2 = m_Q^2 - (M_R - M_H)^2$.

F A complement of the lattice data for the D -meson masses

In this appendix we list the lattice results for the D -meson masses from ETM collaboration, provided by the authors [40]. The results are listed in Table F.1 and F.2.

am_π	am_K	$a\mu_c$	discr.	am_D	am_{D_s}	am_{D^*}	$am_{D_s^*}$
0.1240(4)	0.2512(3)	0.2772	(\pm, \mp)	0.8979(9)	0.9412(2)	0.9782(16)	1.0225(7)
		0.2270	(\pm, \mp)	0.7994(8)	0.8441(2)	0.8880(16)	0.9338(7)
		0.2772	(\pm, \pm)	0.9154(14)	0.9610(3)	0.9759(15)	1.0185(7)
		0.2270	(\pm, \pm)	0.8181(12)	0.8655(3)	0.8859(15)	0.9289(8)
0.1412(3)	0.2569(3)	0.2768	(\pm, \mp)	0.9002(10)	0.9420(3)	0.9776(20)	1.0213(9)
		0.2389	(\pm, \mp)	0.8258(9)	0.8692(3)	0.9104(20)	0.9545(9)
		0.2768	(\pm, \pm)	0.9162(13)	0.9623(4)	0.9743(19)	1.0169(9)
		0.2389	(\pm, \pm)	0.8433(12)	0.8904(4)	0.9067(18)	0.9501(9)
0.1440(6)	0.2589(4)	0.2768	(\pm, \mp)	0.9006(8)	0.9425(3)	0.9801(23)	1.0252(8)
		0.2389	(\pm, \mp)	0.8268(12)	0.8697(2)	0.9153(19)	0.9589(8)
		0.2768	(\pm, \pm)	0.9160(13)	0.9627(3)	0.9813(16)	1.0208(7)
		0.2389	(\pm, \pm)	0.8432(11)	0.8911(3)	0.9145(15)	0.9544(7)
0.1988(3)	0.2764(3)	0.2929	(\pm, \mp)	0.9327(8)	0.9668(5)	1.0148(17)	1.0496(12)
		0.2299	(\pm, \mp)	0.8164(13)	0.8520(4)	0.9092(16)	0.9449(11)
		0.2929	(\pm, \pm)	0.9500(12)	0.9879(5)	1.0098(44)	1.0434(20)
		0.2299	(\pm, \pm)	0.8358(10)	0.8746(5)	0.9026(41)	0.9381(18)

Table F.1.: Masses for the D mesons from ETMC, provided by the authors of [40] (continued).

am_π	am_K	$a\mu_c$	discr.	am_D	am_{D_s}	am_{D^*}	$am_{D_s^*}$
0.1074(5)	0.2133(4)	0.2230	(\pm, \mp)	0.8473(10)	0.8780(5)	0.9140(31)	0.9474(10)
		0.1727	(\pm, \mp)	0.7501(8)	0.7827(4)	0.8262(29)	0.8601(9)
		0.2230	(\pm, \pm)	0.8588(16)	0.8922(7)	0.9112(25)	0.9443(10)
		0.1727	(\pm, \pm)	0.7629(14)	0.7978(6)	0.8224(24)	0.8566(10)
0.1549(2)	0.2279(2)	0.2230	(\pm, \mp)	0.8543(5)	0.8824(3)	0.9268(11)	0.9536(7)
		0.1727	(\pm, \mp)	0.7549(5)	0.7841(3)	0.8362(11)	0.8637(8)
		0.2230	(\pm, \pm)	0.8666(8)	0.8961(4)	0.9218(11)	0.9500(6)
		0.1727	(\pm, \pm)	0.7683(7)	0.7991(3)	0.8322(17)	0.8597(7)
0.1935(4)	0.2430(4)	0.2230	(\pm, \mp)	0.8559(8)	0.8784(5)	0.9309(18)	0.9521(13)
		0.1727	(\pm, \mp)	0.7600(11)	0.7850(4)	0.8443(18)	0.8669(13)
		0.2230	(\pm, \pm)	0.8690(8)	0.8928(5)	0.9273(14)	0.9484(11)
		0.1727	(\pm, \pm)	0.7763(7)	0.8007(5)	0.8413(14)	0.8629(11)
0.0703(4)	0.1697(3)	0.2230	(\pm, \mp)	0.6655(12)	0.6981(4)	0.7161(18)	0.7456(10)
		0.1919	(\pm, \mp)	0.6072(11)	0.6402(3)	0.6621(18)	0.6923(10)
		0.2230	(\pm, \pm)	0.6706(15)	0.7035(5)	0.7078(24)	0.7430(10)
		0.1919	(\pm, \pm)	0.6123(14)	0.6460(4)	0.6536(23)	0.6898(10)
0.0806(3)	0.1738(5)	0.2227	(\pm, \mp)	0.6661(19)	0.6983(4)	0.7209(26)	0.7452(12)
		0.1727	(\pm, \mp)	0.5712(14)	0.6041(4)	0.6325(25)	0.6586(11)
		0.2227	(\pm, \pm)	0.6721(22)	0.7037(5)	0.7209(20)	0.7452(10)
		0.1727	(\pm, \pm)	0.5775(17)	0.6102(4)	0.6335(23)	0.6587(10)
0.0975(3)	0.1768(3)	0.2230	(\pm, \mp)	0.6666(16)	0.6980(5)	0.7183(23)	0.7458(13)
		0.1727	(\pm, \mp)	0.5720(12)	0.6036(4)	0.6308(24)	0.6587(13)
		0.2230	(\pm, \pm)	0.6713(13)	0.7033(5)	0.7169(19)	0.7451(8)
		0.1727	(\pm, \pm)	0.5770(12)	0.6098(4)	0.6290(22)	0.6579(11)

Table F.2.: Masses for the D mesons from ETMC, provided by the authors of [40](continued).

Bibliography

- [1] Eric S. Swanson. The New heavy mesons: A Status report. *Phys.Rept.*, 429:243–305, 2006.
- [2] Shi-Lin Zhu. New hadron states. *Int.J.Mod.Phys.*, E17:283–322, 2008.
- [3] S. Godfrey and Nathan Isgur. Mesons in a Relativized Quark Model with Chromodynamics. *Phys.Rev.*, D32:189–231, 1985.
- [4] D. Ebert, R. N. Faustov, and V. O. Galkin. Properties of heavy quarkonia and B_c mesons in the relativistic quark model. *Phys. Rev.*, D67:014027, 2003.
- [5] B. Aubert et al. Observation of a narrow meson decaying to $D_s^+ \pi^0$ at a mass of 2.32-GeV/ c^2 . *Phys.Rev.Lett.*, 90:242001, 2003.
- [6] D. Besson et al. Observation of a narrow resonance of mass 2.46-GeV/ c^2 decaying to $D^* + (s) \pi^0$ and confirmation of the $D^*(sJ)(2317)$ state. *Phys.Rev.*, D68:032002, 2003.
- [7] Kazuo Abe et al. Measurements of the D_{sJ} resonance properties. *Phys. Rev. Lett.*, 92:012002, 2004.
- [8] Hua-Xing Chen, Wei Chen, Xiang Liu, Yan-Rui Liu, and Shi-Lin Zhu. A review of the open charm and open bottom mesons. 2016.
- [9] Stephen Godfrey and Richard Kokoski. The Properties of p Wave Mesons with One Heavy Quark. *Phys.Rev.*, D43:1679–1687, 1991.
- [10] Massimo Di Pierro and Estia Eichten. Excited heavy - light systems and hadronic transitions. *Phys.Rev.*, D64:114004, 2001.
- [11] Bernard Aubert et al. A Study of the $D^*(sJ)(2317)$ and $D(sJ)(2460)$ Mesons in Inclusive c anti- c Production Near $(s)^*(1/2) = 10.6$ -GeV. *Phys.Rev.*, D74:032007, 2006.
- [12] P. Colangelo and F. De Fazio. Understanding $D(sJ)(2317)$. *Phys. Lett.*, B570:180–184, 2003.
- [13] Jie Lu, Xiao-Lin Chen, Wei-Zheng Deng, and Shi-Lin Zhu. Pionic decays of $D(sj)(2317)$, $D(sj)(2460)$ and $B(sj)(5718)$, $B(sj)(5765)$. *Phys.Rev.*, D73:054012, 2006.
- [14] J. Gasser and H. Leutwyler. Chiral Perturbation Theory: Expansions in the Mass of the Strange Quark. *Nucl.Phys.*, B250:465, 1985.
- [15] J. Gasser and H. Leutwyler. Low-Energy Expansion of Meson Form-Factors. *Nucl.Phys.*, B250:517–538, 1985.
- [16] J. Gasser and H. Leutwyler. $\eta \rightarrow 3 \pi$ to One Loop. *Nucl.Phys.*, B250:539, 1985.
- [17] Nathan Isgur and Mark B. Wise. Weak decays of heavy mesons in the static quark Approximation. *Phys.Lett.*, B232:113, 1989.
- [18] Nathan Isgur and Mark B. Wise. Weak transition form factors between heavy mesons. *Phys.Lett.*, B237:527, 1990.
- [19] Mark B. Wise. Chiral perturbation theory for hadrons containing a heavy quark. *Phys.Rev.*, D45:2188–2191, 1992.

-
- [20] Gustavo Burdman and John F. Donoghue. Union of chiral and heavy quark symmetries. *Phys.Lett.*, B280:287–291, 1992.
- [21] Tung-Mow Yan, Hai-Yang Cheng, Chi-Yee Cheung, Guey-Lin Lin, Y.C. Lin, et al. Heavy quark symmetry and chiral dynamics. *Phys.Rev.*, D46:1148–1164, 1992.
- [22] M.F.M. Lutz and E.E. Kolomeitsev. Relativistic chiral SU(3) symmetry, large N(c) sum rules and meson baryon scattering. *Nucl.Phys.*, A700:193–308, 2002.
- [23] A. Gasparyan and M.F.M. Lutz. Photon- and pion-nucleon interactions in a unitary and causal effective field theory based on the chiral Lagrangian. *Nucl.Phys.*, A848:126–182, 2010.
- [24] Tran N. Truong. Chiral Perturbation Theory and Final State Theorem. *Phys.Rev.Lett.*, 61:2526, 1988.
- [25] J. A. Oller and Ulf G. Meissner. Chiral dynamics in the presence of bound states: Kaon nucleon interactions revisited. *Phys. Lett.*, B500:263–272, 2001.
- [26] J.A. Oller, E. Oset, and A. Ramos. Chiral unitary approach to meson meson and meson - baryon interactions and nuclear applications. *Prog.Part.Nucl.Phys.*, 45:157–242, 2000.
- [27] E.E. Kolomeitsev and M.F.M. Lutz. On Heavy light meson resonances and chiral symmetry. *Phys.Lett.*, B582:39–48, 2004.
- [28] J. Hofmann and M.F.M. Lutz. Open charm meson resonances with negative strangeness. *Nucl.Phys.*, A733:142–152, 2004.
- [29] Matthias F.M. Lutz and Madeleine Soyeur. Radiative and isospin-violating decays of D(s)-mesons in the hadrogenesis conjecture. *Nucl.Phys.*, A813:14–95, 2008.
- [30] Feng-Kun Guo, Christoph Hanhart, and Ulf-G. Meissner. Interactions between heavy mesons and Goldstone bosons from chiral dynamics. *Eur.Phys.J.*, A40:171–179, 2009.
- [31] M. Altenbuchinger, L. S. Geng, and W. Weise. Scattering lengths of Nambu-Goldstone bosons off D mesons and dynamically generated heavy-light mesons. *Phys. Rev.*, D89(1):014026, 2014.
- [32] Matthias F. M. Lutz et al. Resonances in QCD. *Nucl. Phys.*, A948:93–105, 2016.
- [33] John B. Kogut. A Review of the Lattice Gauge Theory Approach to Quantum Chromodynamics. *Rev.Mod.Phys.*, 55:775, 1983.
- [34] C. Aubin, C. Bernard, Carleton E. DeTar, M. Di Pierro, Elizabeth Dawn Freeland, et al. Charmed meson decay constants in three-flavor lattice QCD. *Phys.Rev.Lett.*, 95:122002, 2005.
- [35] E. Follana, C.T.H. Davies, G.P. Lepage, and J. Shigemitsu. High Precision determination of the pi, K, D and D(s) decay constants from lattice QCD. *Phys.Rev.Lett.*, 100:062002, 2008.
- [36] A. Bazavov et al. B- and D-meson decay constants from three-flavor lattice QCD. *Phys.Rev.*, D85:114506, 2012.
- [37] Daniel Mohler, C.B. Lang, Luka Leskovec, Sasa Prelovsek, and R.M. Woloshyn. $D_{s0}^*(2317)$ Meson and D-Meson-Kaon Scattering from Lattice QCD. *Phys.Rev.Lett.*, 111(22):222001, 2013.
- [38] Graham Moir, Michael Peardon, Sinead M. Ryan, Christopher E. Thomas, and Liuming Liu. Excited spectroscopy of charmed mesons from lattice QCD. *JHEP*, 1305:021, 2013.
- [39] A. Bazavov et al. Charmed and light pseudoscalar meson decay constants from four-flavor lattice QCD with physical light quarks. *Phys.Rev.*, D90(7):074509, 2014.

-
- [40] Martin Kalinowski and Marc Wagner. Masses of D mesons, D_s mesons and charmonium states from twisted mass lattice QCD. *Phys. Rev.*, D92(9):094508, 2015.
- [41] Daniel Mohler and R.M. Woloshyn. D and D_s meson spectroscopy. *Phys.Rev.*, D84:054505, 2011.
- [42] Martin Kalinowski and Marc Wagner. Masses of mesons with charm valence quarks from $2+1+1$ flavor twisted mass lattice QCD. *Acta Phys.Polon.Supp.*, 6(3):991–996, 2013.
- [43] M. F. M. Lutz, R. Bavontaweepanya, C. Kobdaj, and K. Schwarz. Finite volume effects in the chiral extrapolation of baryon masses. *Phys. Rev.*, D90(5):054505, 2014.
- [44] B. Borasoy and Ulf-G. Meissner. Chiral Expansion of Baryon Masses and Sigma-Terms. *Annals Phys.*, 254:192–232, 1997.
- [45] John F. Donoghue and Barry R. Holstein. Improved treatment of loop diagrams in SU(3) baryon chiral perturbation theory. *Phys. Lett.*, B436:331–338, 1998.
- [46] Shi-Lin Zhu, S. Puglia, and M. J. Ramsey-Musolf. Recoil order chiral corrections to baryon octet axial currents. *Phys. Rev.*, D63:034002, 2001.
- [47] A. Semke and M.F.M. Lutz. Baryon self energies in the chiral loop expansion. *Nucl.Phys.*, A778:153–180, 2006.
- [48] Matthias Frink, Ulf-G. Meissner, and Ilka Scheller. Baryon masses, chiral extrapolations, and all that. *Eur. Phys. J.*, A24:395–409, 2005.
- [49] A. Semke and M. F. M. Lutz. Discontinuous quark-mass dependence of baryon octet and decuplet masses. *Nucl. Phys.*, A789:251–259, 2007.
- [50] L. S. Geng, M. Altenbuchinger, and W. Weise. Light quark mass dependence of the D and D_s decay constants. *Phys. Lett.*, B696:390–395, 2011.
- [51] A. Semke and M.F.M. Lutz. On the quark-mass dependence of the baryon ground-state masses. *Phys.Rev.*, D85:034001, 2012.
- [52] Matthias F. M. Lutz, Yonggoo Heo, and Xiao-Yu Guo. On the convergence of the chiral expansion for the baryon ground states. 2016.
- [53] G. Ecker. Chiral perturbation theory. *Prog.Part.Nucl.Phys.*, 35:1–80, 1995.
- [54] Stefan Scherer. Introduction to chiral perturbation theory. *Adv.Nucl.Phys.*, 27:277, 2003.
- [55] Matthias Neubert. Heavy quark symmetry. *Phys.Rept.*, 245:259–396, 1994.
- [56] A.V. Manohar and M.B. Wise. *Heavy Quark Physics*. Cambridge Monographs on Particle Physics, Nuclear Physics and Cosmology. Cambridge University Press, 2007.
- [57] J. Beringer et al. Review of Particle Physics (RPP). *Phys.Rev.*, D86:010001, 2012.
- [58] T.P. Cheng and L.F. Li. *Gauge Theory of Elementary Particle Physics*. Oxford Science Publications. Clarendon Press, 1984.
- [59] K.A. Olive et al. Review of Particle Physics. *Chin.Phys.*, C38:090001, 2014.
- [60] Murray Gell-Mann, R.J. Oakes, and B. Renner. Behavior of current divergences under SU(3) x SU(3). *Phys.Rev.*, 175:2195–2199, 1968.

-
- [61] Stephen L. Adler. Axial vector vertex in spinor electrodynamics. *Phys.Rev.*, 177:2426–2438, 1969.
- J.S. Bell and R. Jackiw. A pcac puzzle: $\pi_0 \rightarrow \gamma\gamma$ in the σ -model. *Nuovo Cimento A*, 60(1):47–61, 1969.
- [62] Kazuo Fujikawa. Path Integral Measure for Gauge Invariant Fermion Theories. *Phys.Rev.Lett.*, 42:1195, 1979.
- [63] Gerard 't Hooft. Symmetry Breaking Through Bell-Jackiw Anomalies. *Phys.Rev.Lett.*, 37:8–11, 1976.
- [64] H. Leutwyler. On the foundations of chiral perturbation theory. *Annals Phys.*, 235:165–203, 1994.
- [65] Steven Weinberg. Pion scattering lengths. *Phys. Rev. Lett.*, 17:616–621, 1966.
- [66] Steven Weinberg. Phenomenological Lagrangians. *Physica*, A96:327, 1979.
- [67] Sidney R. Coleman, J. Wess, and Bruno Zumino. Structure of phenomenological Lagrangians. 1. *Phys.Rev.*, 177:2239–2247, 1969.
- [68] Jr. Callan, Curtis G., Sidney R. Coleman, J. Wess, and Bruno Zumino. Structure of phenomenological Lagrangians. 2. *Phys.Rev.*, 177:2247–2250, 1969.
- [69] S. Weinberg. *The Quantum Theory of Fields*, volume II. Modern Applications. Cambridge University Press, 1995.
- [70] G. Ecker, J. Gasser, A. Pich, and E. de Rafael. The Role of Resonances in Chiral Perturbation Theory. *Nucl.Phys.*, B321:311, 1989.
- [71] G. Ecker, J. Gasser, H. Leutwyler, A. Pich, and E. de Rafael. Chiral Lagrangians for Massive Spin 1 Fields. *Phys.Lett.*, B223:425, 1989.
- [72] J.F. Donoghue, E. Golowich, and B.R. Holstein. *Dynamics of the Standard Model*. Cambridge Monographs on Particle Physics, Nuclear Physics and Cosmology. Cambridge University Press, 1994.
- [73] J. Gasser, M.E. Sainio, and A. Svarc. Nucleons with Chiral Loops. *Nucl.Phys.*, B307:779, 1988.
- [74] Benjamin Grinstein. The Static Quark Effective Theory. *Nucl.Phys.*, B339:253–268, 1990.
- [75] Howard Georgi. AN EFFECTIVE FIELD THEORY FOR HEAVY QUARKS AT LOW-ENERGIES. *Phys.Lett.*, B240:447–450, 1990.
- [76] Adam F. Falk, Benjamin Grinstein, and Michael E. Luke. Leading mass corrections to the heavy quark effective theory. *Nucl.Phys.*, B357:185–207, 1991.
- [77] Estia Eichten and Brian Russell Hill. STATIC EFFECTIVE FIELD THEORY: $1/m$ CORRECTIONS. *Phys.Lett.*, B243:427–431, 1990.
- [78] Michael E. Luke. Effects of subleading operators in the heavy quark effective theory. *Phys.Lett.*, B252:447–455, 1990.
- [79] Joan Soto and Rodanthy Tzani. Anomalies in the effective theory of heavy quarks. *Phys.Lett.*, B297:358–366, 1992.
- [80] Thomas Mannel, Winston Roberts, and Zbigniew Ryzak. A Derivation of the heavy quark effective Lagrangian from QCD. *Nucl.Phys.*, B368:204–220, 1992.

-
- [81] Veronique Bernard, Norbert Kaiser, Joachim Kambor, and Ulf G. Meissner. Chiral structure of the nucleon. *Nucl.Phys.*, B388:315–345, 1992.
- [82] G. Ecker. The Standard model at low-energies. *Czech.J.Phys.*, 44:405–430, 1995.
- [83] Michael E. Luke and Aneesh V. Manohar. Reparametrization invariance constraints on heavy particle effective field theories. *Phys.Lett.*, B286:348–354, 1992.
- [84] R. Casalbuoni, A. Deandrea, N. Di Bartolomeo, Raoul Gatto, F. Feruglio, et al. Phenomenology of heavy meson chiral Lagrangians. *Phys.Rept.*, 281:145–238, 1997.
- [85] Adam F. Falk. Hadrons of arbitrary spin in the heavy quark effective theory. *Nucl.Phys.*, B378:79–94, 1992.
- [86] Adam F. Falk, Matthias Neubert, and Michael E. Luke. The Residual mass term in the heavy quark effective theory. *Nucl.Phys.*, B388:363–375, 1992.
- [87] C. Glenn Boyd and Benjamin Grinstein. Chiral and heavy quark symmetry violation in B decays. *Nucl.Phys.*, B442:205–227, 1995.
- [88] C.G. Itzykson and J.B. Zuber. *Quantum Field Theory*. Dover Books on Physics. Dover Publications, Incorporated, 2005.
- [89] John F. Donoghue, Carlos Ramirez, and German Valencia. The Spectrum of QCD and Chiral Lagrangians of the Strong and Weak Interactions. *Phys.Rev.*, D39:1947, 1989.
- [90] J.S.R. Chisholm. Change of variables in quantum field theories. *Nucl.Phys.*, 26:469–479, 1961.
- [91] S. Scherer and H. W. Fearing. Field transformations and the classical equation of motion in chiral perturbation theory. *Phys. Rev.*, D52:6445–6450, 1995.
- [92] Steven Weinberg. Effective chiral Lagrangians for nucleon - pion interactions and nuclear forces. *Nucl.Phys.*, B363:3–18, 1991.
- [93] V. Bernard, Norbert Kaiser, and Ulf-G. Meissner. Nucleon electroweak form-factors: Analysis of their spectral functions. *Nucl.Phys.*, A611:429–441, 1996.
- [94] Thomas Becher and H. Leutwyler. Baryon chiral perturbation theory in manifestly Lorentz invariant form. *Eur. Phys. J.*, C9:643–671, 1999.
- [95] Veronique Bernard. Chiral Perturbation Theory and Baryon Properties. *Prog. Part. Nucl. Phys.*, 60:82–160, 2008.
- [96] Paul J. Ellis and Hua-Bin Tang. Pion nucleon scattering in a new approach to chiral perturbation theory. *Phys. Rev.*, C57:3356–3375, 1998.
- [97] Matthias Lutz. Effective chiral theory of nucleon-nucleon scattering. *Nucl.Phys.*, A677:241–312, 2000.
- [98] J. Gegelia and G. Japaridze. Matching heavy particle approach to relativistic theory. *Phys. Rev.*, D60:114038, 1999.
- [99] T. Fuchs, J. Gegelia, G. Japaridze, and S. Scherer. Renormalization of relativistic baryon chiral perturbation theory and power counting. *Phys.Rev.*, D68:056005, 2003.
- [100] M. Altenbuchinger, L. S. Geng, and W. Weise. SU(3) Breaking Corrections to the D , D^* , B , and B^* decay Constants. *Phys. Lett.*, B713:453–456, 2012.

-
- [101] D. Djukanovic, J. Gegelia, A. Keller, and S. Scherer. Complex-mass renormalization in chiral effective field theory. *Phys. Lett.*, B680:235–238, 2009.
- [102] Peter C. Bruns, Ludwig Greil, and Andreas Schäfer. Chiral behavior of vector meson self energies. *Phys. Rev.*, D88:114503, 2013.
- [103] Peter C. Bruns and Ulf-G. Meissner. Infrared regularization for spin-1 fields. *Eur. Phys. J.*, C40:97–119, 2005.
- [104] Ross Daniel Young, Derek Bruce Leinweber, and Anthony William Thomas. Convergence of chiral effective field theory. *Prog. Part. Nucl. Phys.*, 50:399–417, 2003. [,399(2002)].
- [105] Silas R. Beane. In search of the chiral regime. *Nucl. Phys.*, B695:192–198, 2004.
- [106] Veronique Bernard, Thomas R. Hemmert, and Ulf-G. Meissner. Cutoff schemes in chiral perturbation theory and the quark mass expansion of the nucleon mass. *Nucl. Phys.*, A732:149–170, 2004.
- [107] C. Aubin, C. Bernard, C. DeTar, J. Osborn, Steven Gottlieb, et al. Light hadrons with improved staggered quarks: Approaching the continuum limit. *Phys.Rev.*, D70:094505, 2004.
- [108] A. Walker-Loud, H.-W. Lin, D.G. Richards, R.G. Edwards, M. Engelhardt, et al. Light hadron spectroscopy using domain wall valence quarks on an Asqtad sea. *Phys.Rev.*, D79:054502, 2009.
- [109] Derek Bruce Leinweber, Anthony William Thomas, and Ross Daniel Young. Extrapolation of lattice QCD results beyond the power-counting regime. *Nucl. Phys.*, A755:59–70, 2005.
- [110] Vladimir Pascalutsa and Marc Vanderhaeghen. The Nucleon and delta-resonance masses in relativistic chiral effective-field theory. *Phys. Lett.*, B636:31–39, 2006.
- [111] Shi-Lin Zhu, G. Sacco, and M. J. Ramsey-Musolf. Recoil order chiral corrections to baryon octet axial currents and large $N(c)$ QCD. *Phys. Rev.*, D66:034021, 2002.
- [112] Massimiliano Procura, Thomas R. Hemmert, and Wolfram Weise. Nucleon mass, sigma term and lattice QCD. *Phys. Rev.*, D69:034505, 2004.
- [113] M. K. Banerjee and J. Milana. Baryon mass splittings in chiral perturbation theory. *Phys. Rev.*, D52:6451–6460, 1995.
- [114] M. K. Banerjee and J. Milana. The Decuplet revisited in χ (PT). *Phys. Rev.*, D54:5804–5811, 1996.
- [115] Thomas R. Hemmert, Barry R. Holstein, and Joachim Kambor. Systematic $1/M$ expansion for spin $3/2$ particles in baryon chiral perturbation theory. *Phys. Lett.*, B395:89–95, 1997.
- [116] Thomas R. Hemmert, Barry R. Holstein, and Joachim Kambor. Chiral Lagrangians and $\delta(1232)$ interactions: Formalism. *J. Phys.*, G24:1831–1859, 1998.
- [117] Jonathan M. M. Hall and Vladimir Pascalutsa. Limitations of the heavy-baryon expansion as revealed by a pion-mass dispersion relation. *Eur. Phys. J.*, C72:2206, 2012.
- [118] S. Aoki et al. Review of lattice results concerning low-energy particle physics. 2016.
- [119] R. Frezzotti, G. Martinelli, M. Papinutto, and G.C. Rossi. Reducing cutoff effects in maximally twisted lattice QCD close to the chiral limit. *JHEP*, 0604:038, 2006.
- [120] Ph. Boucaud et al. Dynamical twisted mass fermions with light quarks. *Phys.Lett.*, B650:304–311, 2007.

-
- [121] Philippe Boucaud et al. Dynamical Twisted Mass Fermions with Light Quarks: Simulation and Analysis Details. *Comput.Phys.Commun.*, 179:695–715, 2008.
- [122] Remi Baron et al. Light Meson Physics from Maximally Twisted Mass Lattice QCD. *JHEP*, 1008:097, 2010.
- [123] R. Baron, Ph. Boucaud, J. Carbonell, A. Deuzeman, V. Drach, et al. Light hadrons from lattice QCD with light (u,d), strange and charm dynamical quarks. *JHEP*, 1006:111, 2010.
- [124] Remi Baron et al. Computing K and D meson masses with $N_f = 2+1+1$ twisted mass lattice QCD. *Comput.Phys.Commun.*, 182:299–316, 2011.
- [125] Gregorio Herdoiza, Karl Jansen, Chris Michael, Konstantin Ottnad, and Carsten Urbach. Determination of Low-Energy Constants of Wilson Chiral Perturbation Theory. *JHEP*, 1305:038, 2013.
- [126] Krzysztof Cichy, Martin Kalinowski, and Marc Wagner. The continuum limit of the D meson, D_s meson and charmonium spectrum from $N_f = 2 + 1 + 1$ twisted mass lattice QCD. 2016.
- [127] A. Bazavov, D. Toussaint, C. Bernard, J. Laiho, C. DeTar, et al. Nonperturbative QCD simulations with 2+1 flavors of improved staggered quarks. *Rev.Mod.Phys.*, 82:1349–1417, 2010.
- [128] Stephen R. Sharpe. Rooted staggered fermions: Good, bad or ugly? *PoS*, LAT2006:022, 2006.
- [129] C. McNeile, C.T.H. Davies, E. Follana, K. Hornbostel, and G.P. Lepage. Heavy meson masses and decay constants from relativistic heavy quarks in full lattice QCD. *Phys.Rev.*, D86:074503, 2012.
- [130] G.C. Donald, C.T.H. Davies, J. Koponen, and G.P. Lepage. Prediction of the D_s^* width from a calculation of its radiative decay in full lattice QCD. *Phys.Rev.Lett.*, 112:212002, 2014.
- [131] C.T.H. Davies, E. Follana, I.D. Kendall, G. Peter Lepage, and C. McNeile. Precise determination of the lattice spacing in full lattice QCD. *Phys.Rev.*, D81:034506, 2010.
- [132] Heechang Na, Christine T.H. Davies, Eduardo Follana, G. Peter Lepage, and Junko Shigemitsu. The $D \rightarrow K, l \nu$ Semileptonic Decay Scalar Form Factor and $|V_{cs}|$ from Lattice QCD. *Phys.Rev.*, D82:114506, 2010.
- [133] Heechang Na, Christine T.H. Davies, Eduardo Follana, G. Peter Lepage, and Junko Shigemitsu. $|V_{cd}|$ from D Meson Leptonic Decays. *Phys.Rev.*, D86:054510, 2012.
- [134] E. Follana et al. Highly improved staggered quarks on the lattice, with applications to charm physics. *Phys.Rev.*, D75:054502, 2007.
- [135] Liuming Liu, Kostas Orginos, Feng-Kun Guo, Christoph Hanhart, and Ulf-G. Meissner. Interactions of Charmed Mesons with Light Pseudoscalar Mesons from Lattice QCD and Implications on the Nature of the $D_{s0}^*(2317)$. *Phys.Rev.*, D87:014508, 2013.
- [136] S. Aoki et al. 2+1 Flavor Lattice QCD toward the Physical Point. *Phys.Rev.*, D79:034503, 2009.
- [137] Aida X. El-Khadra, Andreas S. Kronfeld, and Paul B. Mackenzie. Massive fermions in lattice gauge theory. *Phys.Rev.*, D55:3933–3957, 1997.
- [138] Mehmet B. Oktay and Andreas S. Kronfeld. New lattice action for heavy quarks. *Phys. Rev.*, D78:014504, 2008.
- [139] J. Martin Camalich, L. S. Geng, and M. J. Vicente Vacas. The lowest-lying baryon masses in covariant SU(3)-flavor chiral perturbation theory. *Phys. Rev.*, D82:074504, 2010.
-

-
- [140] Li-sheng Geng, Xiu-lei Ren, J. Martin-Camalich, and W. Weise. Finite-volume effects on octet-baryon masses in covariant baryon chiral perturbation theory. *Phys. Rev.*, D84:074024, 2011.
- [141] M. F. M. Lutz and A. Semke. On the consistency of recent QCD lattice data of the baryon ground-state masses. *Phys. Rev.*, D86:091502, 2012.
- [142] Yan-Rui Liu, Xiang Liu, and Shi-Lin Zhu. Light Pseudoscalar Meson and Heavy Meson Scattering Lengths. *Phys.Rev.*, D79:094026, 2009.
- [143] Liuming Liu, Huey-Wen Lin, and Kostas Orginos. Charmed Hadron Interactions. *PoS, LATTICE2008:112*, 2008.
- [144] M. Altenbuchinger and Li-Sheng Geng. Off-shell effects on the interaction of Nambu-Goldstone bosons and D mesons. *Phys. Rev.*, D89(5):054008, 2014.
- [145] Feng-Kun Guo, Christoph Hanhart, Siegfried Krewald, and Ulf-G. Meissner. Subleading contributions to the width of the $D^*(s_0)(2317)$. *Phys. Lett.*, B666:251–255, 2008.
- [146] Zhi-Hui Guo, Ulf-G. Meißner, and De-Liang Yao. New insights into the $D_{s_0}^*(2317)$ and other charm scalar mesons. *Phys. Rev.*, D92(9):094008, 2015.
- [147] De-Liang Yao, Meng-Lin Du, Feng-Kun Guo, and Ulf-G. Meißner. One-loop analysis of the interactions between charmed mesons and Goldstone bosons. *JHEP*, 11:058, 2015.
- [148] M.E. Peskin and D.V. Schroeder. *An Introduction To Quantum Field Theory*. Frontiers in physics. Westview Press, 1995.
- [149] Gerard 't Hooft. A Planar Diagram Theory for Strong Interactions. *Nucl.Phys.*, B72:461, 1974.
- [150] Edward Witten. Baryons in the $1/n$ Expansion. *Nucl.Phys.*, B160:57, 1979.
- [151] Aneesh V. Manohar. Large N QCD. In R. Gupta, editor, *Probing the Standard Model of Particle Interactions*, pages 1091–1169. 1998.
- [152] Richard F. Lebed. Phenomenology of large $N(c)$ QCD. *Czech.J.Phys.*, 49:1273–1306, 1999.
- [153] G. Veneziano. Some Aspects of a Unified Approach to Gauge, Dual and Gribov Theories. *Nucl.Phys.*, B117:519–545, 1976.
- [154] George Leibbrandt. Introduction to the Technique of Dimensional Regularization. *Rev. Mod. Phys.*, 47:849, 1975.
- [155] J. Gasser and H. Leutwyler. Light Quarks at Low Temperatures. *Phys. Lett.*, B184:83–88, 1987.
- [156] J. Gasser and H. Leutwyler. Spontaneously Broken Symmetries: Effective Lagrangians at Finite Volume. *Nucl. Phys.*, B307:763–778, 1988.
- [157] M. Doring, Ulf-G. Meissner, E. Oset, and A. Rusetsky. Unitarized Chiral Perturbation Theory in a finite volume: Scalar meson sector. *Eur. Phys. J.*, A47:139, 2011.
- [158] M. Luscher. Volume Dependence of the Energy Spectrum in Massive Quantum Field Theories. 2. Scattering States. *Commun. Math. Phys.*, 105:153–188, 1986.
- [159] Luka Leskovec and Sasa Prelovsek. Scattering phase shifts for two particles of different mass and non-zero total momentum in lattice QCD. *Phys. Rev.*, D85:114507, 2012.

Acknowledgements

Over the past more than four years, I have received great support and encouragement from my supervisor Prof. Dr. Matthias F.M. Lutz. During this period, he introduced me to the subject I am working on and illuminated a lot of deep insights on the issues raised in my field. Throughout the years, I have benefited also from his rigorous and suspicious attitude in doing research. His confidence and enthusiasm always inspired me to insist on pursuing what I am convinced in. I am indebted to Matthias also for his having provided me the numerical fits involved in this thesis, and having given corrections to my thesis with endless patience.

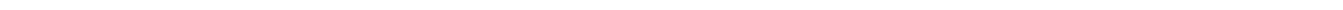
I am grateful to Prof. Dr. Bengt Friman for being my external supervisor of my PhD committee. His erudition and wisdom always shed light on many different topics in physics in a profound manner and made me benefit a lot. I also highly appreciate the efforts he made in order to let me get continuous financial supports.

I would like to acknowledge HGS-HIRE and GSI for providing me scholarship during my study.

In the last years, I learned a lot from my groupmates Dr. Yonggoo Heo and Dr. Igor Danilkin. I want to say thanks to them. Special thanks to Yonggoo for his careful checks with the results involved in my thesis. I would like to thank Dr. Pok Man Lo for those of delightful discussions with him. Grateful acknowledgements are also given to Prof. Dr. Marc Wagner and Martin Kalinowski for providing their unpublished lattice results based on ETMC configurations. Special thanks go to Prof. Dr. Qionggui Lin, Dr. Zhi-Gang Luo and Prof. Dr. Meirong Zhang for illuminating discussions about generic convergence properties of complex functions.

I am cherishing the memory of joyful moments with Enrico Speranza, and memorable good time with Gabor Almasi, Sofija Antic, Dr. Hans-Friedrich Fuhrmann and Ulrich Sauerwein during my PhD study. Thank you my friends. And thanks to all the GSI theory group members for hosting me and helping me during the years. Many thanks to my friend Dr. Xiaodong Xu. His optimistic spirit always inspires me. And thanks also to my friend Dr. Zhan-Wei Liu.

Finally, I give my most gratitude to my wife, Dandan Liu, and my parents. Especially, my wife has come to Germany in parallel with me, though not in the same city, and I cannot imagine how my life in Germany would be if my wife weren't here. With encouragement from all of you, I have made myself tougher to overcome tough obstacles. Without my wife and my parents, I would not have such an ambition and courage to insist on doing what I am interested in.



Lebenslauf

Xiaoyu Guo

[REDACTED]
[REDACTED]

09.2004 ~ 06.2008

Bachelorstudium an der Wuhan University,
Wuhan, China.

06.2008

Abschluss: Bachelor of Science.

09.2009 ~ 06.2012

Masterstudium an der Peking University,
Beijing, China.

07.2012

Abschluss: Master of Science,
Masterarbeit: *Study on Nambu-Jona-Lasinio Model
with Heavy Quarks.*

seit 10.2012

Promotionsstudium an der Technischen Universität Darmstadt
Doktorand in der Theorie-Abteilung des GSI helmholzzentrums
für Schwerionenforschung und Anfertigung der Dissertation,
Darmstadt, Deutschland.